Dear Editor

We thank you for soliciting two thorough, informed, and constructive reviews on our Solid Earth Discussion article by Richard Styron and Folarin Kolawole, which will undoubtedly improve our manuscript. Below, we have copied the reviewer's comments in italics and replied to them in blue, cambria text with how we would like to incorporate them into a revised manuscript to submit to *Solid Earth*. Unless otherwise stated, line numbers refer to the clean version of the manuscript without tracked changes unless.

We thank you for consideration of this manuscript and look forward to hearing from you.

Kind regards

Jack Williams (on behalf of all co-authors)

Reviewer 1

The paper by Williams et al. provides a high-quality map of active faults in southern Malawi, and presents a clever method for partitioning regional deformation rates onto the rift structures, with a thorough exploration of the uncertainties. The work (the mapping, rate estimation, and manuscript) are executed competently, and there is nothing that is strictly incorrect, although some topics would benefit from a bit more explanation if not revision. The mapping is quite high quality, and is the most solid contribution made here.

Although the authors may not want to do this, I think that the work could benefit from being split into two different, shorter papers: one that presents the fault mapping and discusses it in a bit more detail and context (although not too much more), and another that presents the parameter estimates, ideally as a part of a PSHA. (Note that I am not asking that this be done for major revisions–it's just something to consider doing.)

We thank the reviewer for their suggestion, which we have considered very seriously. Our preference is to keep the mapping and parameter estimates together in one paper, as we feel they are inherently linked and that a strength of the current study is the fact that it spans traditional discipline boundaries, Nevertheless, we see the importance of more distinctly separating between our observations and interpretations. As outlined below with respect to major issue #1, and in the introduction in the main text (Lines 68-94) we have recognised this by describing and providing two distinct GIS file databases in this study, the 'South Malawi Active Fault Database' (Sect. 3) and 'South Malawi Seismogenic Sources Database' (Sect. 4). In this way, the reader will be more able to separate between the fault mapping and the parameter estimates, and any user has a choice between adapting the fault mapping only or also including our parameter estimates.

Major issues:

1. Separation of data and estimates

The first issue is that there is no apparent separation in the fault data and attributes between observation (and associated interpretation firmly based in observations) and rough estimation based on little to no data. Although the authors are helpfully conforming to the schema laid out by the GEM Faulted Earth (GFE) project (e.g. Christophersen et al. 2015), I believe that the GFE is intended to hold observations or measurements, rather than the estimates made in this project. For example, recurrence intervals would be derived from paleoseismology rather than calculated from the slip rate and assumed magnitudes. Only considering measured recurrence intervals makes the recurrence intervals independent of assumptions of earthquake magnitude, scaling relations, or other factors. Christophersen et al (2015) state that the database is often sparse where observations don't exist.

The coupling of the fault traces (which are observations or data, as far as I am concerned, even if there is an interpretive component) with the parameter estimations crosses a traditional boundary. Typically, the fault data are considered to be somewhat objective and immutable (though subject to revision) while the derivation of earthquake rates is considered to be part of the modeling process and often done while making fault sources for a PSHA. Model results are a bit more subjective and mutable, as they are dependent on assumptions that are explored during the modeling process and/or are project-dependent. A good modeler will have a process for testing and refining some of these assumptions (i.e. magnitude scaling relations or slip partitioning) through comparisons with instrumental seismicity or other observations. However the observed data are usually not revised to *improve a data-model fit. A user who wants to incorporate this dataset into a seismic hazard model, but who may not agree with some of the model assumptions used here (i.e. scaling relations, magnitude ranges, or the style of partitioning between internal and border faults) may have a hard time knowing what to keep and what to discard, without reading a long paper. This can be a big challenge for the many seismic hazard modelers who do not have a great facility with the English language. Similarly, if this data were incorporated into other fault databases, the end user may not be able to cleanly separate data from model results.*

This does not mean that what the authors have done is wrong or necessarily needs to be changed. It is just to raise their awareness of a potential concern (that these estimates may be confused for observations) and that many hazard modelers would prefer to redo the estimation rather than rely on these results. I am not sure of the best course of action. If it were me doing the work, I would separate these processes and release both 'only data' and 'data plus estimates' datasets. I would also consider publishing them independently, and perhaps incorporating the rate estimation work into a PSHA rather than going part way as is done here. But there is no 'right' or scientifically optimal decision here, and a lot depends on the particular circumstances of the authors.

Another possibility is to keep the parameter estimation through the slip rate estimation but stop there, which would avoid the problems of choosing a magnitude-frequency distribution, estimating the seismogenic thickness of the crust, etc. In a typical project, these tasks are often done by the hazard modeler rather than the geologist who prepares the fault data up through slip rate estimations.
I can state that as a fault data compiler, I am a bit hesitant to bring any of the estimated parameters into the GEM Global Active Faults Database, as they are too poorly constrained and data-limited, and I don't want users to confuse them for measurements.

As noted above, to follow the advice to release both 'only data' and 'data plus estimates' datasets, in this revised manuscript we have described and included two separate GIS databases of faults in South Malawi:

1. The South Malawi Active Fault Database (SMAFD, Sect. 3, Table 1): this database incorporates the objective mapping and geomorphic 'trace' attributes included in the previous version of the SMAFD. In addition, individual GIS features represent faults (see minor comment for Reviewer #1 Line 325). In this way, the SMAFD conforms to the 'only data' dataset requested by the reviewer and will also be readily comparable to the newly published GEM Global Active Fault Database (Styron and Pagani, 2020).
2. The South Malawi Seismogenic Source Database (SMSSD, Sect. 4, Table 2): this database incorporates the modelling derived attributes included in the original version of the SMAFD that are required to turn the mapped faults into earthquake sources for PSHA (e.g. fault segmentation, fault width, slip rates, earthquake magnitudes, and recurrence intervals). Here, individual GIS features represent fault segments, which can each be considered distinct sources for PSHA. Furthermore, in line with other earthquake source databases (Basili et al., 2008; Field et al., 2014; Stirling et al., 2012) faults in the SMSSD are mapped as straight lines that connect segment tips, as opposed to truly honouring the surface trace of the faults (see for example the comparison for the Chingale Step Fault in Fig. 4). In this way, the SMSSD will conform to the 'data plus estimate' dataset requested by the reviewer.

By distinctly describing these two datasets in the revised manuscript, whilst also clearly outlining how they are linked, we thus address the reviewer's concern about how users of these databases may be confused by which fault attributes are objective measurements, and which are model-driven. Furthermore, we maintain the multidisciplinary aspect of this manuscript, and allow seismic hazard modellers to understand the limitations for geologists investigating active faults in a region where data is sparse and vice versa (Lines 96-98). Work to include the SMAFD and SMSSD into PSHA in southern Malawi is ongoing, and this will be the topic of a subsequent study.

2. *Estimation of uncertainty:*

The second issue is that the logic tree framework used to propagate uncertainties and explore the parameter space is perhaps more complex than it needs to be based on the lack of input data. It is a clever method and there seems to be nothing incorrect in the implementation, but I question the wisdom of using it southern Malawi where there is essentially no data to feed in. The old saying in modeling is "garbage in, garbage out"; in this case it's more like "nothing in, nothing out" (I am not suggesting the work is garbage!). The exercise seems to simply quantify the obvious, that each fault slips somewhere between 0-5 mm/yr. I am not sure that it provides much value. The further work, estimating recurrence intervals, has larger theoretical issues (discussed below) in addition to adding several more layers of uncertainty into the results. It could easily be removed from the database (though perhaps kept in the paper for discussion).

As a subordinate issue, I don't think a logic tree framework is really the most appropriate method of propagating uncertainty as used; it is more appropriate when the parameters that make up the branches in the tree are discrete variables with a few choices, rather than continuous random variables. For example, an appropriate use of logic trees is to consider different scaling relationships.

With continuous random variables (i.e., extension rate or dip), the use of unweighted logic trees considers the lower, mid, and high values to all have equal probability. Do the authors consider this to be the case? Do the authors believe that the resulting low, mid and high values are equally probable? Even if the inputs are all equal, if there are no correlations between the different parameters, the middle values should be more probable (see for example the Central Limit Theorem).

In my opinion, a more appropriate method for representing the uncertainty in the results (i.e., slip rates or recurrence intervals) would be to define distributions for each continuous random variable (i.e., dip or total geodetic extension at that latitude) and then randomly sample from these distributions, and then characterize the resulting distributions for the results parameters. This is a simple Monte Carlo method. The major strength of this method is that the sampling will cover far more of the parameter space than a coarse 'low/med/high' sampling method. It is also quite trivial to introduce distributions for each parameter that may reflect prior knowledge (i.e., a PDF of regional dips based on focal mechansisms or structural measurements).

One way to think of this is that the representation of uncertainty in the model should reflect the real uncertainty of the parameter. Continuous variables should be represented through continuous distributions, while discrete variables (i.e. the choice of scaling relationships) should be represented through discrete distributions (i.e. lists or arrays, perhaps weighted).

The strategy employed here does a good job of defining the absolute range of the results based on the inputs, but a worse job of defining the central values (broadly like the mean and one standard deviation rather than three standard deviations). If the authors believe this is the better choice, that is fine, but I would like to hear their arguments.

We can appreciate why the reviewer might question the usefulness of the large uncertainties in our slip rate and recurrence intervals estimates. However, the fact remains that even being able to quantify slip rate estimates of 0-5 mm/yr in southern Malawi represents a significant advance, given that prior to this study, no slip rate estimates have been previously made (Lines 78-79). Furthermore, as highlighted in the manuscript (Lines 672-675) the large range of values we obtain in our recurrence interval estimates are not unusual compared to other low strain rate regions with limited paleoseismic information (Villamor et al., 2018) and can still be incorporated into PSHA (Hodge et al., 2015). Indeed, these large ranges can be considered as an important outcome of the study, as they can be used to the highlight the parameters that need further study to reduce uncertainty (Sect. 5.4 of the manuscript).

We note that logic trees have been used elsewhere to propagate uncertainty in seismic hazard in regions with little paleoseismic data (Villamor et al., 2018). However, we do agree with the reviewer's comments on how we should consider our lower, intermediate, and upper estimates; indeed, and note in the revised manuscript that the upper and lower values obtained from the logic tree required an unlikely set of parameter combinations (Lines 675-678), and that treating these values as a continuous variable and assigning a probability distribution function to them would be a more appropriate method of treating them in PSHA (lines 1599-1600).

A more complex treatment than the intermediate, lower, and upper slip rate and recurrence interval estimates obtained from the logic tree are beyond the scope of this study, but already under consideration for our next paper. In this revised manuscript, we have therefore included a distinct section on how the fault data included in the SMAFD and SMSSD could be incorporated into PSHA (Sect. 6.3), where we more explicitly discuss some of the reviewer's excellent suggestions. This would also address Major Issue #3 (see below).

3. The calculations of recurrence rate:

The authors choose to calculate recurrence rates under the assumption that all of the seismic moment that accumulates on each fault is released during earthquakes of identical magnitude. This is essentially the "characteristic earthquake hypothesis" which featured quite prominently in mid-late 20th century paleoseismology and PSHA but was always quite contentious (for example see "Characteristic Earthquake Model, 1884-2011, RIP" by Kagan et al. 2012, Seismological Research Letters). This hypothesis is believed by fewer and fewer scientists with each passing year, as our observations of variable rupture segmentation and per-event displacement accrue. The few remaining national-level PSHA models that still use a 'pure' characteristic earthquake model (not a distribution that includes aleatoric variability) do so primarily because it simplifies time-dependent hazard analysis. The modern state of practice is to consider a range of earthquake sizes on each fault, and to distribute moment throughout the range of earthquake sizes by specifying the relative frequencies of different magnitudes of earthquakes, and then calculating the absolute frequencies through moment rate balancing.

The canonical reference for this is Youngs and Coppersmith (1985 BSSA), which provides equations for multiple magnitude-frequency distributions. GEM's Open-Quake Engine and OQ Model Building Toolkit also has some Python code for this purpose, if the authors are interested in using or studying a functional implementation (https://github.com/gem/oq-engine/tree/master/openquake/hazardlib/mfd; https://github.com/GEMScienceTools/oqmbtk/blob/master/openquake/mbt/tools/fault_modeler/fault_modeling_utils.py#L2379). If the authors favor the pure characteristic earthquake hypothesis, then they should provide some supporting arguments. Otherwise they may either calibrate the magnitude frequency distributions, or simply drop this part of the estimation procedure (even if they retain the estimates up through the slip rate calculations).

We recognise that we make a large simplification by considering characteristic whole-fault or segment ruptures only, and that fully incorporating the SMAFD into PSHA requires further evaluation of individual faults' magnitude-frequency distribution. We have now ensured that this simplification is spelled out in the revised manuscript (Lines 682-685), but also noted that by considering both whole fault or segmented fault ruptures, our study already partially recognises that the characteristic earthquake hypothesis does not necessarily apply in southern Malawi, because the faults will not always host similar sized events Furthermore, some recent studies have noted that the characteristic earthquake hypothesis, and its use in PSHA, is not necessarily 'dead' (Stirling and Gerstenberger, 2018).

It is also worth reflecting that in studies where faults are allowed to host a range of earthquake magnitudes in PSHA, these are built from many years of detailed geological mapping, historical, instrumental and paleo-, seismicity data, and hazard modelling (Basili et al., 2008; Field et al., 2014). Conversely, prior to this study, there has been very little systematic investigation of possible earthquake magnitudes and recurrence intervals at all in southern Malawi. Hodge et al., (2015) is an exception, and this was based on a very limited active fault mapping. So even though the recurrence interval and earthquake magnitude estimates in this study are poorly constrained compared to other countries' seismic hazard assessments, we still consider them to represent a step change in our understanding of southern Malawi's seismic hazard.

Therefore, similar to Major Issue #2 above, our preference has been to incorporate the reviewer's comments in a distinct section where we discuss how this study could be used into PSHA (Sect. 6.3).

Minor issues:

Data license, distribution and updates:

One of the promises of 21st century science is that new technologies enable rapid and low-friction sharing, integrating, and updating of data. However, it raises some new topics that have been heretofore ignored by most. The first is the license of the data. As the creators of a nice dataset, the authors are entitled to specify the terms and conditions under which others may use it. A good "open-data" choice is the Creative Commons Attribution license, which is what the articles published by the EGU/Copernicusjournals use.

However, the authors may wish to specify a different license, such as a non-commercial license (meaning that it can't be sold or used for other commercial purposes), a share-alike license (meaning that any modifications to the data, which are allowed by the Creative Commons licenses, must be redistributed under the same conditions), or various others. There are also more and less restrictive licenses, but these may start to conflict a bit with the release of the data in this journal.

It may sound like a bit of boring lawyer stuff, but it's very important to many of us that deal with others' data regularly. If the authors want the data to be most useful, please explicitly state what the license is, so the potential users can have some clarity about what they can or can't do with it. It's an easy process: just put a 'license.txt' file in the zip with the GIS data.

Similarly, the data will probably see a lot more use if it is easy to get to, and in a place where it's easy for the authors to update. The easiest here is using GitHub (github.com) which has turned into the default small data distribution channel for many, including the GEM Global Active Faults Database. GitHub, or other similar services such as GitLab, provide a great platform for licensing, distributing and updating data, in a way that makes the history of the data transparent to the users by being integrated with a version control system.

Something else to consider is whether the authors would welcome updates or extensions to the mapping (and perhaps parameter estimation). It may be that other users who are interested or have some need for a fault database over a wider area than just that covered in this dataset, and may want to expand along strike. This is the kind of collaborative science that is quite easy to do now, especially with services such as GitHub, but I don't think the academic publication process, and allotment of credit (citationsetc.) has caught up. Nevertheless, if the authors support this (in principle, no need to blindly accept changes) they could write a sentence or two in the manuscript or in a text file with the data describing this.

We recognise the importance of findable, accessible, interoperable, and reusable data (i.e. the FAIR principles), and thank the reviewer for their advice. Indeed, it is these principles that partly guided our decision to submit this study to *Solid Earth*. As the reviewer recommends, when resubmitting the SMAFD and SMSSD, we have been explicit that this is licenced under Creative Commons Attribution ShareAlike (CC-BY-SA 4.0) Licence (in keeping with the GEM Global Fault Active Database).

Publication of code to perform parameter estimation:

I think that by default, any code used in a scientific work should be published with the paper. This would definitely include any code used to perform the parameter estimation (one assumes it wasn't done on a hand calculator). There may be some extenuating circumstances where publication of code isn't a good idea, but this would involve prior intellectual property restrictions or something. I wouldn't consider messy scripts to be exempted here. Detailed inspection of methods and reproducibility is central to the scientific process, and code is perhaps the most perfect form of scientific inquiry thatallows for this. Please publish the code, even if it's a messy script of zip file of them. (Ialso think that EGU/Copernicus asks for this but I could be wrong.)

As outlined above with respect to sharing our GIS file, we appreciate the importance of data that follows the FAIR principle. In this case we will include the excel file where our earthquake source estimates are calculated with our resubmitted file.

Line edits:

Line 5 (and throughout manuscript): Superscripts are formatted as subscripts. This is particularly annoying with exponents.

This was a formatting error when converting the word document to a pdf file, and will of course be corrected in the typeset version of the manuscript

Line 18: All seismically active areas on earth have instrumental records much shorter than the 'repeat times' of the larger earthquake produced in these regions (hundreds to tens of thousands of years).

We recognise that the phrasing of this sentence was not precise, and this has been corrected in the abstract (Line 17-18). However, we also note that tough the reviewer is correct in what they say, we would argue that this problem is particularly acute in low strain rate regions where earthquake recurrence intervals may be ~10,000-100,000 years (i.e. the ~100 year long instrumental record covers 0.1-1% of a fault's seismic cycle). as opposed to 100-1000's of years in high strain rate regions (where the instrumental record covers 10-100% of a fault's seismic cycle). We discuss this further in the revised manuscript at lines 82-84.

Line 56: Actually, active fault databases have been developed for close to all seismically active regions; the GEM Global Active Faults database is referenced elsewhere in the paper, which has global coverage. Some areas (like the EARS) need better mapping and slip rate measurements, but active fault data does exist

We have correct for this in our revised submission (Lines 53-55), but as the reviewer acknowledges, emphasis that though there is global coverage of active fault maps, the mapping in many regions, including Africa is still patchy, and many of the underlying attributes required to use these faults in PSHA is still lacking (Lines 56-58).

Line 79 (and elsewhere): I would be more careful with the suggestions that PSHA based on instrumental seismicity is likely to underestimate seismicity in moderately low strain rate regions. The cited references don't do a good job of backing this assertion up, which is not surprising as many earthquake scientists who are not actively involved in PSHA overestimate their knowledge of it (Stein being a prime offender). The justification that this study will provide better constraints on earthquake rates than PSHA models that incorporate instrumental seismicity (which, when done correctly, is quite capable of dealing with incomplete catalogs) is cringe-inducing in light of the extremely poor constraints on earthquake rates produced in this work.

The reviewer makes excellent points, and we did not wish to assert that instrumental data provide less constraint than our estimates or that corrections cannot be made to incorporate incomplete catalogues in PSHA. We have therefore removed the sentences that discuss whether instrumental seismicity can be reliably used as a PSHA source in low strain rate settings (Lines 79-83 in the original discussion paper).

Instead, we have more specifically related this section to the East African Rift (Lines 92-94), where it is noted more generally that although previous PSHA has typically considered the instrumental record alone (Poggi et al., 2017), prelimary studies by Hodge et al. (2015) suggest that fault source data can improve the assessment of the magnitude and location of future earthquakes. Indeed, it is now becoming increasingly routine for PSHA to consider fault sources (Gerstenberger et al., 2020).

Line 160: The GEM Global Active Faults Database has now been through peer review, and the citation should be changed to Styron, Richard, and Marco Pagani. "The GEM Global Active Faults Database." Earthquake Spectra, Aug. 2020, doi:10.1177/8755293020944182.

We have updated this reference in the revised manuscript (e.g. Line 55).

Line 324: Note that the GEM neotectonics database is part of the GEM Faulted Earth project, which ended around 2015, and is quite distinct from the GEM Global Active Faults Database (Styron and Pagani, 2020). Please more explicitly refer to the earlier neotectonics database as the Faulted Earth database for clarity.

We thank the reviewer for clarifying the distinction between the GEM Faulted Earth Project and the GEM Global Active Faults Database, and in the revised manuscript we have carefully distinguish between these projects (e.g. Lines 53-55).

Line 325: It is worth noting (but not necessarily changing the fault data or the manuscript) that the hierarchy developed by Christophersen et al (2015) as part of the GFE is a bit contentious and has *been abandoned at GEM. The newer Global Active Faults database does not incorporate it, as I decided it was too cumbersome and instead chose a 'flat' system where the 'trace' units in the GFE system would be mapped as a single, continuous trace (in most cases it's somewhat obvious that the traces connect in the bedrock regardless of surface expression, as most faults in these databases have a kilometer or more displacement which can't geologically drop to zero where the traces don't quite join). This simplifies the mapping, drastically reduces the file size of the fault database, and makes for easier hazard modeling as the maximum earthquake can be calculated from the area of a single feature rather than manual joining of multiple features. Many other institutions, such as the USGS, are considering following suit if they have not done so already–the simplicity of the system allows for easier updates and more automated pipelines for incorporating faults into PSHA.*

It is our intention that the fault databases we produce are as consistent with the GEM Global Active Fault database as possible. Therefore, in the revised manuscript we have revised the South Malawi Active Fault Database (SMAFD) data-only GIS file so that each fault is a single continuous GIS 'feature' (Sect. 3.4; though as outlined for our response to Major Comment #1, individual faults can consist of multiple GIS features in the seismogenic source database, SMSSD).

Line 383: The calculations here are another instance of what many would consider to be modeling decisions rather than something incorporated directly into fault databases.

As outlined for Major Comment #1, by more clearly distinguishing between our observations and modelling parameters, we will address this comment. In this case, by placing fault width as a parameter in the data + estimates SMSSD (Sect. 4.1), but not the data-only SMAFD (Table 2, Sect. 4.1)

Line 639: This is not in any way a test of the results. The comparison of very broadly estimated rates with data-based estimates for faults hundreds of kilometers away does not meaningfully indicate the validity of the rate estimates here.

We recognise our use of the term 'test' here was misguided and have removed this term (Lines 594-596). Nevertheless, though these estimates are 100's of km away from southern Malawi, the tectonic setting (i.e. amagmatic continental rift with border faults and intrabasinal faults) and extension rates (1-3 mm/yr; Saria et al., 2014) between these two regions are comparable. Furthermore, we would also argue that when taking a heavily model dependent approach to estimate slip rates and seismic hazard, any 'real-world' constraints that can support our approach, even within an order of magnitude, are useful; it would be worrying, for example, if the intrabasinal faults in northern Malawi had slip rates of <0.01 or >1 mm/yr. Therefore, we still consider this a useful 'comparison.'

Line 651: This is also not a very meaningful comparison. The reasons that the projected date of initiation of the rifting derived from geodetic data (an extrapolation of 1,000,000x) don't match geologic data are manifold to the point where it may not be worth discussing; consider removing this paragraph.

Unlike the comparison above which deals with fault slip rates measured over 75 Ka, we recognise this comparison is much more uncertain and dependent on several poorly constrained parameters. We have removed it in the revised manuscript.

Line 669: Why exactly are only half of the 128 parameter combinations considered in this? How were these 'carefully selected' in a way that is not cherry picking? Computers re pretty fast these days and if this analysis is worth doing (it is interesting it is worth doing with all of the combinations. Surely it wouldn't take more than a few seconds.

As described fully in Appendix A, these combinations are not 'cherry-picked' but selected based on a rigorous statistical analysis (Box et al., 1978; Rabinowitz and Steinberg, 1991) such that they provide comparable results to an exploration of all the parameter space. We have clarified this in the main text of the revised manuscript (Lines 605-609).

Lines 691-730: I don't think these bits of discussion add anything to the paper, and removing them would improve the focus of the paper. The digression about fault growth is interesting but not very relevant. The second paragraph has some sloppy scholarship; the 30-60 km long normal faults here are not at all on the long side of normal faults worldwide, as is clearly evident in the GEM Global Active Faults Database which is cited a few times. The Jackson and White reference is very out of date.

We accept the reviewer's comments that this section (Section 6.1 of the discussion paper) detracts from the main focus of the study, and so will remove it from the resubmitted manuscript. This has also created space for further discussion on incorporating the databases into PSHA (Sect. 6.3), without lengthening the paper.

The paragraph on seismic risk is important but could be tightened up and placed in the introduction, where it is more appropriate. The next paragraph, comparing the lengths of faults in this database to earthquakes also suffers a bit because it compares a small number of global earthquakes to a local fault database, which isn't a good point of comparison (longer normal faults exist in several orogens and generally have similarly slow slip rates, i.e. the Basin and Range in the US).

As requested by the reviewer, in the resubmitted manuscript we have revised a comparison of fault lengths in Malawi to those of other normal faults from the Global Earthquake Model Global Active Fault Database (Styron and Pagani, 2020), as opposed to specifically just normal fault earthquake ruptures (Lines 636-638).

Line 758: This paragraph is troubling. It seems to discourage others from attempting to collect real data to use in PSHA, though there is no reason to think that the rough estimates provided in this work are superior to field measurements.

It was certainly never our intention to discourage the collection of on-fault data to feed into active fault databases. In the revised manuscript, we have emphasised that such data should still be collected (Lines 655-656) and that our approach is most appropriate in places like southern Malawi precisely because there is currently no paleoseismic data (e.g. Line 317). Furthermore, a motivation of this study was to identify where future data collection should be targeted, with the collection of paleoseismic data clearly highlighted, along with tighter geodetic constraints, as a priority area (Sect. 6.2).

Line 798: The probability distributions listed here describe aleatory variability in recurence, but the topic under discussion is epistemic uncertainty. In this case these are not comparable.

We have removed the discussion on these types of probabilities distributions

Reviewer 2

This manuscript presents a new systematic approach useful for parametrizing seismic hazards in areas with limited instrumental seismicity. The study was carried out in the southern part of Malawi, and documents the large faults that are capable of accommodating medium-large magnitude earthquakes in the region, as well as the attributes of these faults that are relevant for the hazard analysis. Also, the study discusses both the seismic hazard and tectonic implications of the results, as well as the uncertainties in the estimates. I believe that this approach is great and useful in active plat boundary settings where there is poor earthquake monitoring infrastructure. Such settings abound in several continents, and seismic instrumentation is expensive; thus, necessitating a need for creative, less expensive approaches as presented in this study. The manuscript is well written and easy to read. I believe that this manuscript contains material fit for publication in EGU Solid Earth.

However, I believe this manuscript could appropriate for publication in the journal after moderate revisions to the paper. I'm recommending moderate revision because of the issues I consider to be major flaws in the interpretation of the tectonic domains and associated structural elements in the study area, which directly impact either the input data or specific features of the implementation of the analysis performed in the study. Here below, are the 7 major issues I have with the manuscript, and 2 comments/questions that I think the authors could consider incorporating into the discussion part of the manuscript. Also, I made comments in different parts of the text that are either minor corrections/comments, or are related to the major issues stated below (see attached an annotated pdf).

Regards, Folarin Kolawole

Major Issues

Major Issue 1: The interchanging use of "southern Malawi" and "southern Malawi Rift". These two terms should not be used interchangeably in this text as it can bring confusion. "Southern Malawi" refers to a geopolitical region that hosts rift segments of different tectonic affiliations; whereas, "Southern Malawi Rift" refers to the southernmost segment of the Malawi Rift which includes only the Makanjita Trough & Malombe Graben (bifurcation around the Shire Horst), and the Zomba Graben. This interchanging use occurs at too many parts of the manuscript, so I decided to just mention it here instead of commenting on it in the text (attached pdf). This issue also leads to and is related to my Major Issue 2…see below.

We acknowledge our interchangeable use of 'southern Malawi' and 'the southern Malawi Rift' will be confusing to readers not familiar with the area, and further adds to the confusion in the various ways that the southern end of the Malawi Rift has been defined previously (Chapola and Kaphwiyo, 1992; Chorowicz and Sorlien, 1992; Ebinger et al., 1987; Laõ-Dávila et al., 2015). In our revised submission, we have carefully outlined that the database covers the geopolitical region of southern Malawi, as opposed to the southern 'Malawi Rift' (albeit with the necessity that it will include some faults that extend into Mozambique, Lines 107-113). This choice also reflects that seismic hazard is typically considered at a national level, and so it makes sense that active fault databases are defined by national, and not geological, boundaries, with the necessary exception that faults that cross geopolitical boundaries are included.

Major Issue 2: Definition of principal grabens of the southern Malawi Rift. The authors identified the graben "Lower Shire Graben" as a principal graben of southern Malawi Rift (pg 19 lines 458-459). I have issue with the characterization of this graben as a tectonic element of the Malawi Rift. This is very misleading as this Lower Shire Graben is a sub-basin in the Shire Rift, not the Malawi Rift (Castaing, 1991). I understand that this graben is located within the Malawi geopolitical boundary, whereas most of the other sections of the Shire Rift are located in Mozambique. However, geopolitical location does not automatically make this graben a part of the Malawi Rift. Moreover, the Shire Rift has a distinctly different structure, orientation, and tectonic history from those of the southern Malawi Rift. Shire Rift is a multiphase rift basin (Mesozoic-Cenozoic; Castaing, 1991), whereas, southern Malawi Rift is Late Cenozoic (e.g., Wedmore et al., 2019; Scholz et al., 2020). Infact, exposed basement highs separate the Zomba Graben (which is at the southernmost tip of the Malawi Rift) from this Lower Shire Graben and the other sections of the Shire Rift. Therefore, in order not to confuse a reader, I'll suggest that the authors use the term "southern Malawi" in the context of describing the location of the 'Lower Shire graben' (i.e. use geographical description), rather than the term "southern Malawi Rift".

As discussed above with reference to Major Issue 1, by explicitly outlining that the South Malawi Active Fault Database (SMAFD) and the South Malawi Seismogenic Source Database (SMSSD) cover the political region of southern Malawi, not the southern 'Malawi Rift,' we have addressed this comment (Lines 107-113).

Major Issue 3: The descriptions of the "Makanjira Graben" in the manuscript and the modelling done in Fig.A3a shows that the authors consider that term to incorporate both the Makanjira Trough and Malombe Graben. The Malawi Rift bifurcates around the Shire Horst into these two segments and further south, they link-up and transition into the Zomba Graben. The Makanjira Trough is bounded to the west by Chirobwe-Ncheu Fault, and to the East by Shire Horst, whereas the Malombe Graben is bounded to the west by the Malombe Fault and to the east by the Mwanjage Fault. The surface+subsurface structure of this section of the Malawi Rift (Lao-Davila et al., 2015) shows that the Malombe Graben has a greater hanging wall subsidence and thus, border fault offset than the Makanjira Trough. Here are the evidences:

1.) *The floor of the Makanjira trough is mostly dominated by exposed basement, whereas, the Malombe Graben is relatively better developed graben structure with a wider-spread sediment accumulation and even a lake development at the foot of its border fault. The zone of sediment accumulation on the northern half of the Makanjira trough is associated with subsidence along the southern extension of the N-S trending eastern border fault of the Nkhotakota Segment of the Malawi Rift (for location of Nkhotakota Segment see Lao-Davila et al., 2015; for the described subsidence and fault location, see Fig.5b of Scholz et al., 2020).*

2.) *The floor of the Makanjira half-graben is at a higher elevation compared to that of the Malombe Graben, indicating that subsidence is most-likely greater in the Malombe Graben. For reference see the across-rift profiles in Figs.4L-4M of Lao-Davila et al. (2015). I am guessing that the authors consider that because the Chirobwe-Nchue Fault has a higher footwall elevation/escarpment along the rift section, therefore, it must have the largest throw. If that is the consideration upon which the border fault definition and Fig.A3a model are based, I refer the authors to the Rukwa Rift where border fault footwall elevation/uplift is not representative of the subsurface fault throw (Morley et al., 1999). Thus, based on the* *observed geologic structure, I think the model in Fig.A3a is problematic because it ignores the presence of the fault with the larger offset and hanging wall subsidence at the so-called "Makanjira Graben". Also, the model assumes the Chirobwe-Ncheu to has the greatest offset/hanging wall subsidence along the profile which is not representative of the distribution of subsidence across this section of the rift (Figs. 4L-4M in Lao-Davila et al., 2015). Therefore, in my opinion, if possible, I think this model needs to be revised. If impossible due to modelling limitations, then it should be stated.*

We firstly recognise that the hanging-wall flexural modelling in a discussion manuscript was based on several large assumptions and have removed this from the revised manuscript. Nevertheless, the point remains due to thick elastic crust, and comparatively small border fault throws (<1000 m), the amount of hanging-wall flexural extensional strain in southern Malawi is negligible (Lines 426-429; Wedmore et al., 2020a)

We address the reviewer's concerns on how we define border faults and intrabasinal faults further below (Major Issue #4). In the context of the Malombe Fault, as the reviewer correctly points out, the Shire Horst divides the rift section that we term the Makanjira Graben. However, though this structure may have been important in the tectonic evolution of the rift (Laõ-Dávila et al., 2015), for the reasons outlined below we do not consider that it strongly influences the current distribution of extensional strain in the Makanjira Graben.

With respect to the reviewer's first set of concerns, we disagree that the 'Makanjira trough' is dominated by exposed basement with any sediment accumulation necessarily related to subsidence along the Nkhotakota rift segment: (1) geological maps and boreholes indicate that sediments have not just accumulated along the northern half of the Makanjira trough, but along its entire length (Dawson and Kirkpatrick, 1968; Walshaw, 1965; Fig. 1b of our discussion paper) and including to the south of the Nkhotakota fault as mapped by Scholz et al., (2020), (2) there is geomorphic evidence of recent multiple earthquakes along the Bilila-Mtakataka Fault (BMF; Hodge et al., 2018, 2019, 2020; Jackson and Blenkinsop, 1997), indicating that this is a highly active part of the rift capable of creating accommodation space for sediment accumulation, (3) boreholes indicate that these sediments in this section of the rift thicken to the west against the BMF (Dawson and Kirkpatrick, 1968; Walshaw, 1965), indicating that it is the BMF not the Nkhotakota fault that is primarily generating accommodation space, and (4), where there is exposed basement in the hanging-wall of the Chirobwe-Ncheu fault, this can be related to footwall uplift of the interior BMF (Lines 231-235).

With respect to the reviewer's second concerns, the higher elevation of the Makanjira trough relative to the Malombe trough does not require that these should be separated as distinct basins. There are other (albeit smaller) horst structures and basement highs that the Malawi Rift bifurcates around in the Central and North Basins of Lake Malawi (Ebinger et al., 1987; Scholz et al., 2020; Shillington et al., 2020). These also result in complex across-rift topography; however, they have not necessitated the division of the rift across strike. We suggest too that the formation of Lake Malombe does not require that the Malombe Fault has accommodated considerable throw as: (1) it only extends across the northern section of the fault and (2) it has a maximum depth of 5 m (Weyl et al., 2004). Indeed, this part of the rift has very little variation in subsidence with the Shire River experiencing only a 1.5 m drop in elevation in the 85 km distance between Mangochi and Liwonde; (Dulanya, 2017).

We agree with the reviewer that ideally subsurface data should be used to characterise the structure of the Malawi Rift. However, south of Lake Malawi, such data are scarce, and in their absence, we prefer to use the data we *do* have from the rift's topography and basement-penetrating boreholes to characterise its structure (Fig. S1; Bloomfield, 1965; Bloomfield and Garson, 1965; Walshaw, 1965). Cumulatively, we suggest that these observations indicate that the Malombe Fault should be considered as an intrabasinal fault (see Major Issue #4), albeit it could be one with considerable displacement (>500 m).

In this context, it could be considered similar to some of the high displacement horst-forming intrabasinal faults (up to 2.5 km throw) in Lake Malawi (Scholz et al., 2020; Shillington et al., 2020).

To further demonstrate how we have used topography and borehole data to characterise the rift's structure, in the revised manuscript we have included across-rift cross sections for each basin in southern Malawi (Fig. 8). For the Makanjira Graben cross section, as highlighted by the reviewer, we have also noted the Shire Horst structure and the lower elevation in the eastern side of the graben, as these structures were not described in sufficient detail in the discussion paper (Lines 524_426). Also note that Figure 4L-M in Lao-Davila et al. 2015 would not be a good reference for such a figure, as although they suggest a ~500 m thick sequence of sediments in the Malombe Trough, it is not clear what evidence they have for this assertion.

Major Issue 4: Age of the Thyolo Fault and modelling of strain in Lower Shire graben (Fig. A3c and pg 37 lines 895-896, pg 38 lines914-915). The authors suggest that the Thyolo Fault is Karoo age. There is no evidence suggesting that there exists karoo-agesedimentary or volcaniclastic deposits on the hanging wall of the Thyolo Fault (Habgood, 1963; Habgood et al., 1973). Mesozoic activity along the Thyolo Fault would require subsidence of its hanging wall and creation of accommodation space for the deposition of volcanic and sedimentary sequences. Both Habgood (1963) and Castaing (1991) suggested that the Mwanza-Namalmbo Fault system is the eastern border fault of the Mesozoic Shire Rift. Castaing (1991) suggested that the Thyolo Fault is Cenozoic, bounding the currently active eastern domain of the Shire Rift. Therefore, I think this idea of Thyolo Fault being a Karoo fault needs to be revised except the authors provide data showing the presence of Mesozoic deposits on the hanging wall of the Thyolo Fault.

As discussed for Major Issue #3, we have removed the hanging-wall flexure modelling in the revised manuscript. Therefore, there are no parts in this manuscript that explicitly discuss the age of the Thyolo Fault, nor is this study an appropriate place to do so. The key point is that it is active.

Major Issue 5: Definition of "border fault" in southern Malawi (Fig. 2a). The Lisungwe Fault, Malombe Fault, and Mwanza Faults are excluded from the 'border fault' definition and I am not particularly sure why. This is an issue for me, particularly because the structure of the basins point directly to the essence of these faults. For example, the Malombe Fault is the principal border fault of the Malombe Graben, not the Mwanjage Fault which you've assigned as the main border fault. Even the distribution of the amplitudes and wavelengths of the magnetic fabrics beneath the Malombe Graben in Fig.2c (Laõ-Dávila et al., 2015) clearly shows that the hanging wall of the Malombe Fault has significantly larger subsidence than that of the Mwanjage Fault. Also, the Mwanza Fault is a major border fault of the NW half of the Shire Rift (as shown in the maps in Figure 2). There is also evidence that the exposed segment of the Mwanza fault has been reactivated in the Cenozoic given by accumulation of Quaternary sediments on its hanging-wall (Habgood 1963).

We thank the reviewer for bringing these points to our attention, and for demonstrating that the classification of border faults and intrabasinal faults is not always as clear-cut as the manuscript suggests in its current form. In the resubmitted manuscript, we have included a section where we more explicitly define the difference in border and intrabasinal faults, and how this was applied to southern Malawi (including the use of geological cross sections as outlined for Major Comment #3). We define border faults using the simplest geometric criteria: the fault at the edge of the rift's surface expression (Lines 399-403). In other words, this definition is purely based on the geometry and distribution of brittle deformation across the rift. This definition is not inconsistent with differences between border and intrabasinal faults noted in previous studies (e.g. cumulative offset, slip rate, length; Agostini et al., 2011; Ebinger, 1989; Gawthorpe and Leeder, 2000; Muirhead et al., 2019; Wedmore et al., 2020b), but equally this definition is not dependent on these factors.

To specifically reply to the reviewer's comments on individual faults: the justification for not including the Malombe Fault as a border fault is discussed in Major Comment #3. With regards to the Mwanza Fault, we agree that it has been active during the East African Rifting, hence its inclusion in the SMAFD. Nevertheless, on the basis of the reviewer's comments and more recent mapping by Daly et al.,(2020) that suggests this part of the rift may extend further into Mozambique and the Lower Zambezi Rift where it forms a different microplate boundary (Angoni-San), we now consider the Mwanza Fault as the border fault of a different rift section to the Lower Shire Graben (Lines 140, 547, and Fig. 8e). Unfortunately, in this case there are no geodetic constraints on the extension rate across the Zambezi Rift. In this case, we have calculated fault slip rates using values of between 0.2-1 mm/yr (Table 3, Lines 455-458), where the lower estimate represents the minimum strain accrual measurable by geodesy (Calais et al., 2016) and the upper estimate represents that extension rates in the Zambezi Rift are unlikely to be higher than in the Lower Shire Graben given that the Mwanza Fault has only accumulated EAR sediments along its south-eastern most extent (Habgood, 1963).

The topography at the western edge of the Zomba Graben, where it grades into the Kirk Plateau, is very complex and so it is difficult to fit the Zomba Graben into conventional half-graben/graben models (Wedmore et al., 2020a). In particular, there are a number of N-S trending deeply incised valleys that lie to the west of the Lisungwe Fault and which have been previously interpreted as 'rift valley faults' (Bloomfield and Garson, 1965, see Figure 1 below). In addition, there are a number ENE-WSW trending valleys that are interpreted as 'cross faults' (i.e. strike-slip) faults (Bloomfield and Garson, 1965). Though only one of these faults (the Wamkurumadzi Fault) meet our definition of being active and is included in the SMAFD (section 3.1 of the discussion paper), inclusion of this fault, and the generally complex topography, requires that the Lisungwe Fault does not meet the definition of the border fault as outlined above. In the revised manuscript, we have more carefully outline how we have come to this decision and hope that this study will stimulate further studies into the question of fault activity at the western edge of the Zomba Graben (Lines 528-539, Fig. 8b).

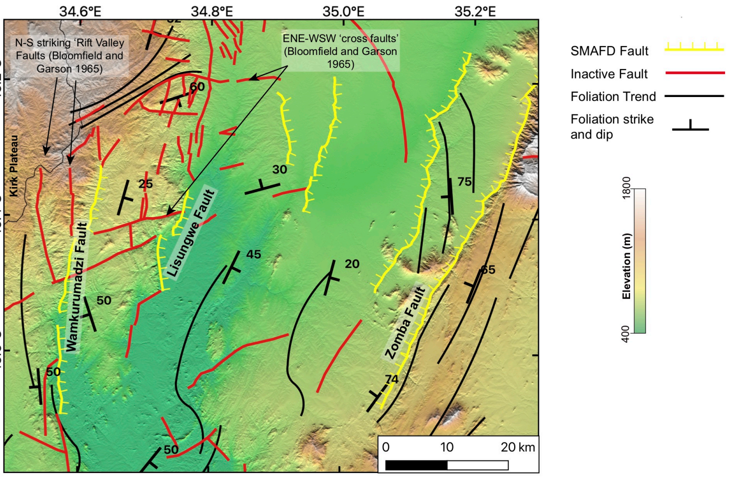

Figure 1: Fault map for Zomba Graben underlain by TanDEM-X 12 m resolution digital elevation model. 'Inactive faults' as mapped by Bloomfield and Garson, (1965). TanDEM-X data was obtained via DLR proposal DEM_GEOL0686.

Major Issue 6: Related to "Issue 4" above, the authors classified Namalambo Fault as an active Fault (e.g., Figs. 1b & 2). Namalambo Fault cannot be classified as an East African Rift System Fault because there is no evidence supporting its Cenozoic reactivation (see Bloomfield, 1958; Habgood, 1963; Castaing, 1991). The mentioned geological reports specifically stated that there is no Quaternary sediment deposition on top of the karoo sedimentary units at the base of its scarp, suggesting it has not been reactivated in the Cenozoic. Also, this fault does not satisfy the criteria stated by the author in Pg11 lines 260-267. Are the authors including it because they're assuming that it could be reactivated sometime in the future? If yes, I think this should be stated in the relevant figure captions and in the manuscript (particularly because this fault is a prominent fault in the area, and could be confusing to a reader without this additional information).

Although we noted in the database that the Namlambo Fault formed during Karoo-age rifting, we accept the reviewers comments that there is very little evidence for its reactivation during East African Rifting, and so in the resubmitted manuscript we have removed this fault from the SMAFD and include it in the 'Malawi OtherFault' database instead.

Major Issue 7 (minor): A 'declaration' that I think is not clearly made in the set-up of the premise of the manuscript is that the parameterization approach focuses on tectonically active continental settings. I do not think that the authors imply that the approach is applicable to relatively more stable intraplate settings where much lower strain rates generally abound and potentially dangerous faults are buried, although some of those areas could be seismically active (e.g., intraplate induced seismicity). Therefore, I'll suggest that the authors state this clearly, at least in the abstract and introduction sections of the paper. I noticed that in different parts of the text, it is subtly implied with phrases relating to plate boundary, interplate setting etc., however, I think it will be beneficial to the reader if this is stated clearer from the onset.

The reviewer is correct that the approach outlined for characterising seismic hazard is most applicable to low strain rate regions (plate boundary slip rates 0.1-10 mm/yr; Scholz et al 1986), which are distinct from both high strain rate regions (plate boundary slip rates >10 mm/yr) *and* stable cratons (plate boundary slip rates <0.1 mm/yr). We have stated this in the revised manuscript (Lines 84-85).

Question/Comment 1: Pg29 lines 703-707. The authors highlighted the anomalously large seismogenic thickness of the southern Malawi area, with continuous 30-60 km long fault sections. Crustal thickness map of southern Malawi (Njinju et al., 2019a) shows that an unusually thick crust dominates the area. In addition, heat flow map of the same area (Njinju et al., 2019b) shows an anomalous thermal gap in the area. Both of these have been associated it with an eastern extension of the Niassa Craton. Do you think that there is a possibility that these have an impact on the observed seismogenic thickness?

The contribution of low heat flow to the anomalously thick seismogenic crust in southern Malawi is acknowledged (Line 165), however, we thank the reviewer for the suggested reference, which we have included in the revised manuscript. It is also worth noting that Fagereng, (2013) demonstrated that an anomalously low heat flow alone (63 mW/m^{-2}) is not sufficient to explain the thick seismogenic crust in this region, with other factors such as strain rate and crustal composition also important. Furthermore, the seismogenic crust is unusually thick throughout Malawi (>30 km), even in places where the heat flow is higher (e.g. 65-70 mW/m^{-2} in Karonga; Ebinger et al 2019).

Question/Comment 2: It is well-known that the patterns of seismogenic fault reactivation are influenced by the frictional stability of faults. Asides from strain rate and lithology/mineralogical composition, another important factor that influence the frictional stability is geothermal gradient/heat flow. Well-constrained heat flow & geothermal gradient maps of southern Malawi (Njinju et al., 2019b) show interesting thermal anomalies within the areas analyzed in this study. I am curious as to how the heat flow distribution in the area may affect the results/conclusions of this study.

Although the reviewer raises an interesting point, as noted above there are other factors beyond heat flow that will control fault reactivation in this region. We consider that to discuss them all will go beyond the scope of this study, which is focussed on active faulting, not crustal rheology. Furthermore, classic Mohr-Coulomb theory suggests that brittle fault reactivation is temperature independent (Sibson 1985), although it will partially influence thickness of the seismogenic crust (as discussed above).

Comments on Reviewer Supplement

Line 31: This sentence, as it is written here, implies circular logic. This is because measurements of fault length is one of the inputs into your model estimates of EQ magnitude. How about "These potentially high magnitudes for continental normal faults are compartible with the observed 11-140 km-long faults and thick (30-35 km) seismogenic crust of southern Malawi."

We have removed this sentence from the abstract

Line 61: The repetition of "estimate" sound awkward...could reword as "fault slip rates can be estimated using geodetic constraints"?

We will correct this in the revised manuscript to geodetic 'data' (Line 86)

Line 87: I suggest a rewording of this text. Southern Malawi lies NEAR the southern incipient end of the EARS, not "AT" the end.
Rather, it is Central/Southern Mozambique that lies AT the southern incipient end of the EARS and has all those characteristics you've mentioned...see papers on the MOZART project (e.g., Fonseca et al. (2014), Urema Graben, Mazenga Graben, Chissenga-Urema Graben System, and the Changani Graben System (Mueller & Jokat, 2019).

We have corrected this in the revised manuscript and outline that southern Malawi lies *near* and/or *towards* the southern end of the EARS (e.g. Line 116).

Line 112: I think the authors should include the Salambidwe Igneous structure (Cooper, 1961) and the flood basalts associated with the Lupata Volcanic Complex (footwall and hanging wall of the Panga Fault; Habgood, 1963).
We thank the reviewer for noting these omissions. However, we have removed the section so this sentence was not included in from the revised manuscript.

Line 123: By definition, can a graben can be bounded by 1 border fault? I suggest need rewording

We have replaced 'graben' with 'basin' and/or 'half-graben' in the revised manuscript where appropriate (e.g. Line 398)

Lines 136-144: This paragraph is written with a mixed context that could create confusion...i.e. written with a context of a political territory (i.e. southern Malawi) and a rift basin (Malawi Rift). I will say this is very 'dangerous' as it propogates a very common problem with the way geology has been carried out in Africa for a very long time. Therefore, I will suggest that the authors stick to "Malawi Rift" since this study and this particular paragraph focuses more on tectonic history.

On the aspect of the evolution of the Malawi Rift, I will refer the author to Scholz et al. (2020) which demonstrates clearly the southward episodic propagation of the Malawi Rift. In addition, studies have showed that Karoo sandstones outcrop along the Karonga border fault of the Karonga Basin, and Accardo et al. 2018 observed an anomalous velocity interval that suggests highly lithified Karoo sedimentary rocks directly overlying the basement beneath the Karonga and Usisya Basin fill.

As outlined for Major Issue #1 we have more carefully defined the term 'Malawi Rift' in our revised manuscript and note that the databases cover the political region of southern Malawi, not the Malawi Rift (Lines 107-113). We have also incorporated the Scholz et al (2020) reference into the revised manuscript, however, note that this study provides age constraints for the southern end of Lake Malawi, not southern Malawi itself (Lines 122-124).

Lines 146-150: The inferences made in this section, as written, sounds highly speculative, and since it is placed in the "geologic setting" section, I will suggest rewording. First, the text totally ignores the Malombe Graben as the primary hydrologic linkage between the Lake Malawi and the Zomba Graben (i.e. hosts the axial stream). Second, the text implies that sedimentation in the grabens referred to are only associated with flooding episodes. This is very strange to me. The area described is defined by the southward bifurcation of the Malawi Rift into two narrower branches: a graben in the east (Malombe Graben), another graben to the west (Makanjira Graben). The Malombe Graben has a well-developed lake from which the axial stream Shire River flows southwards. South of the bifurcation, the two branches merge back into a weakly-extended graben (Zomba Graben) south of which the basement is exposed and faulting is diffused. The point here is than the bifurcation troughs are actively subsiding, fault-bounded tectonic elements with structurally-controlled axial (Shire River) and transverse streams (from the rift flanks) channelling sediments into the subsiding basins. Thus, it is more likely that both faulting and climate control sedimentation within these basins, and not 'only climate' (as it is described here). For general reference on interactions between faulting and climate in humid rift settings, I refer the authors to Gawthorpe & Leeder (2000).

In the revised manuscript we have noted that faulting in the rift will have influenced sedimentation (Lines 211-214). Nevertheless, it should be noted that base level changes in Lake Malawi are thought to be primarily driven by climatic forcing (e.g. Scholz et al 2007; Lyons et al 2015).

Lines 151-152: What does this sentence mean? ...you mean the steep gradient of the rift floor does not correspond to a fault escarpment? As this sentence is written, it precludes every form of structural control on the gradient...and I am highlighting this because this particular zone is a transfer zone between the Malawi Rift and the currently active part of the Shire Rift. Transfer zones in areas of incipient rifting are typically characterized by elevated/exposed basement...for reference, see Heilman et al. (2019) and Gawthorpe & Leeder (2000).

This sentence refers to the point that no active faults were identified in the region between the Zomba and Lower Shire Graben from fieldwork and analysis of high resolution digital elevation models (although we of course cannot exclusively prove that there are no active faults in this region). We have clarified this in the resubmitted manuscript (Lines 541-543). Note too that this sentence does not preclude that this gradient may reflect pre-existing topography from previous phases of deformation (e.g. Karoo).

Lines 157-158: First, I think it should also be added that the Castaing (1991) mapping was infact, only limited to the Shire Rift part of southern Malawi...the mapped faults in the paper did not extend into Southern Malawi Rift.

Second, I have seen a lot of these faults mapped previously in the Malawi Geological Survey reports (e.g., Bloomfield, 1958; Habgood, 1963; Habgood et al., 1973)... some of which were cited in this manuscript. I could see that the authors mentioned some of these faults on pg 12, however, I think the contributions should also be acknowledged here.

We will make it clearer in the revised manuscript that Castiang (1991) only considered EARS faults in the Lower Shire (Line 143-144). With respect to the second point, we now also discuss the Malawi Geological Survey Reports in this section (Lines 146-150), though note that fault traces mapped in these reports were not included in the Global Earthquake Model global active fault database (Christophersen et al., 2015; Styron and Pagani, 2020).

Line 161: The mapping in the Geological Survey reports looks pretty fine-scale to me because they were done on the field. I think the detailed info on slip rates and recent faulting are the parts that are missing which this current study provide.

We are referring here specifically to the Global Earthquake Model global active fault database here (Fig. 2a; Christophersen et al., 2015; Styron and Pagani, 2020), which do not incorporate the faults mapped by the Malawi Geological Survey, but those mapped by Macgregor, (2015). We have clarified this in the revised manuscript (Line 146)

Line 178-179: This sentence sounds weird with the "to 1965". Pls check

We will revise this sentence in the resubmitted manuscript as requested (Line 161).

Lines 181-188: Wondering if it will also be worth mentioning the crustal thickness in southern Malawi (Njinju et al., 2019a; Tectonics), and heat flow distribution in southern Malawi (Njinju et al., 2019b; J. Volc. & Geoth. Res.)

Njinju, E.A., Atekwana, E.A., Stamps, D.S., Abdelsalam, M.G., Atekwana, E.A., Mickus, K.L., Fishwick, S., Kolawole, F., Rajaonarison, T.A. and Nyalugwe, V.N. (2019a). Lithospheric structure of the Malawi Rift: Implications for magma-poor rifting processes. Tectonics, 38(11), pp.3835-3853.

Njinju, E.A., Kolawole, F., Atekwana, E.A., Stamps, D.S., Atekwana, E.A., Abdelsalam, M.G. and Mickus, K.L. (2019b). Terrestrial heat flow in the Malawi Rifted Zone, East Africa: Implications for tectono-thermal inheritance in continental rift basins. Journal of Volcanology and Geothermal Research, 387, p.106656.

As outlined for Question/Comment 1 we have incorporate these references into the revised manuscript (Line 167).

Lines 202-203: True. However, another possibility that could be mentioned here is local stress rotations (see Morley, 2010...case study on the Rukwa Rift).

As discussed in Williams et al., (2019) stress rotations do not explain the discrepancy in extension direction when inferred from geodesy or earthquake focal mechanisms in southern Malawi, as the orientation of recent joint sets in the region is uniform across the rift suggesting that the regional stress field is uniform. Furthermore, the hypothesis of Morley, (2010) is that that stress rotations reflect changes in foliation orientation, in which case it would not account faults locally cross cutting the foliation in southern Malawi.

Line 237: also depth of medium-large magnitude EQ ruptures?

We have included focal depth as a factor of whether an earthquake ruptures to the surface in the revised manuscript (Line 203)

Line 250: "little" sounds awkward here, because how little is "little"? I'll suggest "limited" instead

We have clarified this in the revised manuscript (Lines 218-220), and note that there is some limited dating from <10 ka sediments around Lake Malombe (Van Bocxlaer et al., 2012).

Lines 458-459: See comments in 'major issues'.

See reply to comment on Major Issue 3

Lines 464-464: Isn't this graben is known as the Urema Graben/Rift (Castaing, 1991; Fonseca etal. 2014; Lloyed et al., 2019). Why give it a different name?

Castaing, C. (1991), Post-Pan-African tectonic evolution of South Malawi in relation to the Karroo and recent East African rift systems. Tectonophysics, 191(1-2), pp.55-73.

Fonseca, J.F.B.D., Chamussa, J., Domingues, A., Helffrich, G., Antunes, E., van Aswegen, G., Pinto, L.V., Custódio, S. and Manhiça, V.J., 2014. MOZART: A seismological investigation of the East African Rift in central Mozambique. Seismological Research Letters, 85(1), pp.108-116.

Lloyd, R., Biggs, J. and Copley, A., 2019. The decade-long Machaze–Zinave aftershock sequence in the slowly straining Mozambique Rift. Geophysical Journal International, 217(1), pp.504-531.

As for the Malawi Rift, there is little consensus on the extent of the Urema Graben (see also, Steinbruch, (2010) which suggest it refers to mainly the basins around the river Urema 150 km along strike to the south). Our preference here is to avoid using this term as it may imply that our fault mapping covers the full extent of the Urema Graben, and this will be clarified in the revised manuscript (Line 138).

Lines 473-474: Does this estimate include subsurface measurement of the total throw at the hanging wall cut-off of the faults? Please, provide reference. Also, based on the wording, does this refer to southern Malawi Rift (excluding the 'Lower Shire Graben') or does it refer to all the faults in southern Malawi geopolitical boundary?
Yes, this estimate includes the limited subsurface data that does exist in southern Malawi (i.e. groundwater boreholes, Fig. S1; Bloomfield, 1965; Bloomfield and Garson, 1965; King and Dawson, 1976; Walshaw, 1965), and we have clarified this in the revised manuscript (Lines426-428).

Lines 687-689: For the sake of the reader, I think the hazard part should be stated before implications for continental rift as seismic hazard is the primary focus of this study. Thus, I'll

suggest a rewording to: "In the following section, we examine some key results of the SMAFD in terms of its implications for seismic hazard in southern Malawi, its contribution to our understanding of fault growth in continental rifts, and future strategies to...".
As discussed with respect to the comments for Lines 690-711 from Reviewer #1, we will be removing this section on 'controls on fault growth in southern Malawi' in the revised manuscript.

Line691: This relates to my comment above... While this section is important and relevant, for the reader, it seems like a sudden digression from the seismic hazard story to bring it in at this early part of the discussion. Pls consider swaping it with '6.2 Implications for seismic hazard in southern Malawi'.
See our reply to the previous comment.

Line 694: Could also include Scholz et al. (2020)

Scholz, C.A., Shillington, D.J., Wright, L.J., Accardo, N., Gaherty, J.B. and Chindandali, P., 2020. Intrarift fault fabric, segmentation, and basin evolution of the Lake Malawi (Nyasa) Rift, East Africa. Geosphere.

We thank the reviewer for bringing this article to our attention and have incorporated it into the revised manuscript e.g. Line 124).

Line 843: growth,

Corrected (Line 717)

Line 895-896: This statement, as written, is misleading. Please revise. Castaing (1991) argued that the Thyolo Fault is Cenozoic and along with the reactivated Mwanza Fault, is accommodating strike-slip in present day. He suggested that the Mwanza Fault was the primary eastern Karoo and Cretaceous border fault of the Shire Rift. See pages 65-66 and figs. 7,9,&10 of Castaing et al. (1999).

As discussed for Major Issue #3, we have removed the hanging-wall flexural modelling from our revised manuscript, so this sentence was removed anyway.

Lines 897-899: This statement, as written, is speculative. As I explained in my "Major issues 1 & 2", the Shire Rift is a multiphase rift of which the Lower Shire graben is the easternmost sub-basin. The Malawi Rift and Shire Rift have different tectonic histories and structure, and only linked up at the current location of southern Zomba Graben. Although the development of the Lower Shire graben could be syn-tectonic with the southward propagation of the Malawi Rift, the pre-rift and early-phase structures in the Shire Rift (which are absent in the Zomba and Makanjira grabens) could greatly impact the strain in the Lower-Shire Graben...e.g., consider the influence of the mechanical load of the thick sequences of volcanic flows in the hanging wall of the Panga Fault and buried Mwanza Fault (all beneath a part of the Lower-Shire graben), which could impact the throw on the Thyolo Fault. Thus, in the absence of actual subsurface data on Thyolo fault throw, I think it is speculative to make a statement like this. I understand that there is a need to assume a maximum throw limit for the modelling, thus, I'll suggest that the authors revise this sentence by stating that the estimate is an assumption.

As also discussed for Major Issue #3, we have removed the hanging-wall flexural modelling from our revised manuscript, so this section was removed anyway. In the revised manuscript, we make no reference to the total throw across the Thyolo Fault.

Lines 900-901: See my comments in "Major Issue 3" related to the structure of this rift segment as implemented in the model.

Again, by removing the hanging-wall flexure modelling section, this sentence is not included in the revised manuscript.

Line 909: The lower Shire graben is no more than 38-40 km wide (at its widest). I'm curious to know how the extent of this basin is estimated?

Again, by removing the hanging-wall flexure modelling section, this section is not included in the revised manuscript.

Line 914-915: This statement assumes that the Thyolo Fault is a Karoo-age border fault, which I think is problematic considering the observations in Castaing (1991). See "Major Issue 4".

See our reply to Major Issue #4

Line 1620/Figure 1b: For figure 1b: It will be very helpful if you can add symbols or number the colored polygons of the different terranes shown. The colored polygons are faded into the grey scale hillshade map which makes the color slightly different from the ones shown in the legend....by adding symbols or numbering, it makes it easier for the reader to identify where what terrane is.

As suggested, we have added text labels for the terranes in the revised manuscript

Line 1621/Figure 1a: I'll suggest that you include the Aswa Shear Zone to this map as it is one of the most well-known lithospheric-scale shear zones in East Africa (see Daly et al., 1989; Ruotoistenmäki et al., 2014; Katumwehe et al., 2016; Saalmann et al., 2016). Other ones you could also include are the Lurio Shear Zone and the Sanangoe Shear Zone.

For clarity, we no longer include major shear zones in this figure.

Line 1639/Figure 2c: You might want to check the N-striking (80deg-dip) foliation anotated on the Namalambo Fault in Fig2c. The foliation trends in the Nsanje horst are NE-trending. The Namalambo Fault cuts the foliation. For reference, see "Structual Map of the Northern PortHerald Hills" in Bloomfield (1958).

As suggested by the reviewer, we will remove this strike and dip measurements to reflect the regional NE-striking fabrics in the Nsanje Horst (albeit with local variations).

Line 1732/Figure A3: The orientation of the Zomba and Lower Shire profiles should also be stated in this caption.

By removing the hanging-wall flexure modelling from the revised manuscript, this figure is not included anyway.

Line 1736/Figure A3: You mean WSW-ENE?

By removing the hanging-wall flexure modelling from the revised manuscript, this figure is not included anyway.

References

- Agostini, A., Bonini, M., Corti, G., Sani, F. and Manetti, P.: Distribution of Quaternary deformation in the central Main Ethiopian Rift, East Africa, Tectonics, 30(4), doi:10.1029/2010TC002833, 2011.
- Basili, R., Valensise, G., Vannoli, P., Burrato, P., Fracassi, U., Mariano, S., Tiberti, M. M. and Boschi, E.: The Database of Individual Seismogenic Sources (DISS), version 3: Summarizing 20 years of research on Italy's earthquake geology, Tectonophysics, 453(1–4), 20–43, doi:10.1016/j.tecto.2007.04.014, 2008.
- Bloomfield, K.: The Geology of the Zomba Area, Bull. Geol. Surv. Malawi, 16, 1965.
- Bloomfield, K. and Garson, M. S.: The Geology of the Kirk Range-Lisungwe Valley Area, Bull. Geol. Surv. Malawi, 17, 1965.
- Van Bocxlaer, B., Salenbien, W., Praet, N. and Verniers, J.: Stratigraphy and paleoenvironments of the early to middle Holocene Chipalamawamba Beds (Malawi Basin, Africa), Biogeosciences, 9(11), 4497–4512, doi:10.5194/bg-9-4497-2012, 2012.
- Box, G. E. P., Hunter, W. G. and Hunter, J. S.: Statistics for experimenters, John Wiley and sons New York., 1978.
- Calais, E., Camelbeeck, T., Stein, S., Liu, M. and Craig, T. J.: A new paradigm for large earthquakes in stable continental plate interiors, Geophys. Res. Lett., 43(20), 10,621-10,637, doi:10.1002/2016GL070815, 2016.
- Castaing, C.: Post-Pan-African tectonic evolution of South Malawi in relation to the Karroo and recent East African rift systems, Tectonophysics, 191(1–2), 55–73, doi:10.1016/0040-1951(91)90232-H, 1991.
- Chapola, L. S. and Kaphwiyo, C. E.: The Malawi rift: Geology, tectonics and seismicity, Tectonophysics, 209(1–4), 159–164, doi:10.1016/0040-1951(92)90017-Z, 1992.
- Chorowicz, J. and Sorlien, C.: Oblique extensional tectonics in the Malawi Rift, Africa, Geol. Soc. Am. Bull., 104(8), 1015–1023, doi:10.1130/0016-7606(1992)104<1015:OETITM>2.3.CO;2, 1992.
- Christophersen, A., Litchfield, N., Berryman, K., Thomas, R., Basili, R., Wallace, L., Ries, W., Hayes, G. P., Haller, K. M., Yoshioka, T., Koehler, R. D., Clark, D., Wolfson-Schwehr, M., Boettcher, M. S., Villamor, P., Horspool, N., Ornthammarath, T., Zuñiga, R., Langridge, R. M., Stirling, M. W., Goded, T., Costa, C. and Yeats, R.: Development of the Global Earthquake Model's neotectonic fault database, Nat. Hazards, 79(1), 111–135, doi:10.1007/s11069-015-1831-6, 2015.
- Daly, M. C., Green, P., Watts, A. B., Davies, O., Chibesakunda, F. and Walker, R.: Tectonics and Landscape of the Central African Plateau and their Implications for a Propagating Southwestern Rift in Africa, Geochemistry, Geophys. Geosystems, 21(6), doi:10.1029/2019GC008746, 2020.
- Dawson, A. L. and Kirkpatrick, I. M.: The geology of the Cape Maclear peninsula and Lower Bwanje valley, Bull. Geol. Surv. Malawi, 28, 1968.
- Dulanya, Z.: A review of the geomorphotectonic evolution of the south Malawi rift, J. African Earth Sci., 129, 728–738, doi:10.1016/j.jafrearsci.2017.02.016, 2017.
- Ebinger, C. J.: Tectonic development of the western branch of the East African rift system, Geol. Soc. Am. Bull., 101(7), 885–903, doi:10.1130/0016-

7606(1989)101<0885:TDOTWB>2.3.CO;2, 1989.

- Ebinger, C. J., Rosendahl, B. R. and Reynolds, D. J.: Tectonic model of the Malaŵi rift, Africa, Tectonophysics, 141(1–3), 215–235, doi:10.1016/0040-1951(87)90187-9, 1987.
- Fagereng, Å.: Fault segmentation, deep rift earthquakes and crustal rheology: Insights from the 2009 Karonga sequence and seismicity in the Rukwa-Malawi rift zone, Tectonophysics, 601, 216–225, doi:10.1016/j.tecto.2013.05.012, 2013.
- Field, E. H., Arrowsmith, R. J., Biasi, G. P., Bird, P., Dawson, T. E., Felzer, K. R., Jackson, D. D., Johnson, K. M., Jordan, T. H. and Madden, C.: Uniform California earthquake rupture forecast, version 3 (UCERF3)—The time-independent model, Bull. Seismol. Soc. Am., 104(3), 1122–1180, 2014.
- Fritz, H., Abdelsalam, M., Ali, K. A., Bingen, B., Collins, A. S., Fowler, A. R., Ghebreab, W., Hauzenberger, C. A., Johnson, P. R., Kusky, T. M., Macey, P., Muhongo, S., Stern, R. J. and Viola, G.: Orogen styles in the East African Orogen: A review of the Neoproterozoic to Cambrian tectonic evolution, J. African Earth Sci., 86, 65–106, doi:10.1016/j.jafrearsci.2013.06.004, 2013.
- Gawthorpe, R. L. and Leeder, M. R.: Tectono-sedimentary evolution of active extensional basins, Basin Res., 12(3–4), 195–218, doi:10.1111/j.1365-2117.2000.00121.x, 2000.
- Gerstenberger, M. C., Marzocchi, W., Allen, T., Pagani, M., Adams, J., Danciu, L., Field, E. H., Fujiwara, H., Luco, N., Ma, K. F., Meletti, C. and Petersen, M. D.: Probabilistic Seismic Hazard Analysis at Regional and National Scales: State of the Art and Future Challenges, Rev. Geophys., 58(2), e2019RG000653, doi:10.1029/2019RG000653, 2020.
- Habgood, F.: The geology of the country west of the Shire River between Chikwawa and Chiromo, Bull. Geol. Surv. Malawi, 14, 1963.
- Hodge, M., Biggs, J., Goda, K. and Aspinall, W.: Assessing infrequent large earthquakes using geomorphology and geodesy: the Malawi Rift, Nat. Hazards, 76(3), 1781–1806, doi:10.1007/s11069-014-1572-y, 2015.
- Hodge, M., Fagereng, A., Biggs, J. and Mdala, H.: Controls on Early-Rift Geometry: New Perspectives From the Bilila-Mtakataka Fault, Malawi, Geophys. Res. Lett., 45(9), 3896–3905, doi:10.1029/2018GL077343, 2018.
- Hodge, M., Biggs, J., Fagereng, A., Elliott, A., Mdala, H. and Mphepo, F.: A semi-automated algorithm to quantify scarp morphology (SPARTA): Application to normal faults in southern Malawi, Solid Earth, 10(1), 27–57, doi:10.5194/se-10-27-2019, 2019.
- Hodge, M., Biggs, J., Fagereng, Mdala, H., Wedmore, L. N. J. and Williams, J. N.: Evidence From High-Resolution Topography for Multiple Earthquakes on High Slip-to-Length Fault Scarps: The Bilila-Mtakataka Fault, Malawi, Tectonics, 39(2), e2019TC005933, doi:10.1029/2019TC005933, 2020.
- Jackson, J. and Blenkinsop, T.: The Bilila-Mtakataka fault in Malawi: an active, 100-km long, normal fault segment in thick seismogenic crust, Tectonics, 16(1), 137–150, doi:10.1029/96TC02494, 1997.
- King, A. W. and Dawson, A. L.: The Geology of the Mangochi-Makanjila Area, Bull. Geol. Surv. Malawi, 35, 1976.
- Laõ-Dávila, D. A., Al-Salmi, H. S., Abdelsalam, M. G. and Atekwana, E. A.: Hierarchical segmentation of the Malawi Rift: The influence of inherited lithospheric heterogeneity and kinematics in the evolution of continental rifts, Tectonics, 34(12), 2399–2417, doi:10.1002/2015TC003953, 2015.
- Macgregor, D.: History of the development of the East African Rift System: A series of interpreted maps through time, J. African Earth Sci., 101, 232–252, doi:10.1016/j.jafrearsci.2014.09.016, 2015.
- Morley, C. K.: Stress re-orientation along zones of weak fabrics in rifts: An explanation for

pure extension in “oblique” rift segments?, Earth Planet. Sci. Lett., 297(3–4), 667–673, doi:10.1016/j.epsl.2010.07.022, 2010.

- Muirhead, J. D., Wright, L. J. M. and Scholz, C. A.: Rift evolution in regions of low magma input in East Africa, Earth Planet. Sci. Lett., 506, 332–346, doi:10.1016/j.epsl.2018.11.004, 2019.
- Poggi, V., Durrheim, R., Tuluka, G. M., Weatherill, G., Gee, R., Pagani, M., Nyblade, A. and Delvaux, D.: Assessing seismic hazard of the East African Rift: a pilot study from GEM and AfricaArray, Bull. Earthq. Eng., 1–31, doi:10.1007/s10518-017-0152-4, 2017.
- Rabinowitz, N. and Steinberg, D. M.: Seismic hazard sensitivity analysis: a multi-parameter approach, Bull. - Seismol. Soc. Am., 81(3), 796–817, 1991.
- Saria, E., Calais, E., Stamps, D. S., Delvaux, D. and Hartnady, C. J. H.: Present-day kinematics of the East African Rift, J. Geophys. Res. Solid Earth, 119(4), 3584–3600, doi:10.1002/2013JB010901, 2014.
- Scholz, C., Shillington, D., Wright, L., Accardo, N., Gaherty, J. and Chindandali, P.: Intrarift fault fabric, segmentation, and basin evolution of the Lake Malawi (Nyasa) Rift, East Africa, Geosphere, doi:10.1130/GES02228.1, 2020.
- Shillington, D. J., Scholz, C. A., Chindandali, P. R. N., Gaherty, J. B., Accardo, N. J., Onyango, E., Ebinger, C. J. and Nyblade, A. A.: Controls on Rift Faulting in the North Basin of the Malawi (Nyasa) Rift, East Africa, Tectonics, 39(3), e2019TC005633, doi:10.1029/2019TC005633, 2020.
- Steinbruch, F.: Geology and geomorphology of the Urema Graben with emphasis on the evolution of Lake Urema, J. African Earth Sci., 58(2), 272–284, doi:10.1016/j.jafrearsci.2010.03.007, 2010.
- Stirling, M. and Gerstenberger, M.: Applicability of the Gutenberg-Richter relation for major active faults in New Zealand, Bull. Seismol. Soc. Am., 108(2), 718–728, doi:10.1785/0120160257, 2018.
- Stirling, M., McVerry, G., Gerstenberger, M., Litchfield, N., Van Dissen, R., Berryman, K., Barnes, P., Wallace, L., Villamor, P., Langridge, R., Lamarche, G., Nodder, S., Reyners, M., Bradley, B., Rhoades, D., Smith, W., Nicol, A., Pettinga, J., Clark, K. and Jacobs, K.: National seismic hazard model for New Zealand: 2010 update, Bull. Seismol. Soc. Am., 102(4), 1514–1542, doi:10.1785/0120110170, 2012.
- Styron, R. and Pagani, M.: The GEM Global Active Faults Database, Earthq. Spectra, 1–21, doi:10.1177/8755293020944182, 2020.
- Thomas, D. S. G., Bailey, R., Shaw, P. A., Durcan, J. A. and Singarayer, J. S.: Late Quaternary highstands at Lake Chilwa, Malawi: Frequency, timing and possible forcing mechanisms in the last 44 ka, Quat. Sci. Rev., 28(5–6), 526–539, doi:10.1016/j.quascirev.2008.10.023, 2009.
- Villamor, P., Barrell, D. J. A., Gorman, A., Davy, B., Hreinsdóttir, S., Hamling, I. J., Stirling, M. W., Cox, S. C., Litchfield, N. J., Holt, A., Todd, E., Denys, P., Pearson, C., C, S., Garcia-Mayordomo, J., Goded, T., Abbot, E., Ohneiser, C., Lepine, P. and F, C.-T.: Unknown faults under cities, Lower Hutt., 2018.
- Walshaw, R. D.: The Geology of the Nchue-Balaka Area, Bull. Geol. Surv. Malawi, 19, 1965.
- Wedmore, L. N. J., Biggs, J., Williams, J. N., Fagereng, Dulanya, Z., Mphepo, F. and Mdala, H.: Active Fault Scarps in Southern Malawi and Their Implications for the Distribution of Strain in Incipient Continental Rifts, Tectonics, 39(3), e2019TC005834, doi:10.1029/2019TC005834, 2020a.
- Wedmore, L. N. J., Williams, J. N., Biggs, J., Fagereng, Å., Mphepo, F., Dulanya, Z., Willoughby, J., Mdala, H. and Adams, B. A.: Structural inheritance and border fault

reactivation during active early-stage rifting along the Thyolo fault, Malawi, J. Struct. Geol., 139, 104097, doi:10.1016/j.jsg.2020.104097, 2020b.

- Weyl, O. L. F., Mwakiyongo, K. R. and Mandere, D. S.: An assessment of the nkacha net fishery of Lake Malombe, Malawi, African J. Aquat. Sci., 29(1), 47–55, doi:10.2989/16085910409503791, 2004.
- Williams, J. N., Fagereng, Å., Wedmore, L. N. J., Biggs, J., Mphepo, F., Dulanya, Z., Mdala, H. and Blenkinsop, T.: How Do Variably Striking Faults Reactivate During Rifting? Insights From Southern Malawi, Geochemistry, Geophys. Geosystems, 20(7), 3588–3607, doi:10.1029/2019GC008219, 2019.

A systems-based approach to parameterise seismic hazard in regions with little historical or instrumental seismicity: active fault and seismogenic source databases for southern Malawi

Jack N. Williams[a*], Hassan Mdala[b], Åke Fagereng[a], Luke N.J. Wedmore[c], Juliet Biggs[c], Zuze Dulanya[d], Patrick Chindandali[e], Felix Mphepo[b]

Affiliations

[a]*School of Earth and Environmental Sciences, Cardiff University, Cardiff, UK*

[b]*Geological Survey Department, Mzuzu Regional Office, Mzuzu, Malawi*

[c]*School of Earth Sciences, University of Bristol, Bristol, UK*

[d]*Geography and Earth Sciences Department, University of Malawi, Zomba, Malawi*

[e]*Geological Survey Department, Zomba, Malawi*

*Corresponding author: Jack Williams (williamsj132@cardiff.ac.uk)

Abstract

Seismic hazard is commonly characterised using instrumental seismic records. However, these records are short relative to earthquake repeat times and extrapolating to estimate seismic hazard can misrepresent the probable location, magnitude, and frequency of future large earthquakes. Although paleoseismology can address this challenge, this approach requires certain geomorphic setting, is resource intensive, and can carry large inherent uncertainties. Here, we outline how fault slip rates and recurrence intervals can be estimated by combining fault geometry, earthquake-scaling relationships, geodetically derived regional strain rates, and geological constraints of regional strain distribution. We apply this approach to southern Malawi, near the southern end of the East African Rift, and where, although no on-fault slip rate measurements exist, there are constraints on strain

Deleted: The South Malawi Active Fault Database

Deleted: *Ocean*

Deleted: frequently

Deleted: and historical

Deleted: in regions where

Deleted: instrumental

Deleted: is

Deleted: times, and

Deleted: it

Deleted: s

Deleted: and

Deleted: ies

Deleted: through an approach that

Deleted: es

Deleted: then

Deleted: the

Deleted: which lies

Deleted: at

Deleted: Rift

Deleted: wher

Deleted: although no

Deleted: exist

Deleted: ,

Deleted: t

Deleted: theoretical and observational

Deleted: how

partitioning between border and intrabasin faults. This has led to the development of the South Malawi Active Fault Database (SMAFD), a geographical database of 23 active fault traces, and the South Malawi Seismogenic Source Database (SMSSD), in which we apply our systems-based approach to estimate earthquake magnitudes and recurrence intervals for the faults compiled in the SMAFD. We estimate earthquake magnitudes of M_W 5.4-7.2 for individual fault sections in the SMSSD, and M_W 5.6-7.8 for whole fault ruptures. However, low fault slip rates (intermediate estimates ~0.05-0.8 mm/yr) imply long recurrence intervals between events: 10^2-10^5 years for border faults and 10^3-10^6 years for intrabasin faults. Sensitivity analysis indicates that the large range of these estimates can best be reduced with improved geodetic constraints in southern Malawi. The SMAFD and SMSSD provide a framework for using geological and geodetic information to characterize seismic hazard in regions with few on-fault slip rate measurements, and could be adapted for use elsewhere in the East African Rift and globally.

1. Introduction

Earthquake ruptures tend to occur on pre-existing faults (Brace and Byerlee, 1966; Jackson, 2001; Scholz, 2002; Sibson, 1989). Thus, the identification and systematic mapping of active faults, which are then compiled with other fault attributes (e.g. slip rate and slip sense) into a geospatial active fault database, provides an important tool in assessing regional seismic hazard (Christophersen et al., 2015; Hart and Bryant, 1999; Langridge et al., 2016; Shyu et al., 2016; Styron et al., 2020; Styron and Pagani, 2020; Taylor and Yin, 2009). Not only can these databases inform on the surface rupture risk (Hart and Bryant, 1999; Villamor et al., 2012), they can also be converted into earthquake sources for Probabilistic Seismic Hazard Assessment (PSHA) to forecast future levels of ground shaking (Beauval et al., 2018; Cornell, 1968; Gerstenberger et al., 2020; Hodge et al., 2015; Morell et al., 2020; Stirling et al., 2012). Furthermore, the data contained in active fault databases are

Deleted: is distributed

Deleted: al

Deleted: the first database of its kind in the East African Rift System (EARS) and designed so that the outputs can be easily incorporated into Probabilistic Seismic Hazard Analysis.

Deleted: AFD

Deleted: 6

Deleted: 0

Deleted: These potentially high magnitudes for continental normal faults reflect southern Malawi's 11-140 km long faults and thick (30-35 km) seismogenic crust.

Deleted: s (intermediate estimates

Deleted:)

Deleted: al

Deleted: most significantly from

Deleted: an improved understanding of the rate and partitioning of rift-extension

Deleted: , earthquake scaling relationships, and earthquake rupture scenarios

Deleted: Hence these are critical areas for future research.

Deleted: s

Deleted: low strain rate settings

Deleted: S

Deleted: or

inherently useful in understanding regional geological evolution (Agostini et al., 2011b; Basili et al., 2008; Taylor and Yin, 2009).

Active fault databases with worldwide coverage have been compiled (Christophersen et al., 2015; Yeats, 2012), including recent development of the Global Earthquake Model Foundation Global Active Fault Database (Styron and Pagani, 2020). However, in some regions, the fault mapping in these databases has only been performed at a coarse scale, and the fault attributes (e.g. slip rates, earthquake recurrence intervals) that are required to use them as earthquake sources in PSHA have not been measured. This partly reflects that obtaining these attributes from dating faulted surfaces and/or paleoseismology is time-intensive, requires certain geomorphic settings, and can involve large uncertainties (Cowie et al., 2012; McCalpin, 2009; Nicol et al., 2016b). Alternatively, decadal time-scale fault slip rates can be estimated using geodetic data and block models where the crust is divided by mapped faults (e.g. Field et al., 2014; Wallace et al., 2012; Zeng and Shen, 2014). However, not all fault systems are covered by sufficiently dense geodetic networks to perform this analysis, the resulting slip rates may be biased by the short time over which this data has been collected relative to earthquake cycles, and/or sometimes geodetic data cannot resolve how strain is distributed (Calais et al., 2016; Morell et al., 2020; Stein et al., 2012).

In this study, we first describe the South Malawi Active Fault Database (SMAFD), a systematic attempt to map active faults and collate their geomorphic attributes in southern Malawi. Located within the East African Rift System (EARS), southern Malawi lies in a region specifically highlighted by Styron and Pagani, (2020) as a priority area for future active fault mapping, and where population growth and seismically vulnerable building stock is driving an increased exposure to seismic hazard (World Bank, 2019; Goda et al., 2016; Hodge et al., 2015; Kloukinas et al., 2019; Ngoma et al., 2019; Novelli et al., 2019).

Deleted:

Deleted: Despite their benefits, active fault databases have yet to be developed for many seismically active regions (Christophersen et al., 2015).

Deleted: he difficulty in estimating fault slip rates and earthquake recurrence intervals, as instrumental seismic records typically cover only a fraction of a fault's seismic cycle (Stein et al., 2012), whilst obtaining

Deleted: these

Deleted: offset

Deleted: estimates

Deleted: plate boundaries

Deleted: networks

Deleted: all known

Deleted: The SMAFD has been compiled from a review of high resolution digital elevation models, fieldwork, geophysical datasets, and legacy geological maps, It thus represents the most complete active fault database to be compiled so far within the

Within southern Malawi itself, faults capable of hosting M_W 7-8 earthquakes have been previously identified (Hodge et al., 2019, 2020; Jackson and Blenkinsop, 1997; Wedmore et al., 2020a). However, there are currently no reports of historical surface rupturing earthquakes, on-fault slip rate measurements, or paleoseismic investigations. In the second part of this study, we thus describe a new systems-based approach for combining geodetic and geological information to estimate slip rates and earthquake recurrence intervals. In particular, it may be useful for low-slip rate interplate regions (regional slip rates ~1-10 mm/yr; Scholz et al., 1986) where the instrumental record is relatively short compared to fault recurrence intervals and where earthquakes may be especially damaging (England and Jackson, 2011). It would not, however, be appropriate for low strain intraplate settings where geodetic data cannot resolve deformation rates (Calais et al., 2016).

By applying this approach to southern Malawi, we have developed the Southern Malawi Seismogenic Source Database (SMSSD), a complementary database to the SMAFD, but where the attributes (e.g. fault segmentation, earthquake recurrence intervals) are: (1) targeted towards it inclusion in PSHA, and (2) derived from modelling and so are mutable. Notably, previous PSHA in the EARS has typically been conducted using the ~65 year long instrumental seismic record alone (Ayele, 2017; Goitom et al., 2017; Midzi et al., 1999; Poggi et al., 2017). However, fault-based earthquake sources, such as the SMSSD, may play an important role in characterising the EARS's ever increasing seismic risk (Goda et al., 2016; Hodge et al., 2015).

We describe the SMAFD and SMSSD together here so that the assumptions and uncertainties of our approach are clear, particularly for hazard modellers who may wish to incorporate these databases into a PSHA. This study first describes the seismotectonic setting of southern Malawi (Sect. 2), and the approach used for mapping its active faults in the SMAFD (Sect. 3). In Sect. 4 we then describe

Formatted: Subscript

Deleted: urface rupturing earthquakes

Deleted: by

Deleted: , we present a new systems-based approach

Deleted: in regions like southern Malawi that are defined by a within narrow (<100 km width; Buck, 1991) amagmatic continental rifts. However, this method could be adapted for any region tectonic settingwith low strain rates with, well developedwell-developed active fault maps, and an understanding of strain partitioning.

Deleted: train

Deleted: rate

Deleted: regions (plate boundary

Deleted: (

Deleted: is

Deleted: , inherently difficult for geodesy to resolve strain in intraplate region

Deleted:

Deleted: and so this framework would not be appropriate for these settings.

Deleted: slip

Deleted: rates,

Deleted: We then apply this method to southern Malawi, which has culminated in the development of the South Malawi Active Fault Database (SMAFD).

Deleted: ¶
¶
The SMAFD represents the first active fault database to be developed within the East African Rift System (EARS), where population growth and seismically vulnerable building stock is driving an increased exposure to seismic hazard (World Bank, 2019; Goda et al., 2016; Hodge et al., 2015; Kloukinas et al., 2019; Ngoma et al., 2019; Novelli et al., 2019).

Deleted: comparatively short

Deleted: of seismicity

Deleted: ence

Deleted: However, the short duration of this record in the EARS and its low low EARS strain rates (regional extensional rates ~1-6 mm/yr; Stamps et al., 2018) imply that this record is incomplete and may underestimate seismicity ... [1]

Deleted: in the EARS

Deleted: 's

Deleted: its

Deleted: ever-

Deleted: .However, b

Deleted:

Deleted:

Deleted: The SMAFD and SMSSD are therefore described ... [2]

Deleted: and so it is important that the SMAFD and SMSSD ... [3]

Deleted: ¶ ... [4]

the method used to estimate fault slip rates, earthquake magnitudes and recurrence intervals, and whose application to southern Malawi has resulted in the development of the SMSSD. The SMAFD is described in Sect. 5 along with an evaluation of fault slip rate estimates and sensitivity analysis in the SMSSD. Finally, in Sect. 6, we discuss the implication of these databases in terms of southern Malawi's seismic hazard, and the strategies needed to reduce uncertainties in these databases.

2. Southern Malawi seismotectonics

The SMAFD and SMSSD cover the geopolitical term 'southern Malawi,' and so includes all active faults between the southern end of Lake Malawi and the border between Mozambique and Malawi. Faults that lie close to, or cross this national boundary, are also included. The extent of these databases does not therefore correspond directly to the geological region of the 'southern Malawi Rift,' whose definition has varied in previous studies (Chapola and Kaphwiyo, 1992; Ebinger et al., 1987; Laõ-Dávila et al., 2015; Williams et al., 2019). In this section, we briefly summarise the tectonic history and seismic record in the region.

2.1 Southern Malawi tectonic setting

Southern Malawi lies towards the southern incipient end of the EARS Western Branch, where it channels the Shire River from Lake Malawi to its confluence with the Zambezi River (Dulanya, 2017; Ivory et al., 2016). This portion of the EARS is typically considered to represent the divergent boundary between the Rovuma and Nubia plates (Fig. 1a; Saria et al., 2013; Stamps et al., 2008, 2018, 2020). However, recent seismotectonic analysis suggests that the Nubia Plate can be further divided by the Lower Zambezi and Luangwa rifts into the San and Angoni plates, with the EARS in Malawi forming the Angoni-Rovuma plate boundary (Fig. 1a; Daly et al., 2020). EARS activity in southern Malawi is unlikely to have initiated prior to the mid-Pliocene (~4.5 Ma) onset of sediment accumulation in Lake Malawi's south basin (Delvaux, 1995; McCartney and Scholz, 2016; Scholz et

Deleted: using southern Malawi as an example

Deleted: Fault

Deleted: Results from the

Deleted: mapping

Deleted: are

Deleted: ocumented

Deleted: Aand a sensitivity analysis

Deleted: th

Deleted: e SMAFD

Deleted: fault growth in continental rifts,

Deleted: when assessing this hazard

Deleted: ¶

Moved (insertion) [8]

Deleted: We first note here that this study considers

Deleted: ,

Deleted: all

Deleted: and not

Deleted: . As such, the extent of the SMAFD and SMSSD covers

Moved up [8]: all active faults between the southern end of Lake Malawi and the border between Mozambique and Malawi. Faults that lie close to, or cross this national boundary, are also included.

Deleted: ¶
2.1 Tectonic history of southern Malawi¶
Southern Malawi lies at a complex intersection of orogenic belts that formed during the Pan African Orogeny (~800-450 Ma) and possibly earlier Irumide age deformation (~1,020-950 Ma) as the African continent gradually amalgamated during the Proterozoic, and which imparted amphibolite-granulite facies metamorphic fabrics (mineral segregations and alignments) within the rift's basement rocks (Figs. 1 and 2; Andreoli, 1984; Fritz et al., 2013; Fullgraf et al., 2017; Kröner et al., 2001; Manda et al., 2019). Within the Phanerozoic (540 Ma to present day), Permian-Triassic sediments were deposited in the Mwanza and Lower Shire basinsGraben under NW-SE Karoo extension (Fig. 1b; Castaing, 1991; Habgood et al., 1973; Wedmore et al., 2020b). NE-SW striking dykes then formed during the Jurassic, followed by minor accumulations of Cretaceous sediments under NE-SW extension (Castaing, 1991). Evidence for Upper Jurassic to Cretaceous magmatism is also observed across southern Malawi with the emplacement of the Chilwa Alkaline Province (Bloomfield, 1965; Dulanya, 2017; Eby et al., 1995; Manda et al., 2019), Salambidwe Igneous Structure (Cooper and Bloomfield, 1961) and Lupata Volcanic Complex (Chisenga et al., 2019; Habgood, 1963). ¶

Deleted: *2*

Deleted: ,

Deleted: where it represents the divergent boundary between the Rovuma and Nubia plates (Fig. 1; Saria et al., 2013; Stamps et al., 2008, 2018) al., 2020), and almost certainly not before the Oligocene (23-25 Ma) age of the Rungwe Volcanic Province (RVP) in southern Tanzania (Mesko, 2020; Mortimer et al., 2016; Roberts et al., 2012). Though 700 km to the north, the RVP marks the closest surface volcanism to the EARS in southern Malawi, and hence this rift section is considered to be amagmatic.

Like elsewhere in the Western Branch, the EARS in southern Malawi follows Proterozoic orogenic belts, and can be divided along-strike into a number of 50-150 km long linked basins (Ebinger, 1989). Immediately south of Lake Malawi, the EARS bifurcates around the Shire Horst within the NW-SE trending Makanjira Graben before following an arcuate bend in regional Proterozoic fabrics to form the NNE-SSW trending Zomba Graben (Fig 2; Dulanya, 2017; Fullgraf et al., 2017; Laõ-Dávila et al., 2015; Wedmore et al., 2020a; Williams et al., 2019). Along-strike to the south, the EARS then intersects the Lower Shire Basin, a reactivated Karoo-age (i.e. Permo-Triassic) basin (Castaing, 1991; Chisenga et al., 2019; Habgood, 1963; Habgood et al., 1973; Wedmore et al., 2020b), before bending around the Nsanje Horst to link up with the Urema Graben in Mozambique (Bloomfield, 1958; Steinbruch, 2010). Daly et al., (2020) proposed that the Lower Shire Basin also extends to the west along the Mwanza Basin into Mozambique where it links with the Lower Zambezi Rift and forms the San-Angoni plate boundary (Fig. 1a).

Prior to this study, the only systematic active fault mapping in southern Malawi was conducted by Chapola and Kaphwiyo (1992) and, for the Lower Shire Basin, by Castaing (1991). These maps were subsequently incorporated by Macgregor (2015) into EARS-scale maps, and later into the Global Earthquake Model Global Active Fault Database (Styron and Pagani, 2020). However, the faults are mapped at a coarse scale (Fig. 2a), and this database does not include active faults traces identified in legacy geological maps (Bloomfield, 1965; Bloomfield and Garson, 1965; Habgood et

Deleted:

Deleted: grabens/half grabens

Deleted: where it

Deleted: s

Deleted: may

Deleted: o

Deleted: ¶
of EARS rifting in southern Malawi is poorly constrained (Dulanya, 2017; Wedmore et al., 2020a), it is unlikely to be older than the mid-Pliocene (~4.5 Ma) onset of sediment accumulation in Lake Malawi's south basin Lake Malawi (Delvaux, 1995; McCartney and Scholz, 2016; Scholz et al., 2020), and almost certainly not older than the Oligocene (23-25 Ma) age of the northern end of the Malawi Rift EARS in northern Malawi (Mesko, 2020; Mortimer et al., 2016; Roberts et al., 2012). However, it is unclear if the EARSrift in southern Malawi is actually younger than in northern and central Malawi, and/or it is the same age but has been extending at a slower rate due to its proximity to the Nubia-Rovuma Euler pole (Fig. 1a).¶

Deleted: ¶

Deleted: The floors of the Zomba and Makanjira graben sit at an altitude only ~10 m higher than Lake Malawi. Hence, the sediments deposited in these grabens likely formed during base level changes in lake level, when it was up to 150 m higher than present (Ivory et al., 2016; Lyons et al., 2015; McCartney and Scholz, 2016), and would have flooded this section of the rift (Wedmore et al., 2020a). Between the Zomba and Lower Shire grabens, the rift floor elevation drops from ~450 to ~100 m; however, there is no evidence that this is controlled by active faults (Dulanya, 2017; Wedmore et al., 2020a). The Rungwe Volcanic Province, the closest EARS volcanism to southern Malawi, is ~700 km to the north (Fig. 1a), and hot springs in southern Malawi do not indicate a magmatic origin (Dulanya et al., 2010). Nevertheless, minor intrusions into the lower crust cannot be excluded (Wang et al., 2019).¶
¶

Deleted: Castaing (1991) and

Deleted: , whose

Deleted:

Deleted: Global Earthquake Model (GEM)

Deleted: Global Active Faults map (Fig. 2b; https://blogs.openquake.org/hazard/global-active-fault-viewer/, date last accessed 4 June 2020).

Deleted: and there is no additional information such as slip rates or evidence for recent fault activity

Deleted: .

Deleted: that are both vital components of an active fault database.

Deleted: Furthermore

Deleted: , this database does not incorporate

Deleted: that are

al., 1973; Walshaw, 1965) and high resolution digital elevation models (Hodge et al., 2019, 2020; Wedmore et al., 2020b, 2020a).

2.2 Southern Malawi seismicity

There are no known historical accounts of surface rupturing earthquakes in southern Malawi, although a continuous written record only extends to c. 1870 (Pike, 1965; Stahl, 2010). However, in northern Malawi, the previously unrecognised St Mary fault exhibited surface rupture following the 2009 Karonga earthquakes, a sequence consisting primarily of four shallow (focal depths <8 km) M_W 5.5-5.9 events over a 13 day period (Fig. 1b; Biggs et al., 2010; Gaherty et al., 2019; Hamiel et al., 2012; Kolawole et al., 2018b; Macheyeki et al., 2015).

The International Seismological Centre (ISC) record for Malawi is complete from 1965 to present for events with M_W>4.5 (Figs. 1b and 2a; Hodge et al., 2015), with the largest event in this record being the 1989 M_W 6.3 Salima Earthquake (Jackson and Blenkinsop, 1993). Notably, seismicity in Malawi is commonly observed to depths far greater (30-35 km; Craig et al., 2011; Delvaux and Barth, 2010; Jackson and Blenkinsop, 1993) than would be expected for continental crust of typical composition and geothermal gradient (10-15 km). Thick cold anhydrous lower crust (Craig et al., 2011; Jackson and Blenkinsop, 1997; Njinju et al., 2019; Nyblade and Langston, 1995), localised weak viscous zones embedded within strong lower crust (Fagereng, 2013), and/or volumes of mafic material in the lower crust (Shudofsky et al., 1987) that are velocity weakening at temperatures <700 °C (Hellebrekers et al., 2019) have been proposed as explanations for this unusually deep seismicity.

Earthquake focal mechanism stress inversions that encompass events from across Malawi indicate a normal fault stress state (i.e. vertical maximum principal compressive stress) with an ENE-WSW to E-W trending minimum principal compressive stress (σ_3; Fig. 1b Delvaux and Barth, 2010; Ebinger

Deleted: o

Deleted: r from

Deleted: ¶

Formatted: No bullets or numbering

Deleted: *3*

Deleted:

Deleted: sequence

Deleted: This sequence primarily consisted of four shallow (focal depths <8 km) M_W 5.5-5.9 events over a 13 day period (Biggs et al., 2010; Gaherty et al., 2019; Hamiel et al., 2012). Another relevant event for southern Malawi is the 1910 M_S 7.4 Rukwa Earthquake in southern Tanzania (Ambraseys, 1991). The fault source for this event is not certain, though the Kanda fault is a likely candidate (Vittori et al., 1997), and its steep and laterally continuous scarp closely resembles that of some faults in southern Malawi (Hodge et al., 2018a, 2019, 2020; Wedmore et al., 2020a, 2020b).

Deleted: The largest instrumentally recorded earthquake in southern Malawi is a M 6.7 event in 1954 (De Bremaeker, 1956; Delvaux and Barth, 2010).

Deleted: to

Deleted: magnitude (

Deleted:)

Deleted:

Deleted: to 1965

Deleted: ¶

Deleted: ¶
2.4 Estimates of stress and strain in southern Malawi¶

Deleted: for the entire Malawi Rift

et al., 2019; Williams et al., 2019). This σ_3 orientation is comparable to the σ_3 direction inferred from regional joint orientations (Williams et al., 2019), and the geodetically-derived extension direction between the Nubia and Rovuma plates (Fig. 1b; Saria et al., 2014; Stamps et al., 2018, 2020).

Using instrumental catalogues, Probabilistic Seismic Hazard Analyses (PSHA) finds that there is a 10% probability of exceeding 0.15 g peak ground acceleration in the next 50 years in southern Malawi (Midzi et al., 1999; Poggi et al., 2017). Through the SMAFD and SMSSD, we outline how geological and geodetic data can be collated and assessed, so that it may also be incorporated into PSHA in southern Malawi.

3. Mapping and describing active faults in the South Malawi Active Fault Database (SMAFD)

An active fault database consists of an active fault map, where for each fault, attributes are added that detail geomorphic, kinematic, geometric, and geological information about the fault (Christophersen et al., 2015; Styron and Pagani, 2020). Typically, an active fault database is stored in a Geographic Information System (GIS) environment, in which the fault attributes are assigned to a linear feature that represents the fault's geomorphic trace (e.g. Langridge et al., 2016; Machette et al., 2004; Styron et al., 2020). In this section, we describe how active faults were mapped in the South Malawi Active Fault Database (SMAFD) and the geomorphic attributes that were assigned to them. Estimates of associated earthquake source parameters, which are collated separately in the South Malawi Seismogenic Source Database (SMSSD), are described in Sect. 4.

Deleted: ENE-WSW to E-W extension indicates that NE-SW striking faults in Malawi should accommodate oblique slip. However, slickensides and earthquake focal mechanisms indicate approximately dip-slip motion regardless of fault strike in southern Malawi (Fig. 1b; Delvaux and Barth, 2010; Hodge et al., 2015; Wedmore et al., 2020a). This apparent inconsistency between faults that are simultaneously accommodating near pure dip-slip and strike oblique to the regional extension direction can be explained if the lower crust in southern Malawi contains lateral rheological heterogeneities such as an anastomosing shear zone (Fagereng, 2013; Hodge et al., 2018a; Philippon et al., 2015; Wedmore et al., 2020a; Williams et al., 2019). ¶

Deleted: ¶
¶

Deleted: *2.3.5 Seismic hazard assessment in southern Malawi*¶
Using instrumental catalogues, Using instrumental catalogues,

Deleted: P

Deleted: S

Deleted: i

Deleted:

Deleted: have been conducted for southern Malawi as part of EARS-wide studies

Moved (insertion) [9]

Deleted: (Midzi et al., 1999; Poggi et al., 2017). These indicate that there is a 10% probability of exceeding 0.15 g peak ground acceleration in southern Malawi in the next 50 years (Poggi et al., 2017).

Moved up [9]: (Midzi et al., 1999; Poggi et al., 2017)

Deleted: However, these estimates are sensitive to the choice of the maximum expected earthquake (M_{max}) within each PSHA source zone, which given the short nature of the EARS instrumental record, However, can only be arbitrarily ... [5]

Deleted: Thus, the

Deleted: geodetic and geomorphological information incorporated into SMAFD may be a better guide assessing... [6]

Deleted: the

Deleted: SMAFD

Deleted: , and, if available, estimates of the parameters (earthquake magnitudes and recurrence intervals) required to... [7]

Deleted: the methodology for

Deleted: mapping

Deleted: s

Deleted: outhern Malawi

Deleted: assigning some basic

Deleted: ological

Deleted: into the South Malawi Active Fault Database (SMAFD). Note here that to keep the fault mapping complete

Deleted: Note here that to keep the fault mapping complete for this EARS section, some faults in the SMAFD also extend... [8]

Deleted: (including slip rate, earthquake magnitudes and recurrence intervals)

3.1 Identifying active and inactive faults in southern Malawi

There are many inherent limitations in mapping active faults. Even in countries with well-developed databases such as Italy and New Zealand, their success in accurately predicting the locations of future surface rupturing earthquakes is, at best, mixed (Basili et al., 2008; Nicol et al., 2016a). An active fault might not be recognised because evidence of previous surface rupture is subsequently buried, eroded (Wallace, 1980), or the fault itself is blind (e.g. Quigley et al., 2012), which in turn depends on earthquake magnitude, focal depth, thickness of the seismogenic crust, and the local geology. Furthermore, although active and inactive faults are typically differentiated by the age of the most recent earthquake, the precise maximum age that is used to define 'active' varies between different active fault databases depending on the regional strain rate (i.e. plate boundary vs. stable craton) and the prevalence of youthful sediments (Clark et al., 2012; Jomard et al., 2017; Langridge et al., 2016; Machette et al., 2004). Indeed, it may not always be possible to reliably determine if an exposed fault has been recently 'active' or not (Cox et al., 2012; Nicol et al., 2016a).

Deleted: s

Deleted: in some cases

Each of these issues has relevance to mapping active faults in southern Malawi. Firstly, active faults may be buried by sediments deposited due to tectonic subsidence (Gawthorpe and Leeder, 2000), and/or regular (10-100 ka) climate driven ~100 m scale fluctuations in the level of Lake Malawi, which would likely flood the Zomba and Makanjira basins (Ivory et al., 2016; Lyons et al., 2015; Wedmore et al., 2020a). Alternatively, the relatively thick (30-35 km) seismogenic crust in southern Malawi means that even moderate-large earthquakes (M_W>6) do not necessarily result in surface rupture, as illustrated by the M_W 6.3 Salima earthquake (Gupta, 1992; Jackson and Blenkinsop, 1993). Finally, except for studies around Lake Malombe (Van Bocxlaer et al., 2012), there is no chronostratigraphic control for this section of the EARS to help differentiate between inactive and active faults (Dulanya, 2017; Wedmore et al., 2020a).

Deleted: they

Deleted: s

Deleted: during regular (10-100 ka)

Deleted:

Deleted: Finally,

Deleted: there is little chronostratigraphic control for this section of the EARS (Dulanya, 2017; Wedmore et al., 2020a) to help differentiate between inactive and active faults.

For the SMAFD, we therefore define active faults based on evidence of activity within the current tectonic regime. Such an approach has been advocated elsewhere in the EARS (Delvaux et al., 2017) and in other areas with low levels of seismicity, few paleoseismic studies, and/or where there are faults that are favourably oriented for failure in the current stress regime, but which have no definitive evidence of recent activity (Nicol et al., 2016a; De Pascale et al., 2017; Villamor et al., 2018). In practice, this means that faults will be included in the SMAFD if they can be demonstrated to have been active during East African rifting. This evidence can vary from the accumulation of post-Miocene hanging-wall sediments to the presence of a steep fault scarp, offset alluvial fans, and/or knickpoints in rivers that have migrated only a short vertical distance (<100 m) upstream (Hodge et al., 2019, 2020; Jackson and Blenkinsop, 1997; Wedmore et al., 2020a). We note that the absence of post-Miocene sediments in the hanging-wall of a normal fault does not necessarily imply that it is inactive, if for example, faults are closely spaced across strike so that sediments are eroded during subsequent footwall uplift of an interior normal fault (e.g. Chirobwe-Ncheu fault, Fig. 3c; see also Mortimer et al., 2016; Muirhead et al., 2016). In these cases, if there is other evidence of recent activity (e.g. scarp, triangular facets), these faults are still included.

Deleted:

Deleted:

Deleted: Previous active fault mapping in southern Malawi was based on the extent of scarps alone (Hodge et al., 2019; Wedmore et al., 2020a). Therefore, the relaxed definition of an 'active' fault in the SMAFD means that it includes more faults than these maps, and that the lengths of some faults have been increased.

For the sake of completeness, major faults that control modern day topography, but that do not fit the criteria of being active (e.g. Karoo faults), were mapped separately (Fig. 2a). However, this map is not necessarily complete for all other faults in southern Malawi, and we also cannot definitively exclude the possibility that some of these faults are still active although they display no evidence for it. The relatively broad definition of an active fault may also mean that some inactive faults are included in the SMAFD. However, in applying the opposite approach (i.e. requiring an absolute age for the most recent activity on a fault) there is a greater risk that faults mistakenly interpreted to be inactive subsequently rupture in a future earthquake (Litchfield et al., 2018; Nicol et al., 2016a).

Deleted: b

Deleted: inactive

3.2 Datasets for mapping faults in southern Malawi

3.2.1 Legacy geological maps

Between the 1950s and 1970s, the geology of southern Malawi was systematically mapped at 1:100,000 scale. These studies noted evidence of recent displacement on the Thyolo (Habgood et al., 1973), Bilila-Mtakataka, Tsikulamowa (Walshaw, 1965), and Mankanjira faults (King and Dawson, 1976). However, they did not systematically distinguish between active and inactive faults. Furthermore, these studies are in places ambiguous with equivalent structures in the Zomba Graben being variably described as 'terrace features' (Bloomfield, 1965), active fault scarps (Dixey, 1926) and Late Jurassic-Early Cretaceous faults (Dixey, 1938).

Deleted: and these maps, and their associated reports, were consulted in detail when defining and naming faults

Deleted: Tsikulumowa

Deleted: no attempt was made to

Deleted: there is ambiguity in

3.2.2 Geophysical datasets

Regional-scale aeromagnetic data were acquired across Malawi in 2013 by the Geological Survey Department of Malawi (Fig. 2c; Kolawole et al., 2018a; Laõ-Dávila et al., 2015). These survey data were used to refine fault mapping in cases where features interpreted as faults in the aeromagnetic survey extended beyond their surface expression. Gravity surveys have also been used to map blind faults in the Lower Shire Basin (Chisenga et al., 2019), and these have been incorporated into the SMAFD.

Deleted: s

Deleted: , and these have also been incorporated into the SMAFD A revised fault map for the Lower Shire Graben based on gravity surveys

Deleted: was also consulted when compiling the SMAFD.

3.2.3 Digital Elevation Models

The topography of southern Malawi is primarily controlled by EARS faulting (Dulanya, 2017; Laõ-Dávila et al., 2015; Wedmore et al., 2020a) except in the case of the Kirk Range (Fig. 2b), and readily identifiable igneous intrusions and Karoo faults (Figs. 3c and 4b). To exploit this interaction between topography and active faulting, TanDEM-X digital elevation models (DEMs) with a 12.5 m horizontal resolution and an absolute vertical mean error of ± 0.2 m (Wessel et al., 2018) were acquired for southern Malawi (Fig. 2b). This small error means that the TanDEM-X data performs better at identifying the metre-scale scarps common in southern Malawi (Hodge et al., 2019; Wedmore et al., 2020a) than the more widely-used but lower resolution Shuttle Radar Topography Mission (SRTM) 30 m DEMs (Sandwell et al., 2011). Furthermore, TanDEM-X data can be used to assess variations in along-strike scarp height (Hodge et al., 2018a, 2019; Wedmore et al., 2020a, 2020b) and assess the interactions between footwall uplift and fluvial incision (Fig. 4a; Wedmore et al., 2020a). The Mwanza and Nsanje faults partly extended out of the region of TanDEM-X coverage, and these sections were mapped using the SRTM 30 m resolution DEM (Fig. 2b).

3.2.4 Fieldwork

To corroborate evidence of recent faulting recognised in DEMs and geological reports, fieldwork was conducted on several faults (Fig. 2b). This ranged from documenting features indicative of recent displacement on the faults, such as scarps, triangular facets, and displaced Quaternary-recent sediments, to comprehensively sampling the fault and surveying it with an Unmanned Aerial Vehicle (Fig. 3; see also: Hodge et al., 2018; Wedmore et al., 2020a, 2020b; Williams et al., 2019).

3.3 Strategy for mapping and describing active faults in the SMAFD

Following the 'active' fault definition and synthesis of the datasets described above, faults in southern Malawi are mapped following the approach outlined for the Global Earthquake Model Global Active Fault Database (GAF-DB), where each fault constitutes a single continuous GIS feature (Styron and Pagani, 2020). The SMAFD therefore differs from other active fault databases where each distinct geomorphic (i.e. traces) or geometric (i.e. sections) part of a fault is mapped as a separate GIS feature (Christophersen et al., 2015; Machette et al., 2004).

The attributes associated with each fault in the SMAFD are listed and briefly described in Table 1. These resemble the attributes in the GEM GAF-DB that describe a fault's geomorphic attributes and

Deleted: and triangular facets

Deleted: *and describing*

Deleted: e GE

Deleted: neotectonics fault

Deleted:

Deleted: is mapped

Deleted: as

Moved down [7]: We define an individual fault in the SMAFD as a collection of geomorphic traces that are capable of rupturing together in a single earthquake (Christophersen et al., 2015). Empirical observations and Coulomb stress modelling suggests that normal fault earthquakes rarely rupture across steps whose width is >20% of the length of the interacting sections (Biasi and Wesnousky, 2016; Hodge et al., 2018b), and we use this as a criteria to assign whether two *en echelon* sections in the SMAFD are part of the same fault.

Deleted: database (Christophersen et al., 2015; Litchfield et al., 2013). This database uses a hierarchical system to map faults, in which 'traces' are the basic unit, and one or more traces may be used to define 'sections,' and one or more sections define 'faults' (Christophersen et al., 2015; Litchfield et al., 2013). For faults in the SMAFD, which typically propagate to the surface, traces denote a linear, relatively uniform active fault geomorphic expression. The end of a trace is defined by where the geomorphic feature changes. For example, where a scarp may have been eroded to leave a gently dipping escarpment.

Deleted: ¶
¶
'Sections' are portions of faults that have a distinct geometric, kinematic, or paleoseismic attribute (Christophersen et al., 2015; Litchfield et al., 2013; Styron et al., 2020). Except in the case of linking sections, they also represent distinct surface rupturing earthquake sources in PSHA and so should be >5 km in length (Christophersen et al., 2015). Given the lack of paleoseismic information on active faults in the SMAFD, sections are generally defined by geometrical boundaries such as bends or step-overs (Fig. 2d; DuRoss et al., 2016; Jackson and White, 1989; Wesnousky, 2008; Zhang et al., 1991). Along-strike minima in fault displacement (e.g. scarp or knickpoint height) may also be indicative of segmentation (Willemse, 1997), but these do not always coincide with geometrical complexities in southern Malawi (Fig. 4; Hodge et al., 2018a, 2019; Wedmore et al., 2020a, 2020b). This may indicate that deeper structures, not visible in the surficial fault geometry, are also influencing fault ... [9]

Moved down [1]: 'Sections' are portions of faults that have a kinematic, or paleoseismic attribute (Christophersen et al., 2015; Litchfield et al., 2013; Styron et al., 2020). Except in

Deleted: *3.4 Fault traceSMAFD attributes* ¶
Along with the geographic representation of each fault in the SMAFD, a number of

Deleted: are also

Deleted: it

Deleted: , which

Deleted: are The attributes added to each mapped fault in the SMAFD are modelled on

Deleted: from

confidence that it is still active (Styron and Pagani, 2020). To incorporate the multidisciplinary approach we have used to map faults in southern Malawi, we also include a 'Location Method' attribute, which details how the fault was mapped (Table 1). Some fault attributes used in the GEM GAF-DB such as slip rates are not included in the SMAFD, as these data have not been collected in southern Malawi. We instead derive these attributes as outlined in Sect. 4 and incorporate them separately into the SMSSD (Table 2). However, within each database, a numerical ID system is used make the two databases compatible (Tables 1 and 2).

4. A systems-based approach to estimating seismic source parameters: application to southern Malawi

Typically, estimates of fault slip rate, earthquake magnitudes and recurrence intervals are derived from paleoseismology, geodesy, historical records of past earthquakes, or considerations of the seismic moment rate (Basili et al., 2008; Field et al., 2014; Langridge et al., 2016; McCalpin, 2009; Molnar, 1979; Youngs and Coppersmith, 1985). However, as noted in the introduction, these types of data have not been collected in southern Malawi. Indeed, currently very few such records exist across the entire EARS (Delvaux et al., 2017; Muirhead et al., 2016; Siegburg et al., 2020; Zielke and Strecker, 2009), and even in regions with well-developed active fault databases such as California and New Zealand, only a small number of faults have directly measured slip rates and paleoseismic information (Field et al., 2014; Langridge et al., 2016).

In the absence of direct on-fault slip rate estimates, we suggest that they can be estimated through a systems-level approach in which geodetically derived plate motion rates are partitioned across faults in a manner consistent with their geomorphology and regional tectonic regime. Although such an approach has been used before over small regions (Cox et al., 2012; Litchfield et al., 2014), it has not been applied to an entire fault system. In addition, we outline how the uncertainties and

Deleted: below

Deleted: (Sect. 4), we instead derive these attributes from a systems-based

Deleted: In this way, we keep objective and modellingderived fault attributes in southern Malawi separate.

Deleted: to allow easy rison between

Deleted: neotectonics fault database guidelines (Christophersen et al., 2015). These are listed and briefly described in Table 1, along with the hierarchical level it is assigned (i.e. trace, section, or fault). The first set of attributes is linked to information collected about each trace, and so relate to geomorphic observations (Table 1). The attributes 'scale' and 'confidence' reflect that two distinct considerations must be made when mapping a geomorphic feature as an active fault (Barrell, 2015; Styron et al., 2020): (1) its prominence in the landscape, which is indicated by the scale at which a fault is mapped, and (2) the confidence that the feature is an active fault, which indicated by a qualitative score from 1 (high) to 4 (low, Table 1).

Deleted: earthquake

Deleted: the SMAFD

Deleted: ¶
Although important for identifying surface rupture hazards and understanding the geological evolution of the EARS in southern Malawi, the SMAFD cannot be readily incorporated into PSHA. This is because it does not includeIn addition to the active fault map, the GEM neotectonics fault database requires estimates of fault slip rates, and earthquake magnitude and recurrence intervals, which are required to forecast future levels of ground shaking (Cornell, 1968).

Deleted: these attributes

Deleted: (Christophersen et al., 2015). However, given the lack of chronostratigraphic control for faulted surfaces in southern Malawi, no direct measurements of these attributes can be assigned to faults in the SMAFD.

Deleted: Indeed, as noted in the introduction, obtaining these parameters is difficult

Deleted: in

Deleted: for a small number of faults

Deleted: Instead,

Deleted: fault slip rates

Deleted: ,

Deleted: an entire plate boundary

Deleted: also

alternative hypotheses that are inherent to this approach can, in common with seismic hazard practice elsewhere, be explored with a logic tree approach (Fig. 6; Field et al., 2014; Vallage and Bollinger, 2019; Villamor et al., 2018). We use the South Malawi Seismogenic Source Database (SMSSD) as an example of how this approach can be applied to narrow (<100 km width; Buck, 1991) amagmatic continental rifts, where the distribution of regional strain between border faults and intrabasin faults is well constrained by previous studies (Agostini et al., 2011a; Corti, 2012; Gupta et al., 1998; Morley, 1988; Muirhead et al., 2016, 2019; Nicol et al., 1997; Shillington et al., 2020; Wedmore et al., 2020a; Wright et al., 2020).

4.1 Earthquake source geometry

Faults may rupture both along their entire length and in smaller individual section ruptures that are often bounded by changes in fault geometry (DuRoss et al., 2016; Goda et al., 2018; Gómez-Vasconcelos et al., 2018; Hodge et al., 2015; Iezzi et al., 2019; Valentini et al., 2020). Therefore, the basic GIS feature in the SMSSD is a fault section, where individual faults from the SMAFD may be divided into multiple sections by bends in their fault trace (Fig. 2d; DuRoss et al., 2016; Jackson and White, 1989; Wesnousky, 2008; Zhang et al., 1991). Along-strike minima in fault displacement (e.g. scarp or knickpoint height) may also be indicative of segmentation (Willemse, 1997), but these do not always coincide with geometrical complexities in southern Malawi (Fig. 4; Hodge et al., 2018a, 2019; Wedmore et al., 2020a, 2020b). This may indicate that deeper structures, not visible in the surficial fault geometry, are also influencing fault segmentation (Wedmore et al., 2020b). Therefore, where along-strike scarp height measurements exist, these local minima are also used to define fault sections (Figs. 2d and 4).

Faults that are closely spaced across strike, but not physically connected, may also rupture together through 'soft linkages' (Childs et al., 1995; Wesnousky, 2008; Willemse, 1997; Zhang et al., 1991).

Deleted: ¶
¶
The

Deleted: MAFD

Deleted: is used

Deleted: here

Deleted: a

Deleted: (

Deleted: al

Deleted: theoretical and observational

Deleted: However, this framework could be adapted to other tectonic regions with well mapped active faults, few on-fault slip rate measurements, and where the partitioning of regional geodetic strain is, to an extent, predictable; for example fold and thrust belts (Koyi et al., 2000; Poblet and Lisle, 2011) and strike-slip systems (Braun and Beaumont, 1995).

Deleted: ra

Deleted: Discrete faults that closely overlap across steps may also rupture together

In the SMSSD we follow empirical observations and Coulomb stress modelling that suggests that normal fault earthquakes may rupture across steps whose width is <20% of the combined length of the interacting sections, up to a maximum separation of 10 km (Biasi and Wesnousky, 2016; Hodge et al., 2018b), and we use this as a criteria to assign whether two *en echelon* faults in the SMSSD may rupture together.

A number of geometrical attributes are then assigned to both individual sections and whole faults in the SMSSD (Table 2). Section length (L_{sec}) is defined as the straight-line distance between section end points (Fig. 4b). This approach avoids the difficulty of measuring the length of fractal features, and accounts for the hypothesis that small-scale (<km scale) variations in fault geometry in southern Malawi may represent only near-surface complexity (depths <5 km), and that the faults are relatively planar at depth (Hodge et al., 2018a). However, it only provides a minimum estimate of section length. For segmented faults in the SMSSD, fault length (L_{fault}) is the sum of L_{sec}, otherwise L_{fault} is the distance between its tips (Fig. 4b). Since each GIS feature in the SMSSD represents a distinct earthquake source, we consider that L_{sec} and/or L_{fault} must be >~5 km, except in the case of linking sections that rupture only in whole fault ruptures. (Christophersen et al., 2015).

In southern Malawi, fault dip is either unknown or uncertain, because fault planes are rarely exposed, surface processes affect scarp angle (Hodge et al., 2020), and/or dip at depth is not constrained. This difficulty in measuring fault dip is common, and in these cases dip has been parametrised by using a range of reasonable values (Christophersen et al., 2015; Langridge et al., 2016; Styron et al., 2020). In the SMSSD, we therefore assign minimum, intermediate, and maximum dip values of 40°, 53°, and 65°, which encapsulates dip estimates from field data in southern Malawi (Hodge et al., 2018a; Williams et al., 2019), and earthquake focal mechanisms

Moved (insertion) [7]

Deleted: ¶

Deleted: We define an individual fault in the SMAFD as a collection of geomorphic traces that are capable of rupturing together in a single earthquake (Christophersen et al., 2015).

Deleted: E

Deleted: s

Deleted:

Deleted: rarel

Deleted: y

Deleted: >

Deleted: sections

Deleted: AFD

Deleted: are part of the same fault

Moved (insertion) [1]

Deleted: 'Sections' are portions of faults that have a distinct geometric, kinematic, or paleoseismic attribute (Christophersen et al., 2015; Litchfield et al., 2013; Styron et al., 2020). Except in the case of linking sections, they also represent distinct surface rupturing earthquake sources in PSHA and so should be >5 km in length (Christophersen et al., 2015). Given the lack of paleoseismic information on active faults in the SMAFD, sections are generally defined by geometrical boundaries such as bends or step-overs (Fig. 2d; DuRoss et al., 2016; Jackson and White, 1989; Wesnousky, 2008; Zhang et al., 1991). Along-strike minima in fault displacement (e.g. scarp or knickpoint height) may also be indicative of segmentation (Willemse, 1997), but these do not always coincide with geometrical complexities in southern Malawi (Fig. 4; Hodge et al., 2018a, 2019; Wedmore et al., 2020a, 2020b). This may indicate that deeper structures, not visible in the surficial fault geometry, are also influencing fault segmentation (Wedmore et al., 2020b). Therefore, where along-strike scrap height measurements exist, these local minima are also used to define fault sections (Figs. 2d and 4).¶ ¶

Deleted: refore

Deleted: n included in the SMSSD, which

Deleted: 3.5 Section and fault geometry attributes¶ The second set of attributes describes fault geometry, and these …

Deleted: l

Deleted: its

Deleted: possibly

Deleted: actually

Deleted: ly

Deleted: encountered, and in these cases dip is instead

Deleted: W

Deleted: follow this approach by

Deleted: ing

Deleted: minimu

Deleted: m

(Biggs et al., 2010; Ebinger et al., 2019), seismic reflection data (Mortimer et al., 2007; Wheeler and Rosendahl, 1994), and aeromagnetic surveys (Kolawole et al., 2018a) elsewhere in Malawi.

It is typically assumed that fault width (W) can be estimated by projecting the difference in lower and upper seismogenic depth into fault dip (δ), with the assumption that faults are equidimensional up to the point where W is limited by the thickness of the seismogenic crust (Christophersen et al., 2015):

$$W = \begin{cases} L_{fault}, & where\ L_{fault} \leq \dfrac{z}{\sin\delta}; \\ \dfrac{z}{\sin\delta}, & where\ L_{fault} > \dfrac{z}{\sin\delta} \end{cases} \tag{1}$$

In southern Malawi, both seismogenic thickness, z (30-35 km; Jackson and Blenkinsop, 1993; Craig et al., 2011), and δ (40°-65° as justified above) are poorly constrained, so a range of W values must be considered. Furthermore, ruptures unlimited by z are not necessarily equidimensional (Leonard, 2010; Wesnousky, 2008). In the SMSSD, we therefore estimate W from an empirical scaling relationship between fault length and W (Leonard, 2010):

$$W = C_1 L_{fault}^{\beta} \tag{2}$$

where L_{fault} > 5km, and where C_1 and β are empirically derived constants and equal 17.5 and 0.66 respectively for interplate dip-slip earthquakes (Leonard, 2010). As shown in Fig. 5c, by applying Eq. 2 estimates of W in the SMSSD are therefore consistent with: (1) observations of >1 length to width ratios for dip-slip earthquakes (Fig. 5c), and (2) the thick seismogenic crust in East Africa (i.e. W~40 km, Fig. 5c; Craig et al., 2011; Ebinger et al., 2019; Jackson and Blenkinsop, 1993; Lavayssière et al., 2019; Nyblade and Langston, 1995).

Deleted: In the GEM neotectonics database,

Deleted: is

Deleted: by

Deleted: z;

Deleted: not

Deleted: Fig. 5c, wWe therefore compare Eq. 1 with also consider an alternative approach where W is

Deleted: *estimat*

Deleted: ed using an

Deleted: Given that Eq. 2 is

Deleted: aspect

Deleted: ratios

Deleted: of faults when L_{fault} > 5 km

Deleted: nei

Deleted: for faults >50 km

Deleted: , it

When these equations are applied to the mapped length of faults in southern Malawi (Figs. 2 and 5a), both estimate W ~ 40 km, for its longest faults (L_{fault} > 50 km, Fig. 5c). Hence, Eq. 2 is consistent with observations of thick seismogneic crust in East Africa (Craig et al., 2011; Ebinger et al., 2019; Jackson and Blenkinsop, 1993; Lavayssière et al., 2019; Nyblade and Langston, 1995). However, for shorter faults (L_{fault} = 5-50 km), Eq. (2) estimates smaller values of W relative to the approach outlined in Eq. (1) (Fig. 5c). As noted above, this follows empirical observations that the aspect ratio of dip-slip earthquakes will be >1 where L_{fault} > 5 km. In this context, Eq. (2) provides more reasonable W estimates for 5-50 km long faults in south Malawi than Eq. (1) and makes little difference for longer faults; hence it is used preferred to estimate W in the SMAFD

Deleted: Furthermore, along with W, the Leonard (2010) regressions are used to estimate earthquake magnitudes and average displacement in the SMSSDAFD (Sect. 4.2), and so these parameters are all self-consistent.

4.2 Estimating fault slip rates

For a narrow amagmatic continental rift such as the EARS in southern Malawi, the first step to estimate slip rates is to divide the rift along its axis into its basins (Fig. 2b), and then within each basin, divide the mapped faults into border and intrabasin faults. We define border faults geometrically, as a fault located at the edge of the rift with the implicit assumption that all other mapped active faults are intrabasin faults (Fig. 2d; Ebinger, 1989; Gawthorpe and Leeder, 2000; Muirhead et al., 2019; Wedmore et al., 2020b). These geometric definitions have no direct implications for how displacement is partitioned among border and intrabasin faults.

The slip rate for each fault or fault section i is then estimated using the equation:

$$Slip\ rate\ (i) = \begin{cases} \dfrac{\alpha_{bf} v \cos(\theta(i) - \phi)}{n_{bf} cos\delta}, & for\ border\ faults \\ \dfrac{\alpha_{if} v \cos(\theta(i) - \phi)}{n_{if} cos\delta}, & for\ intrabasin\ faults \end{cases} \quad (3)$$

where θ(i) is the fault or fault section slip azimuth, v and ϕ are the horizontal rift extension rate and azimuth, α is a weighting applied to each fault depending on whether it is a border (α_{bf}) or intrabasin (α_{if}) fault, and it is divided by the number of mapped border faults (n_{bf}) or intrabasin faults (n_{if}) in each basin (Fig. 6). Though Eq. 3 is specific for rifts, it could be adapted in other tectonic settings where there is an *a priori* understanding of the rate and distribution of regional strain, for example to distribute regional strain between the basal detachment and thrust ramps in a fold and thrust belt (Poblet and Lisle, 2011), between multiple subparallel faults in a strike-slip system, or assess more complex strain partitioning between kinematically distinct fault populations in transtensional or transpressional systems (Braun and Beaumont, 1995).

Formatted: Normal

Deleted: *1*

Deleted: each of its

Deleted: al

Deleted: .

Deleted: al

Deleted: In the SMSSD, the EARS in southern Malawi is divided into individual basins as indicated in Fig. 2b.

Deleted:

Deleted:

Deleted: hen, t

Deleted: *al*

Deleted: al

Deleted: al

Deleted: graben

The distributed of v between border (α_{bf}) and intrabasin faults (α_{if}) in an amagmatic narrow rift, depends on factors such as total rift extension (Ebinger, 2005; Muirhead et al., 2016, 2019), rift obliquity (Agostini et al., 2011b), hanging-wall flexure (Muirhead et al., 2016; Shillington et al., 2020), lower crustal rheology (Heimpel and Olson, 1996; Wedmore et al., 2020a), and whether border faults have attained their maximum theoretical displacement (Accardo et al., 2018; Olive et al., 2014; Scholz and Contreras, 1998). In some incipient rifts like southern Malawi, extensional strain is observed to be localised (~80-90%) on its border faults (Muirhead et al., 2019; Wright et al., 2020). Furthermore, evidence from boreholes and topography indicates that border faults in southern Malawi have relatively small throws (<1000 m, Fig. S1), which combined with its thick seismogenic crust, indicates that the flexural extensional strain on its intrabasin faults is likely to be negligible (Billings and Kattenhorn, 2005; Muirhead et al., 2016; Wedmore et al., 2020a). However, detailed analysis of fault scarp heights across the Zomba Graben indicate that ~50% of extensional strain is currently distributed onto its intrabasin faults (Wedmore et al., 2020a). To account for this uncertainty in the SMSSD, lower, intermediate, and upper estimates of α_{bf} are set to 0.5, 0.7, and 0.9 respectively (Fig. 6). Since α_{if} = 1- α_{bf}, lower intermediate, and upper estimates are 0.1, 0.3, and 0.5 (Fig. 6).

Where distinct intrabasin faults kinematically interact across steps, we consider these as one fault in Eq. 3, as this equation is considering strain across, not along, the rift. For the Mwanza and Nsanje basins, no intrabasin faults are identified (Fig. 2b), so all the extension strain is assigned to their border faults (i.e. α_{bf} = 1). In the case of the Nsanje basin, however, this is extension is divided into increments of 30, 50, and 70% between the Nsanje fault and a border fault identified 25 km along strike in Mozambique (Fig. S1; Macgregor, 2015) to estimate its lower, intermediate, and upper slip rate.

Deleted: ¶
To estimate slip rates in the SMSMSSDAFD we therefore first divide the EARS in southern Malawi rift into its principal basinsgrabens (Makanjira, Zomba, and Lower Shire, Fig. 2ba). In addition, we include the Nsanje fault, which is located to the south of Malawi's principal EARS grabens (Fig. 2ba) and where it bounds a poorly defined section of the EARS with low footwall relief (~300 m) and no mapped intrabasinal faults. There is, however, an eastern border fault to this section of the rift that has been mapped 25 km along strike in Mozambique (Fig. BA2; Macgregor, 2015), and we group these two faults together into the same 'Nsanje' graben. We also include the Mwanza Fault, as the border fault of the ... [10]

Deleted: When considering how v is

Deleted: amongst

Deleted: al

Deleted: consideration should be given to

Deleted:

Deleted: As an

Deleted: amagmatic

Deleted: in southern Malawi

Deleted: expected

Deleted: the

Deleted: relatively small throws on the border faults

Deleted: of

Deleted: southern Malawi (<1000 m) and thick seismogenic ... [11]

Deleted: in the hanging wall (i.e.

Deleted: the

Deleted: al

Deleted:)

Deleted: (0.1-1.2%, see Appendix A for full analysis;

Deleted: al

Deleted: recognise

Deleted: SM

Deleted: AFD

Deleted: , with this uncertainty explored using a logic tree ... [12]

Deleted: α_{if} is the 'remainder' of the rift extension in each ... [13]

Deleted:),

Deleted: it is

Deleted: set to

Deleted: for lower, intermediate, and upper estimates

Deleted:

Deleted: graben

Deleted: B

Deleted: al

Field Code Changed

Deleted: A2

Deleted: , where the rift consists of just two border faults ... [14]

In the SMSSD, the horizontal extension rate, v, is taken from the plate motion vector between the Rovuma and Nubia plates at the centre of each individual basin (Table 3, Figs. 1b and S1) using the Euler poles reported in Saria et al. (2013). We use the Euler pole (as defined by a location and rotation rate) and the uncertainties associated with the Euler pole (defined by an error ellipse, Fig. A1) to calculate the plate motion and the plate motion uncertainty between the Rovuma-Nubia plates for each basin (Table 3, Fig. 1b) following the methods outlined in Robertson et al. (2016). With this approach, the lower bound of v is negative (i.e. the plate motion is contractional, Table 3). However, the topography and seismicity of southern Malawi clearly indicate it is not a contractional regime, nor is it a stable craton. A lower bound of 0.2 mm/yr horizontal extension is therefore assigned in the SMSSD, which is considered the minimum strain accrual that is measurable using geodesy (Calais et al., 2016). There are no geodetic constraints for the extension rate across the Mwanza basin as it lies along the poorly defined Angoni-San plate boundary (Daly et al., 2020). We therefore assign this basin an extension rate of 0.2-1 mm/yr. This reflects the smaller escarpment height along its border fault (250 m vs ~750 m; Fig. 2b) relative to the Lower Shire Basin, which indicates a slower average extension rate over geological time.

The rift extension azimuth (ϕ) in southern Malawi is derived from a regional focal mechanism stress (073°± 012°, Fig. 1b; Delvaux and Barth, 2010; Ebinger et al., 2019; Williams et al., 2019) as there is considerable uncertainty in this parameter from geodesy (Table 3; Saria et al., 2013). Faults in southern Malawi are considered to be normal (Delvaux and Barth, 2010; Hodge et al., 2015; Williams et al., 2019). Therefore, the slip azimuth ($\theta(i)$) is the dip direction of each fault or fault section, where it is then projected into ϕ in Eq. 3. Although this sets up an apparent inconsistency in which variably striking faults accommodate normal dip-slip under a uniform extension direction, this phenomena that can be explained by lateral heterogeneity in the lower crust in southern Malawi

Deleted: SM

Deleted: AFD

Deleted: graben

Deleted: 2

Deleted: A2

Deleted: B1

Deleted: each graben/half-graben

Deleted: 2

Deleted: 2

Deleted: SM

Deleted: AFD

Deleted: Bs average

Deleted: Along with uncertainty in v, there is also considerable uncertainty in the rift extension azimuth (ϕ) in southern Malawi from geodesy (Table 32) due to the poorly constrained Euler pole (Saria et al., 2013). Independent measurements of regional stress and strain in southern Malawi

Deleted: through

Deleted: inversions, however, provide tighter constraints on ϕ

Deleted: taken from

Deleted: , and so we instead incorporate this additional prior knowledge into the SMSMSSDAFD for all grabens. ¶
¶
As discussed in Sect. 2.3 earthquake focal mechanisms and fault slickensides in southern Malawi indicate that faults accommodate normal dip-slip motion, regardless of strike; a

(Corti et al., 2013; Philippon et al., 2015; Wedmore et al., 2020a; Williams et al., 2019). To account for the uncertainty in ϕ, upper and lower extension rates are obtained by varying ϕ ±012° depending on the fault's dip direction (e.g. upper slip rate estimates for NE and NW dipping fault are estimated with ϕ set to 061° and 085° respectively). An example of these slip rate calculations for the central section of the Chingale Step fault is provided in Fig. 7.

4.3 Earthquake magnitudes and recurrence intervals

We estimate earthquake magnitudes in the SMSSD by applying empirically derived scaling relationships between fault length and earthquake magnitude. Scaling relationships between fault length and average single event displacement ($\bar{D}$) can then be combined with slip rate estimates to calculate earthquake recurrence intervals (R) through the relationship $R=\bar{D}$/slip rate (Wallace, 1970). To select an appropriate set of earthquake scaling relationships for the SMSSD, we consider three previously reported regressions, and apply them to its mapped faults: (1) between normal fault length and M_W (Wesnousky, 2008), (2) interplate dip-slip fault length and M_W (Leonard, 2010), and (3) fault area and M_W (Wells and Coppersmith, 1994) where A is calculated using W derived from Eq. (1).

We find that although generally comparable, for M_W <7.5, the Wells and Coppersmith (1994) regression overestimates magnitudes relative to Leonard (2010) (Fig. 5d). This likely reflects the discrepancy in W between applying Eq. (1) and the Leonard (2010) regression (Eq. (2), Fig. 5c, Sect. 4.1). The Wesnousky (2008) regression overestimates magnitudes for M_W <6.9 relative to Leonard (2010) equations and underestimates them at larger magnitudes (Fig. 5d). This may reflect that the Wesnousky (2008) regression is derived from only 6 events, and these events show a poor correlation between length and M_W (Pearson's regression coefficient = 0.36). Given these considerations, the Leonard (2010) regressions are used in the SMSSD. Furthermore, these

Deleted: Therefore, the slip azimuth (θ(i)) is equivalent to the dip direction of the fault or fault section (Fig. 6, Table 21). It is then necessary to project θ(i) into ϕ in Eq. (3) as these parameters are not necessarily aligned.

Deleted: from

Deleted: by

Deleted: , so that the difference between ϕ and θ tends towards 0° or 180°

Deleted: In converting extension rate to fault slip rate, δ is varied between 40-65° as discussed in Sect. 3.5 (Fig. 6). Finally, unlike in the GEM neotectonic fault database, only the dip-slip rate is reported in the SMAFD as the assumption of normal faulting implies that this is equal to the net slip rate.

Deleted: *2*

Deleted: *s*

Deleted: *ource attributes*

Deleted: The next set of attributes in the GEM neotectonics fault database are related to a fault's earthquake source attributes (i.e. earthquake magnitudes and recurrence intervals, R; Table 1). Although these would ideally be assigned based on historical seismicity or paleoseismicity, where this information is lacking

Deleted: ,

Deleted: can by estimated using

Deleted: ¶
Potential errors exist in the datasets from which earthquake scaling relationships are derived, because of: (1) the possible use of inaccurate historical datasets (Stirling et al., 2013), (2) underestimates of rupture length caused by the low preservation potential of small displacement rupture tips (Hemphill-Haley and Weldon, 1999), and (3) overestimates of $\bar{D}$ from the tendency for paleoseismic investigations to target the largest scarps along a fault (DuRoss, 2008). Furthermore, in the case of southern Malawi, relatively few events from regions with thick seismogenic crust are included in these datasets, and earthquakes in such crust may follow difference scaling relationships (Hodge et al., 2020; Rodgers and Little, 2006; Smekalin et al., 2010). ¶
¶

Deleted: SMAFD

Deleted: moment magnitude

Deleted: Results are shown in Fig. 5d, which indicates

Deleted: 3

Deleted: 5

Deleted:

Deleted: above observations,

Deleted: are applied to

Deleted: SMAFD

regressions are used to estimate *W* (Sect. 4.1) and are self-consistent when estimating M_W and $Đ$ from L_{fault}, which is not necessarily true for the other cases.

M_W and $Đ$ are therefore estimated in the SMSSD by:

$$M_W(i) = \begin{cases} \dfrac{\left(\frac{5}{2}\log L_{sec} + \frac{3}{2}\log C_1 + \log C_2\mu\right) - 9.09}{1.5}, & for\ individual\ section\ ruptures \\ \dfrac{\left(\frac{5}{2}\log L_{fault} + \frac{3}{2}\log C_1 + \log C_2\mu\right) - 9.09}{1.5}, & for\ whole\ fault\ ruptures \end{cases} \tag{4}$$

$$\log Đ(i) = \begin{cases} \frac{5}{6}\log L_{sec} + \frac{1}{2}\log C_1 + \log C_2\mu, & for\ individual\ section\ ruptures \\ \frac{5}{6}\log L_{fault} + \frac{1}{2}\log C_1 + \log C_2\mu, & for\ whole\ fault\ ruptures \end{cases} \tag{5}$$

where μ is the shear modulus (3.3×10^{10} Pa), C_1 is as defined for Eq. (2), and C_2 is another constant derived by Leonard (2010). Both constants are varied between the full range of values derived in a least square analysis (Leonard, 2010) to obtain, lower, intermediate and upper estimates of M_W and $Đ$ (Figs. 6 and 7). Following Eq. (5), recurrence intervals $R(i)$ can be calculated through:

$$R(i) = \frac{Đ(i)}{Slip\ rate(i)} \tag{6}$$

Where upper estimates of *R* are calculated by dividing the upper estimate of $Đ$ by the lowest estimate of fault/section slip rate and vice versa (Fig. 6). An example of these earthquake source calculations for the central section of the Chingale Step fault is provided in Fig. 7.

Deleted: Furthermore, these regressions are already used to estimate *W* (Sect. 4.1) and are self-consistent when estimating M_W and $Đ$, which is not necessarily true for the other cases.

We recognise that segmented normal faults may rupture in both individual sections, as demonstrated in Malawi by the Karonga earthquake sequence (Biggs et al., 2010; Fagereng, 2013), and whole fault ruptures (DuRoss et al., 2016; Goda et al., 2018; Gómez-Vasconcelos et al., 2018; Hodge et al., 2015; Iezzi et al., 2019; Valentini et al., 2020).

Deleted: for each section (except linking sections) or fault *i* in the SMAFD

Deleted: therefore

Deleted: as

Deleted: crust's

Deleted: the same empirically derived constant used in

Deleted: .

Deleted: , lower, intermediate, and upper estimates of each fault or section's

Deleted:

4.3 Miscellaneous attributes

For each fault, a data completeness score is given, where 1 is the highest and 4 is the lowest (Table 1). This score represents the data quality of the trace, fault geometry, and slip rate attributes (Christophersen et al., 2015). In the SMAFD, the highest score is 2, given the uncertainty on fault slip rates and dip. Following the GEM template, other information for each fault includes the date of the most recent event, references for published fault mapping or derivation of fault attributes, the date that the information was last updated, the compiler of the information, and free text details recorded as 'Fault Notes' (Table 1).

5. Key features of the SMAFD and SMSSD

In this section, we briefly describe the fault mapping collated in the SMAFD, and then the present fault slip rates, earthquake magnitudes, and recurrence intervals in the SMSSD as estimated by our systems-based approach.

5.1 Border and intrabasin faults in southern Malawi

The SMAFD contains 23 active faults across five EARS basins. The northernmost faults lie in the NW-SE trending Makanjira Graben, a full graben where two border faults, the Makanjira and Chirobwe-Ncheu, clearly define either side of the rift (Fig. 8a). Four intrabasin faults are identified, with, two of them, the Bilila-Mtakataka and Malombe faults, exhibiting steep scarps (Hodge et al., 2018a, 2019). In particular, one-dimensional diffusional models of scarp degradation suggest the Bilila-Mtakataka fault scarp formed within the past 10,000 years (Hodge et al., 2020). The Malombe fault forms a ~500 m high escarpment that bounds the Shire Horst and which divides post-Miocene deposits in the Makanjira Graben across strike (Fig. 8a; Hodge et al., 2019; Laõ-Dávila et al., 2015).

Along-strike to the south, the NNE-SSW trending Zomba Graben contains a prominent border fault, the Zomba fault, on its eastern edge, and three well defined intrabasin fault scarps in its interior (Fig. 8b; Bloomfield, 1965; Wedmore et al., 2020a). The western edge of the Zomba Graben grades onto the Kirk Plateau where there are several deeply incised N-S trending valleys that have been previously mapped as 'Rift Valley faults' (Fig. 8b; Bloomfield and Garson, 1965). However, only one of these faults has an active scarp and accumulated post-Miocene sediments (the Lisungwe fault; Wedmore et al., 2020a). In addition, the Wamkurumadzi fault, which lies to the west of the Lisungwe, is also included in the SMAFD -albeit with low confidence- as evidence of recent activity is noted by Bloomfield and Garson, (1965), and any recent sediments may have been eroded by the Wamkurumadzi river that flows along its base. Given the complex topography and ambiguity on

Formatted: Heading 2, No bullets or numbering

Deleted: grabens/half grabens

Deleted:

Deleted: F

Deleted: ,

Deleted: several

Field Code Changed

Deleted: (

Deleted: i

Deleted: is

fault activity, we tentatively interpret these faults as intrabasin faults in the SMSSD and note that the western Zomba Graben should be a priority area for future fault mapping.

The floor of the NW-SE trending Lower Shire Basin lies at an elevation 350 m lower than the floor of the Zomba Graben. Between these two EARS sections, basement is exposed, and there is no evidence of tectonic activity that falls within the SMAFD definition of an active fault. Gravity surveys and topographic data indicate that the Lower Shire Basin exhibits a half-graben structure, with the Thyolo Fault bounding it to the northeast (Fig. 8d; Chisenga et al., 2019; Wedmore et al., 2020b). A number of intrabasin faults have been identified in the hanging-wall of the Thyolo Fault (Chisenga et al., 2019), however, none are identified in the Nsanje and Mwanza basins (Figs. 8d and e).

5.2 Fault slip rates, and earthquake magnitudes and recurrence intervals in the SMSSD

By implementing a logic tree approach to assess uncertainty in the SMSSD, three values (lower, intermediate, and upper) are derived for each calculated attribute (Table 2, Fig. 6). However, it is implicit that the upper and lower values have a low probability as they require a unique, and possibly unrealistic, combination of parameters. We therefore primarily report values obtained from applying the intermediate branches in the logic tree but discuss the uncertainties in Sect. 5.4.

Though the SMAFD contains 23 active faults, in the SMSSD these are further subdivided into 74 sections, of which 13 are linking sections. Section lengths (L_{sec}) range between 0.7-62 km, whilst fault lengths (L_{fault}) varies from 6.2 to 144 km (Fig. 5a, Table 4). The highest slip rates are estimated to be on the Thyolo and Zomba faults (intermediate estimates 0.6-0.8 mm/yr). On intrabasin faults in the SMSSD, intermediate slip rate estimates are 0.05-0.1 mm/yr (Fig. 9). Slip rates tend to be relatively fast in the Makanjira Graben (Fig. 9c), as the extension rate is higher (Table 3), and its

Deleted:
Deleted: The Lower Shire Basin is bounded to the northeast by the Thyolo fault
Deleted: al
Deleted: Between the Thyolo and Panga faults, there is a ~40 km wide region of distributed deformation that includes a number of blind faults that were identified by gravity surveys
Deleted: .
Deleted: We do not interpret the Panga Fault as a border fault as it is possible that the this rift section may extend further across strike to the SW, where it is commensurate with the south eastern end of the Zambezi Rift (Daly et al., 2020).
Deleted: Along strike from the Lower Shire Graben, the rift is interpreted to extend to the
Deleted: Basin to the south and Mwanza Basin to the northwest. In both cases, the EARS in this part of southern ... [15]
Formatted: Normal, No bullets or numbering
Deleted: *l*
Deleted: *t geometry,*
Deleted: *earthquake source attributes*
Deleted: Below, we present the results of applying the ... [16]
Deleted: SM
Deleted: AFD
Deleted: 1
Deleted: , with the range of values obtained by applying the ... [17]
Deleted: , by using a logic tree approach,
Deleted: these
Deleted: associated with our estimates approach
Deleted: 3
Deleted: 67
Deleted: XX
Deleted: In total, the SMAFD contains 20 active faults,
Formatted: Font: Not Italic
Deleted: *which comprise a total of 53 sections and 82 traces* ... [18]
Deleted: s
Deleted: 6
Deleted: 0
Deleted: 11
Deleted: 150
Deleted: 3
Deleted: By applying Eq. (2), fault width (*W*) is typically <30 ... [19]
Deleted: al
Deleted: SM
Deleted: AFD
Deleted: 8
Deleted: 8
Deleted: 2

NNW-SSE striking faults are more optimally oriented to the regional extension direction (Fig. 2). The difference between upper and lower slip rate estimates in the SMSSD logic tree is two orders of magnitude; ~0.05-5 mm/yr for the border faults and ~0.005-0.5 mm/yr on the intrabasin faults (Fig. 9).

For whole fault ruptures along border faults, intermediate estimate of earthquake recurrence intervals (*R*) are between 2000-5000 years and for intrabasin whole fault ruptures 10,000-30,000 years (Fig. 10a-c). Considerable uncertainty exists with these values, with the upper and lower estimates for *R* varying from 10^2-10^5 years and ~10^3-10^6 years for border and intrabasin whole fault ruptures respectively (Fig. 10a-c). Furthermore, if these faults rupture in individual sections, *R* may be reduced by up to an order of magnitude (Fig. 10d-f). Intermediate estimates of earthquake magnitudes range from M_W 5.4 to M_W 7.2 for individual section ruptures, and M_W 5.6 to M_W 7.8 for faults that rupture their entire length (Table 4, Fig. 11b). The SMSSD also includes one example where multiple *en-echelon* faults, the Panga Fault System (Fig. 2d), could rupture together given the constraints outlined in Sect 4.1.

5.3 Robustness of fault slip rate estimates

It is possible that slip rate estimates in the SMSSD are effectively upper bounds as some proportion of the geodetically derived rift extension may be accommodated by aseismic creep or along unrecognised faults. With regards to aseismic creep, the discrepancy between geodetic and seismic moment rates in Malawi implies that its faults are strongly coupled (Ebinger et al., 2019; Hodge et al., 2015). This is also consistent with the velocity-weakening behaviour of some samples from the rift in deformation experiments at lower crustal pressure-temperature conditions (Hellebrekers et al., 2019).

Deleted: AF

Deleted: al

Deleted: 8

Deleted: 10,000-30,000 years

Deleted: al

Deleted: 9

Deleted: y

Deleted: al

Deleted: 9

Deleted: 9

Deleted: 6

Deleted: 0

Deleted: 3

Deleted: 0

Deleted: of

Formatted: Font: Italic

Deleted: that

Deleted: imposed

Deleted:

Deleted: Notably, we document 12 faults with the potential for hosting earthquakes greater than the largest recorded event in southern Malawi (i.e. M_W> 6.7, Fig. 10b, assuming intermediate branches for scaling laws in Fig. 6), the largest of which would be a M_W 7.8 ± 0.5 complete rupture of the Bilila-Mtakataka or Mwanza faults.

Deleted: *2*

Deleted: The key advantage of the SMAFD and SMSSD in comparison to other fault mapsseismotectonic studies in made for the EARS (Chapola and Kaphwiyo, 1992; Daly et al., 2020; Delvaux et al., 2017; Macgregor, 2015) is that it provide slip rates estimates for all individual faults and fault sections (Fig. 98).

Deleted: , however,

Deleted: these

Deleted: on hitherto

Deleted: , in which case the SMAFD estimates are effectively upper bounds

Deleted: .

Deleted: , and the low *b*-value (~0.8) for seismicity in the Karonga region

Deleted: in Malawi

Deleted: further supported

Deleted: by

Moved down [5]: We cannot definitively account for blind faults, and we recommend that future PSHA in southern Malawi should still consider 'off-fault' distributed seismic sources by using the instrumental record (e.g. Field et al., 2014; Hodge et al., 2015; Stirling et al., 2012).

Conversely, the possible inclusion of inactive faults in the SMAFD and SMSSD would mean individual fault slip rates may be lower bounds. Without paleoseismic investigations and dating of offset surfaces in southern Malawi, it is difficult to test this point. Nevertheless, reactivation analysis that encompasses the range of fault orientations in southern Malawi indicates that these faults are favourably oriented in the current stress field (Williams et al., 2019). Therefore, even faults that have been inactive for a considerable time (up to the entire age of the EARS) could still theoretically be reactivated. We also note that slip rates of intrabasin faults in the North Basin of Lake Malawi over the last 75 ka (0.15-0.7 mm/yr; Shillington et al., 2020), are within the range of estimates of intrabasin faults in the SMSSD (Fig. 9).

5.4 Sensitivity analysis

Upper and lower estimates of *R* differ by up to three orders of magnitude in the SMSSD (Fig. 10). To investigate these uncertainties, we performed a multi-parameter sensitivity analysis following the methods presented in Box et al. (1978) and Rabinowitz and Steinberg (1991). Full details of this analysis are given in Appendix A. In summary, 7 parameters that contribute to uncertainty in *R* for the central section of the Chingale Step fault are considered (Table 5). By exploring all possible combinations in which these 7 parameters are set at their upper or lower estimates, 128 (i.e. 2^7) different values of *R* can be calculated. However, we instead considered 64 parameter combinations that were chosen following a fractional factorial design (Table S1; Box et al., 1978). In this way, parameter combinations that offer little insight into how a system works are omitted, thereby increasing the efficiency of this analysis at minimal cost to its validity (Rabinowitz and Steinberg, 1991). From these combinations, the natural log of the average value of *R* when a parameter (*k*) is set at its upper ($\overline{\ln R}(k+)$) and lower ($\overline{\ln R}(k-)$) value is calculated and the difference between these values defines the parameter effect (*A*; Rabinowitz and Steinberg, 1991):

Deleted: AF

Deleted: ts

Deleted: estimates are

Deleted: faulted

Deleted: We also note slip rates for intrabasinal faults in the North Basin of Lake Malawi (0.15-0.7 mm/yr), estimated from the vertical offset of a 75 ka horizon in seismic reflection data (Shillington et al., 2020), are within range of estimates of intrabasinal faults in the SMSSD.

Deleted: ¶
An additional comparisontest for the slip rate estimates in the SMSSAFD is provided by comparisons to slip rate estimatess for intrabasinal faults in the North Basin of Lake Malawi, which like southern Malawi represents an amagmatic section of the EARS where extension is localised on the border faults (Accardo et al., 2018). Here, Shillington et al. (2020) estimated slip rates of 0.15-0.7 mm/yr based on the 10-40 m vertical offset of a 75 ka horizon in seismic reflection data, and assuming fault dips of between 50-65°. These rates are consistent with the SMSMSSDAFD only if the upper estimate branches for intrabasinal fault slip rates in the logic tree are used (Fig. 98). Alternatively, high slip rates on intrabasinal faults in northern Malawi may reflect that this section of the EARS is extending more quickly (1-3 mm/yr) as it is further from the Nubia-Rovuma Euler pole (Fig. 1a; Saria et al., 2013; Stamps et al., 2018), and/or that intrabasinal faults in southern Malawi accommodate significantly less hanging-wall flexure (0.1-1.2% vs. 2.5-7%, Appendix BA; Shillington et al., 2020). In this context, the 0.05-0.1 mm/yr intermediate slip rate estimates for intrabasinal faults in the SMSSAFD may be consistent with these estimates in northern Malawi.¶

Deleted: ¶
Given intermediate slip rate estimates of 0.6-0.8 mm/yr (Fig. 8) and fault dips of 53º, the throw accumulated by the border faults in the Makanjira and Zomba grabens (~350-900 m, Table A1) would have accumulated in ~0.5-1 Ma. This is younger than the estimated age for EARS rifting in central and northern Malawi (4.5-25 Ma; Delvaux, 1995; McCartney and Scholz, 2016; Mesko, 2020; Mortimer et al., 2016; Roberts et al., 2012); however, it is unclear if this indicates that the lower border fault slip rate estimates (~0.05 mm/yr) in the SMAFD should be favoured, the onset of rifting occurred later in southern Malawi, or there are additional factors that have not been considered in this comparison (e.g. temporal variations in rift extension rate, footwall erosion). In either case, the range of border fault slip rate estimates in the ... [20]

Deleted: *3*

Deleted: AF

Deleted: 9

Deleted: B

Deleted: However, i

Deleted: 4

Deleted: by using a

Deleted: fractional factorial design (Box et al., 1978),

Deleted: carefully selected

Deleted: C

Deleted: at little cost to the analysis (Table B1).

$$A = \overline{\ln R}(k+) - \overline{\ln R}(k-) \tag{7}$$

This analysis indicates that R is most sensitive to uncertainties in the partitioning of strain between border and intrabasin faults in the rift (i.e. α_{if}/n_{if}), the rift extension rate (v), and the C_2 parameter in Eq. (5), and least sensitive to uncertainties in the rift's extension azimuth, and the C_1 parameter in Eq. (5) (Table 5). If, however, v and its associated uncertainties were estimated using a different Nubia-Rovuma Euler pole solution (Fig. A1, Table 3; Stamps et al., 2008), R estimates are least sensitive to v and most sensitive to C_2 (Table 5). There are no interaction effects between two separate parameters that may influence their effect on R (Table S2).

6. Discussion

6.1 Implications for seismic hazard in southern Malawi

The existence of active faults within southern Malawi poses a significant risk to the 7.75 million people living in this region (Malawi National Statistics Office, 2018), and adjacent to the rift in northern Mozambique (Fig. 11a). Furthermore, with population growth at an annual rate of 2.7% in southern Malawi (Malawi National Statistics Office, 2018) this risk will increase over the coming decades. The rapidly growing city of Blantyre (population 800,000; Malawi National Statistics Office, 2018), which is in the footwall of both the relatively fast slipping (intermediate estimates ~0.8 mm/yr) Zomba and Thyolo faults is at a particularly high risk (Fig. 11a).

Intermediate estimates in the SMSSD for M_W 5.4-7.8 earthquakes and fault recurrence intervals (R) of 10^3-10^4 years (Fig. 11) imply that southern Malawi's seismic hazard is characterised by infrequent large magnitude events. Indeed, faults in this region may host earthquakes comparable to the largest historical continental normal fault earthquakes (~M_W 7.5; Valentini et al., 2020); although

Deleted: al

Deleted: 4

Deleted: B1

Deleted: 2

Deleted: B2

Deleted: Finally, we note that there is no

Deleted: sensitivity

Deleted: B3

Deleted: These results are discussed further in Sect. 6.3

Deleted: *2*

Deleted: 0

Deleted: l

Deleted: arge

Deleted: 0

Deleted: There is therefore an urgent need to quantify the spatial and temporal distribution of this hazard through a PSHA that incorporates the earthquake source data collected in the SMSSAFD.

Formatted: Font: Italic

Deleted: Within the Global Active Faults Database, there are 2800 normal faults (Styron and Pagani, 2020). Of these faults, 241 (i.e. 8.6%) have lengths >100 km, compared to 20% of faults (4/20) in the SMAFD (Fig. 5a). Hence, southern Malawi contains an unusually large proportion of long faults. Furthermore, given that earthquake magnitude scales with fault length, faults in southern Malawi have the potential to host some of the largest continental normal fault earthquake globally (i.e, M_W >7.5, Fig. 11) Indeed, oOut of a global dataset of 61

Deleted: surface rupturing

Deleted: earthquakes

Deleted: ,

relatively rare >150 km long normal faults have been mapped elsewhere, and these would be capable of even larger events (Styron and Pagani, 2020).

6.2 Improving earthquake source estimates in the SMSSD

One of the purposes of collating the SMSSD was to identify current knowledge gaps in our understanding of active faulting and seismic hazard in southern Malawi. Our sensitivity analysis (Sect. 5.4) indicates that the two biggest factors contributing to uncertainty in *R* in the SMSSD is related to our understanding of the distribution and rate of extension (*v*) in southern Malawi (Table 5). In particular, there is considerable uncertainty in the position of the Nubia-Rovuma Euler pole (Fig. A1; Saria et al., 2013), and we would not expect such large differences between upper and lower fault slip rate estimates by following our systems-based approach elsewhere. Although the uncertainties associated with *v* in the SMSSD could be reduced if an alternative solution for the Nubia-Rovuma Euler pole was applied (Fig. A1, Tables 5 and S2; Stamps et al., 2008), this solution uses fewer Global Positioning System (GPS) sites and a shorter position time series (Saria et al., 2013). Therefore, in the short-term, the best refinements to *R* estimates may come from new regional geodetic data and further high resolution topographic analysis (e.g. Daly et al., 2020; Stamps et al., 2020; Wedmore et al., 2020a).

Directly measuring on-fault slip rates and paleoseismicity would provide more robust *R* estimates than the modelling derived-estimates in SMSSD. However, careful site selection would be required for these analyses in southern Malawi because of its potential for large (~10 m) single event displacements (Hodge et al., 2020). Furthermore, these investigations carry large inherent uncertainties in low strain rate regions like southern Malawi if only a few earthquakes are sampled, as these events may be temporally clustered (Nicol et al., 2006, 2016b; Pérouse and Wernicke, 2017; Taylor-Silva et al., 2020).

Deleted: , it is noted that…>150 km long normal faults >150 km long…ave been mapped elsewhere, and hence capable of hosting even larger earthquakes, have …these would be capable of even larger eventsbeen mapped elsewhere ... [21]

Deleted: only six events had a rupture length >50 km, and only one event (the 1887 M_W 7.5 Sonora earthquake) has a length >100 km (Valentini et al., 2020). Hence, the faults compiled within the SMAFD have the potential to produce the largest continental normal fault earthquake globally. However, low regional extension rates imply such events are likely to be very rare, with intermediate estimates of recurrence interval of 10^3-10^4 years (Figs. 109 and 110c).

Deleted: *6.3 Reducing uncertainties* ¶

Formatted: Heading 2

Deleted: *3.1.…Improving earthquake source estimates fault slip rate estimates* ... [22]

Deleted: As… noted in the introduction, o…e of the purposes of collating the SMSSDAFD ... [23]

Moved down [4]: Given the various aleatory (i.e. the uncertainty related to unpredictable nature of future event) and epistemic (i.e. the uncertainty due to incomplete knowledge and data) uncertainties in parameters used to derive earthquake recurrence intervals (*R*), lower and upper estimates differ by over three orders of magnitude (Fig. 9). Although such a range of estimates in a low strain rate region

Deleted: ¶ ¶ ... [24]

Deleted: AF

Deleted: 4.… In particular, we note ... [25]

Field Code Changed

Deleted: B1…1; Saria et al., 2013), and we would not expect such large differences between upper and lower fault slip rate ... [26]

Deleted: B…; Stamps et al., 2008), this solution uses fewer Global Positioning System (GPS) sites and a shorter position ... [27]

Deleted: An alternative approach to constrain *R* estimates would be to obtain on-fault slip rates and paleoseismic ... [28]

Formatted: Font: Italic

Deleted:

Moved (insertion) [2]

Deleted: due…ecause to…f itsthe…potential for large (~10 m) single event displacements …ADDIN CSL_CITATION ... [29]

Deleted: uncertainities

Deleted: variabili…in low strain rate regions like southern Malawity…if only a few earthquakes are sampled, in low ... [30]

Deleted: arthquakes

Deleted: ., as noted previously, this information is difficult to collect, and

Moved down [3]: currently very few records exist across the entire EARS (Delvaux et al., 2017; Zielke and Strecker, ... [31]

Deleted: This latter point reflects the fact that earthquakes may be temporally clustered in low strain rate regions ... [32]

Moved down [6]: elastic stress perturbations (Beanland and Berryman, 1989; Cowie et al., 2012; Harris, 1998; Wedmore

Moved (insertion) [3]

When considering how different rupture magnitude estimates in the SMSSD influence R, the main source of uncertainty is the C_2 parameter from the Leonard (2010) regressions (Table 5). This factor controls the amount of displacement for a given rupture area (Leonard, 2010). It is therefore likely related to earthquake stress drops, and uncertainty in C_2 in southern Malawi will only be reduced by recording more events here or in similar tectonic environments (i.e. normal fault earthquakes in regions with low (~1-10 mm/yr) extension rates and thick (20-35 km) seismogenic crust).

6.3 Incorporation of the SMSSD into Probabilistic Seismic Hazard Analysis

The SMSSD contains the attributes (earthquake magnitudes and R estimates) that allow it to be used as a source model for future PSHA in southern Malawi. However, in common with other low strain rate regions with limited paleoseismic information (e.g. Cox et al., 2012; Villamor et al., 2018), there are various aleatory (i.e. the uncertainty related to unpredictable nature of future event) and epistemic (i.e. the uncertainty due to incomplete knowledge and data) uncertainties. Firstly, as noted in Sect. 5.2, it is unrealistic that the intermediate, lower, and upper value of each attribute in the SMSSD logic tree has an equal probability (Fig. 6). This could be formalised by treating these attributes as continuous variables and assigning probability distribution functions to them.

Implicit in the R estimates in the SMSSD is that each earthquake source can only host events of two sizes: 'individual sections' and 'whole faults.' It therefore does not consider multi-segment ruptures that do not rupture the entire fault. Although not strictly the same, the SMSSD therefore follows many aspects of the characteristic earthquake model (i.e. each earthquake source only hosts event of *one* size) whose applicability remains contentious (Kagan et al., 2012; Page and Felzer, 2015; Stirling and Gerstenberger, 2018). An alternative approach to model R in southern Malawi would be to allow each fault to host a range of earthquake sizes that follow a frequency-magnitude distribution

Deleted: SMESD

Deleted: 4

Deleted: , ideally

Formatted: Outline numbered + Level: 2 + Numbering Style: 1, 2, 3, … + Start at: 3 + Alignment: Left + Aligned at: 0.63 cm + Indent at: 1.27 cm

Deleted: recurrence interval

Deleted: ,

Deleted: in its current form, the SMSSD logic tree is unweighted and so

Deleted: is assigned three discrete values (intermediate, lower, and upper) with

Deleted: However, as noted in Sect. 5.2, we consider the equal probability of these three values as unrealistic as the upper and lower estimates require a unique set of parameter combinations. To formalise this, future PSHA could

Deleted: , for example,

Deleted: variables, and

Moved (insertion) [4]

Deleted: Given the various aleatory (i.e. the uncertainty related to unpredictable nature of future event) and epistemic (i.e. the uncertainty due to incomplete knowledge and data) uncertainties in parameters used to derive earthquake recurrence intervals (R), lower and upper estimates differ by over three orders of magnitude (Fig. 9). Although such a range of estimates in a low strain rate region with limited paleoseismic information is common (e.g. Cox et al., 2012; Villamor et al., 2018) and can still be incorporated into PSHA using synthetic seismicity catalogues (Hodge et al., 2015), reducing uncertainties in these estimates in the SMAFD is an obvious priority.

Deleted: I

Deleted: *recurrence interval*

Deleted: Furthermore, a

Formatted: Font: Italic

Formatted: Font: Italic

that is consistent with its moment rate (Youngs and Coppersmith, 1985), with this moment rate derived from the instrumental record and data incorporated into the SMSSD.

Finally, there are likely active faults in Malawi that are not included in the SMAFD and SMSSD. We therefore recommend that future PSHA in southern Malawi should also consider 'off-fault' areal seismic sources by using the instrumental record (e.g. Field et al., 2014; Gerstenberger et al., 2020; Hodge et al., 2015; Morell et al., 2020; Stirling et al., 2012). Many of the challenges discussed above can be addressed through the creation of synthetic seismic catalogues, which are then used as a PSHA source (Hodge et al., 2015).

7. Conclusions

We describe a new systems-based approach that combines geologic and geodetic data to estimate fault slip rates and earthquake recurrence intervals in regions with little historical or paleoseismic earthquake data. This approach is used to develop the South Malawi Active Fault Database (SMAFD) and South Malawi Seismogenic Source Database (SMSSD), geospatial databases designed to direct future research and aid seismic hazard assessment and planning.

In the SMAFD, we document 23 active faults that have accumulated displacement during East African rifting in southern Malawi. In the SMSSD, fault slip rates, earthquake magnitudes, and recurrence intervals are estimated for the active faults compiled in the SMAFD. The SMSSD indicates the potential for M_W 6.5-7.8 earthquakes throughout southern Malawi. However, slow geodetically-derived extension rates (~1 mm/yr) imply low fault slip rates (0.001-5 mm/yr), and so the recurrence intervals of M_W >7 events are estimated to be 10^2-10^6 years. The large range of these estimated recurrence times reflects aleatory uncertainty on fault rupture scenarios and epistemic uncertainties in fault-scaling relationships, fault slip rates, and fault geometry. Sensitivity analysis

Deleted:

Deleted: ¶

Deleted: ¶
As noted in Sect. 5.3, blind faults may exist that are not included in the SMSSD, and so we recommend that future PSHA in southern Malawi should consider 'off-fault' distributed seismic sources by using the instrumental record (e.g. Field et al., 2014; Hodge et al., 2015; Stirling et al., 2012). By Reduced uncertainty in *R* estimates can also come from a more thorough investigation of the types (i.e. lengths) and probabilities of different rupture scenarios in the SMAFD. Notably, only end member scenarios are currently accounted for, as multi-segment ruptures that do not rupture the entire fault are not currently considered in the SMAFD. By defining faults to consist of sections capable of rupturing together in a single maximum magnitude earthquake (Christophersen et al., 2015), the rupture of multiple 'faults' is also not included in the SMSSD. However, given events such as the 2010 El Mayor-Cucapah (Fletcher et al., 2014) and 2016 Kaikōura earthquakes (Litchfield et al., 2018) in which the rupture 'jumped' unusually large distances (>5 km), the possibility of multi-fault earthquakes in southern Malawi should not be ruled out. Alternatively, faults in ... [34]

Moved (insertion) [6]

Moved (insertion) [5]

Deleted: *6.3.2. Constraining earthquake magnitudes and* ... [33]

Deleted: (e.g. inclusion of off-fault sources, incorporating ... [35]

Deleted: the

Deleted: source for the PSHA

Deleted: W.

Deleted: , and furthermore, the SMAFD and the SMSSD ... [36]

Deleted: ¶ ... [37]

Deleted: ¶

Deleted: *6.4 Development of new active fault databases in* ... [38]

Deleted: Here, we

Deleted: is then applied to faults in southern Malawi, which ... [39]

Deleted: of

Deleted: a

Deleted: The

Deleted: reveals that

Deleted: formed

Deleted: s

Deleted: lts with the potential for

Deleted: >7

Deleted: in

Deleted: exist across

Deleted: That earthquakes of such magnitude can occur ... [40]

Deleted: ¶ ... [41]

Deleted: S

Deleted: that the faults themselves have

Deleted: on the order of

suggests the biggest reduction in uncertainties would come from improved knowledge of fault slip rates through paleoseismic investigations or geodetic studies. Nevertheless, the combination of long, highly-coupled, low slip rate faults and a short (<65 years) instrumental record imply that the SMAFD and SMSSD are important sources of information for future seismic hazard assessments in the region. In this respect, the development of SMSSD is timely as the seismic risk of southern Malawi is growing due to rapid population growth, urbanisation, and seismically vulnerable building stock. Similar challenges exist elsewhere along the EARS, which may also be partially addressed by following the framework provided by the SMAFD and SMSSD.

Appendices

Appendix A: A multiparameter sensitivity analysis for recurrence interval estimates in the South Malawi Active Fault Database

Recurrence interval estimates in the South Malawi Seismogenic Database (SMSSD) vary by over three orders of magnitude (Fig. 10). These uncertainties are not unexpected in a region like Malawi with no paleoseismic data and an incomplete instrumental seismic record (Cox et al., 2012; Villamor et al., 2018), and can be accounted for in Probabilistic Seismic Hazard Assessment (PSHA) using synthetic seismicity catalogues (Hodge et al., 2015). Nevertheless, by conducting a sensitivity analysis on the logic tree approach used to calculate these recurrence intervals (Fig. 6), it is possible to determine which parameters contribute most to this uncertainty, and therefore guide future research directions that will help constrain them in future iterations of the SMSSD. This analysis is briefly described in the main text (Sect. 5.4, Table 5), and is documented fully below.

Here, we follow the multiparameter sensitivity analysis presented by Rabinowitz and Steinberg (1991). This study conducted sensitivity analysis for the parameters that feed into PSHA, where the

Deleted: AF

Deleted: is an

Deleted: within the rift

Deleted: AF

Deleted: . U

Deleted: provided by SMAFD

Deleted: Appendix A: Hanging-wall flexure in southern Malawi

The considerable amounts of throw (>1000 m) along a rift bounding fault can induce a significant amount of flexure within the lithosphere either side of the fault (Muirhead et al., 2016; Olive et al., 2014; Petit and Ebinger, 2000; Shillington et al., 2020). In the case of the hanging-wall, this is a downward flexure that can result in intrabasinal faults accommodating additional slip to that imparted by regional extension alone (Muirhead et al., 2016). This additional flexural strain must therefore be accounted for when considering the distribution of strain in southern Malawi.

Here, strain due to hanging-wall flexure is estimated in profiles across southern Malawi using the methodology described by Muirhead et al. (2016), which is based on the equations presented in Turcotte and Schubert (1982) and Billings and Kattenhorn (2005). or possible rift-widening when the Lower Shire Basin was reactivated during East African Rifting (Castaing, 1991)These flexural profiles are also compared to those made for the North Basin of Lake Malawi using the same method (Shillington et al., 2020). This method calculates flexure by considering a vertical line-load at the point of maximum deflection (i.e. at the upper contact of the border fault hanging wall, Fig. AA1). The deflection (ω) across a border fault hanging wall can then be estimated as:

$$\omega = \omega_0 e^{\frac{-x}{\alpha}} \cos\left(\frac{x}{\alpha}\right)$$

(A1)

where ω_0 is the maximum deflection, x is the position along a hanging wall profile from the deflecting fault (Fig. A1), and α is:

$$\alpha = \left[\frac{Eh^3}{(3\rho_0 g(1-\nu^2))}\right]^{\frac{1}{4}}$$

(A2)

where E is Young's Modulus, ν is Poisson's ratio (0.25), g is acceleration due to gravity (9.8 m/s^2), h is the thickness of elastic crust, which is assumed here to be the equivalent to the thickness of the seismogenic crust (30-35 km, Fig. A1; Jackson and Blenkinsop, 1993; Craig et al., 2011; Ebinger et al., 2019), and ρ_0 is crustal density, for which the average crustal density (2816 kg/m^3) for the Malawi Rift from a thr... [42]

Deleted: B

Deleted:

Deleted: Active Fault

Deleted: AF

Deleted: 9

Deleted: AF

Deleted: 3

Deleted: 4

output metric is the probability of exceedance of a given level of ground shaken. For the SMSSD, we adapt this method to test the sensitivity of seven parameters that are used to calculate earthquake recurrence intervals (R, Eq. A1, Table 5). This metric is chosen as it fully incorporates the aleatory uncertainties in rupture length, and epistemic uncertainties in fault slip rates and the Leonard (2010) scaling relationships (Fig. 6). This analysis is performed for the Chingale Step fault central section (Fig. 4), where like all intrabasin faults in the SMSSD, R is calculated by:

$$R = \frac{\left(\frac{5}{6} logL + \frac{1}{2} logC_1 + logC_2\right)\left(n_{if} cos\delta\right)}{\alpha_{if} v cos\left(\theta - \phi\right)} \quad (A1)$$

Where L is rupture length and depends on whether an individual section (L_{sec}) or whole fault (L_{fault}) rupture is considered, C_1 and C_2 are empirically derived constants from Leonard (2010), δ is fault dip, θ is the fault slip azimuth, v and ϕ are the rift extension rate and azimuth, α_{if} is a weighting of rift extension for intrabasin faults, and n_{if} is the number of mapped intrabasin faults (n_{if}) in the basin.

Eq. A1 is essentially a combination of Eqs. 3, 5, and 6 in the main text, and its application with the SMSSD logic tree to calculate R for the Chingale Step fault central section is shown in Fig. 7. There are 5 intrabasin faults in the Zomba Graben where the Chingale Step fault is situated (Fig. 2), and in this analysis, this parameter is not treated as an uncertainty. However, for simplicity, it is combined with α_{if} to give the 'component of rift extensional strain' parameter, which is defined by α_{if}/n_{if} (Table 5). Assuming that the Chingale Step fault is a normal fault (Wedmore et al., 2020a; Williams et al., 2019), θ is the fault dip direction, and differs by only 4° depending on whether the whole fault ruptures or just the central section (Fig. 7). Hence uncertainity in this parameter is not considered here, and it is set at 290°, which is the average value for these two rupture scenarios. When assessing

Deleted: AF
Deleted: B1
Deleted: 4
Deleted: al
Deleted: AF
Deleted: B1
Deleted: al
Deleted: al
Deleted: graben
Deleted: B1
Deleted: AF
Deleted: al
Deleted: 4

the influence of v, we consider two geodetic models (Fig. A1; Saria et al., 2013; Stamps et al., 2008), and perform this sensitivity analysis for both.

Field Code Changed

Deleted: B

The method presented by Rabinowitz and Steinberg (1991) involves a two-level fractional factorial multiparameter design, where each parameter is restricted to the two levels which will give lower or upper estimates of R (Table 5). Ideally, these levels would be symmetric about the intermediate case, however, in the SMSSD this is not possible for the v, L, and C_2. Compared to a 'one at-a-time (OAT)' parameter analysis, a multiparameter analysis allows us to assess how different parameters interact with each other, and so more fully explore the parameter space (Rabinowitz and Steinberg, 1991). This is achieved through a factorial design, which for the seven parameters (k) tested here would generate 128 (i.e. 2^7) possible combinations in a full two-level factorial approach. However, in a fractional factorial design, just a subset of these combinations is assessed. This approach recognises that many of the combinations in a full factorial design offer little insight into how a system works, and that this can instead be achieved at minimal cost to the results by considering a carefully selected subset of these combinations (Box et al., 1978; Rabinowitz and Steinberg, 1991). In this analysis, 2^{k-p} combinations are assessed where p is the number of generators and is set at 1. This results in the assessment of 64 combinations (Table S1) and a 'resolution' of 5, which means it is possible to estimate the main effects of each parameter (Eq. A2), interactions between two parameters (Eq. A3), but not interactions between three parameters (Box et al., 1978).

Deleted: 4

Deleted: AF

Deleted: B

Deleted: B2

Deleted: B3

The main effect (A) of one parameter (e.g. fault dip, δ) is quantified from the difference between the average of the natural log of recurrence interval ($\overline{\ln R}$) for the 32 combinations in Table S1 when a parameter was at its upper level (i.e. δ+ = 40°) and $\overline{\ln R}$ for the 32 combinations when the parameter was at its low level (i.e. δ- = 65°):

Deleted: B

$$A = \overline{lnR}(\delta +) - \overline{lnR}(\delta -)$$

(A2)

By applying a multiparameter approach it is also possible to the quantify parameter-parameter interaction effects, for example, if the effect of δ depends on the choice of rift extension azimuth (ϕ). To do this, the results in Table S1 can be divided into two sets with 2^{k-p-1} combinations each depending on which level of δ was applied. Following the table designs developed by Box et al. (1978), each set of 32 combinations will have 16 combinations when ϕ was at is upper level (ϕ+) and 16 combinations when ϕ was at its lower level (ϕ-). The effect of δ on each level of ϕ (i.e. δϕ) is then calculated from the corresponding averages differences in $\overline{\ln R}$ (Rabinowitz and Steinberg, 1991):

$$\delta\phi = \left(\overline{lnR}(\delta + \phi +) - \overline{lnR}(\delta - \phi +)\right) - \left(\overline{lnR} - \overline{lnR}(\delta - \phi -)\right)$$

(A3)

If there is no interaction effect between these two parameters, then δϕ is 0. Otherwise, the size of the effect is proportional to the magnitude of δϕ. In addition, we demonstrate our results in terms of an empirical cumulative distribution function for the values of ln*R* reported in Table 1 (Fig. A2a), and following Rabinowitz and Steinberg (1991), values of *A* in a normal probability plot (Fig. A2b).

If the Saria et al. (2013) model is used to provide estimates of *v* in this sensitivity analysis, the parameter that contributes most to uncertainties of *R* in the SMSSD is the component of regional extensional strain that each fault accommodates (A = 3.05, Table 5). This essentially means that ln*R* is higher by 3.05 when this component is set at its high value compared to its lower, or that *R* is ~21 times ($e^{3.05}$) higher when 10% of regional extensional strain is assigned to the Chingale Step fault as opposed to 2%. The importance of this parameter is also demonstrated by the fact that it does not plot close to the normal distribution line in Fig. A2b. The parameters with the next highest main

Deleted: B2

Deleted: B

Deleted: $\delta+\phi--$

Deleted: B3

Deleted: B2a

Deleted: B1b

Deleted: AFD

Deleted: 4

Deleted: B1b

effect on R are v and C_2, whilst estimates of R are least sensitive to uncertainties in ϕ (Table 5). If, however, estimates of v are provided by the Stamps et al. (2008) model (Fig. A1), estimates of R are considerably less sensitive to uncertainites in rift extension rates, and the C_2 parameter has the biggest influence on R (Table 5). Multiparameter effects are all equal to zero (Table S2) regardless of geodetic model, and thus the sensitivity of each of these parameters is independent of changes in other parameters.

The results of the sensitivity analysis reported here are specific to estimates of R for the Chingale Step fault central section, however, results should be broadly applicable to all other faults in the SMSSD as R was calculated following the same steps. There will, however, be differences for faults that are not segmented (where L is not an uncertainty) or that have more than the three sections mapped along the Chingale Step fault (e.g. the seven section Bilila-Mtakataka fault). The uncertainty in the weighting of rift extension may also be different for border faults, as in these cases the weighting factor (α_{bf}) is varied between 0.5-0.9. The results of this analysis are discussed further in Sect. 5.4 and 6.2 in the main text.

Data Availability

The South Malawi Active Fault Database (SMAFD), South Malawi Seismogenic Source Database (SMSSD), and a GIS file for all other faults in Malawi are available in the supplement as Shapefiles. In addition, an excel file is included for the SMSSD where the earthquake source parameters were performed. All files are available under Creative Commons Attribution ShareAlike (CC-BY-SA 4.0) Licence 4.0.

Deleted: 4
Deleted: B1
Deleted: B2
Deleted: B3
Deleted: AF
Deleted: 3
Deleted: 3
Deleted: is
Deleted: S
Deleted: a

Author Contributions

JW and LW led the fault mapping from TanDEM-X data, and HM led the fault mapping using aeromagnetic data. All authors participated in the fieldwork. LW conducted analysis of geodetic data. JW designed the method to obtain fault slip rates and earthquake source parameters with input from all co-authors. JB and AF secured the funding for this project. All authors contributed to manuscript preparation, but JW had primary responsibility.

Competing interests

The authors declare that they have no conflict of interest.

Acknowledgements

This work is supported by the EPSRC-Global Challenges Research Fund PREPARE project (EP/P028233/1). TanDEM-X data were provided through DLR proposal DEM_GEOL0686. The Geological Survey Department of Malawi kindly gave us access to the 2013 aeromagnetic surveys across Malawi. We gratefully acknowledge thoughtful and constructive reviews from Richard Styron and Folarin Kolawole. We also thank Katsu Goda and Mark Stirling for useful discussions on developing this database, and Mike Floyd for his assistance with calculating geodetic extension rates from Euler Poles.

References

Accardo, N. J., Shillington, D. J., Gaherty, J. B., Scholz, C. A., Nyblade, A. A., Chindandali, P. R. N., Kamihanda, G., McCartney, T., Wood, D. and Wambura Ferdinand, R.: Constraints on Rift Basin Structure and Border Fault Growth in the Northern Malawi Rift From 3-D Seismic Refraction Imaging, J. Geophys. Res. Solid Earth, 123(11), 10,003-10,025, doi:10.1029/2018JB016504, 2018.

Agostini, A., Bonini, M., Corti, G., Sani, F. and Manetti, P.: Distribution of Quaternary deformation in the central Main Ethiopian Rift, East Africa, Tectonics, 30(4), doi:10.1029/2010TC002833, 2011a.

Agostini, A., Bonini, M., Corti, G., Sani, F. and Mazzarini, F.: Fault architecture in the Main Ethiopian Rift and comparison with experimental models: Implications for rift evolution and Nubia-Somalia kinematics, Earth Planet. Sci. Lett., 301(3–4), 479–492, doi:10.1016/j.epsl.2010.11.024, 2011b.

Ayele, A.: Probabilistic seismic hazard analysis (PSHA) for Ethiopia and the neighboring region, J. African Earth Sci., 134, 257–264, doi:10.1016/j.jafrearsci.2017.06.016, 2017.

Basili, R., Valensise, G., Vannoli, P., Burrato, P., Fracassi, U., Mariano, S., Tiberti, M. M. and Boschi, E.: The Database of Individual Seismogenic Sources (DISS), version 3: Summarizing 20 years of research on Italy's earthquake geology, Tectonophysics, 453(1–4), 20–43, doi:10.1016/j.tecto.2007.04.014, 2008.

Beauval, C., Marinière, J., Yepes, H., Audin, L., Nocquet, J. M., Alvarado, A., Baize, S., Aguilar, J., Singaucho, J. C. and Jomard, H.: A new seismic hazard model for ecuador, Bull. Seismol. Soc. Am., 108(3), 1443–1464, doi:10.1785/0120170259, 2018.

Biasi, G. P. and Wesnousky, S. G.: Steps and gaps in ground ruptures: Empirical bounds on rupture propagation, Bull. Seismol. Soc. Am., 106(3), 1110–1124, doi:10.1785/0120150175, 2016.

Biggs, J., Nissen, E., Craig, T., Jackson, J. and Robinson, D. P.: Breaking up the hanging wall of a rift-border fault: The 2009 Karonga earthquakes, Malawi, Geophys. Res. Lett., 37(11), doi:10.1029/2010GL043179, 2010.

Billings, S. E. and Kattenhorn, S. A.: The great thickness debate: Ice shell thickness models for Europa and comparisons with estimates based on flexure at ridges, Icarus, 177(2), 397–412, doi:10.1016/j.icarus.2005.03.013, 2005.

Bloomfield, K.: The geology of the Port Herald Area, Bull. Geol. Surv. Malawi, 9, 1958.

Bloomfield, K.: The Geology of the Zomba Area, Bull. Geol. Surv. Malawi, 16, 1965.

Bloomfield, K. and Garson, M. S.: The Geology of the Kirk Range-Lisungwe Valley Area, Bull. Geol. Surv. Malawi, 17, 1965.

Van Bocxlaer, B., Salenbien, W., Praet, N. and Verniers, J.: Stratigraphy and paleoenvironments of the early to middle Holocene Chipalamawamba Beds (Malawi Basin, Africa), Biogeosciences, 9(11), 4497–4512, doi:10.5194/bg-9-4497-2012, 2012.

Box, G. E. P., Hunter, W. G. and Hunter, J. S.: Statistics for experimenters, John Wiley and sons New York., 1978.

Brace, W. F. and Byerlee, J. D.: Stick-slip as a mechanism for earthquakes, Science (80-.)., 153(3739), 990–992, 1966.

Braun, J. and Beaumont, C.: Three-dimensional numerical experiments of strain partitioning at oblique plate boundaries: implications for contrasting tectonic styles in the southern Coast Ranges, California, and central South Island, New Zealand, J. Geophys. Res., 100(B9), doi:10.1029/95jb01683, 1995.

Buck, W. R.: Modes of continental lithospheric extension, J. Geophys. Res., 96(B12), doi:10.1029/91jb01485, 1991.

Calais, E., Camelbeeck, T., Stein, S., Liu, M. and Craig, T. J.: A new paradigm for large earthquakes in stable continental plate interiors, Geophys. Res. Lett., 43(20), 10,621-10,637, doi:10.1002/2016GL070815, 2016.

Castaing, C.: Post-Pan-African tectonic evolution of South Malawi in relation to the Karroo and recent East African rift systems, Tectonophysics, 191(1–2), 55–73, doi:10.1016/0040-1951(91)90232-H, 1991.

Chapola, L. S. and Kaphwiyo, C. E.: The Malawi rift: Geology, tectonics and seismicity, Tectonophysics, 209(1–4), 159–164, doi:10.1016/0040-1951(92)90017-Z, 1992.

Childs, C., Watterson, J. and Walsh, J. J.: Fault overlap zones within developing normal fault systems, J. - Geol. Soc., 152(3), 535–549, doi:10.1144/gsjgs.152.3.0535, 1995.

Chisenga, C., Dulanya, Z. and Jianguo, Y.: The structural re-interpretation of the Lower Shire Basin in the Southern Malawi rift using gravity data, J. African Earth Sci., 149(September), 280–290, doi:10.1016/j.jafrearsci.2018.08.013, 2019.

Christophersen, A., Litchfield, N., Berryman, K., Thomas, R., Basili, R., Wallace, L., Ries, W., Hayes, G. P., Haller, K. M., Yoshioka, T., Koehler, R. D., Clark, D., Wolfson-Schwehr, M., Boettcher, M. S., Villamor, P., Horspool, N., Ornthammarath, T., Zuñiga, R., Langridge, R. M., Stirling, M. W., Goded, T., Costa, C. and Yeats, R.: Development of the Global Earthquake Model's neotectonic fault database, Nat. Hazards, 79(1), 111–135, doi:10.1007/s11069-015-1831-6, 2015.

Clark, D., McPherson, A. and Van Dissen, R.: Long-term behaviour of Australian stable continental region (SCR) faults, Tectonophysics, 566–567, 1–30, doi:10.1016/j.tecto.2012.07.004, 2012.

Cornell, C. A.: Engineering seismic risk analysis, Bull. Seismol. Soc. Am., 58(5), 1583–1606, doi:http://dx.doi.org/10.1016/0167-6105(83)90143-5, 1968.

Corti, G.: Evolution and characteristics of continental rifting: Analog modeling-inspired view and comparison with examples from the East African Rift System, Tectonophysics, 522–523(1), 1–33, doi:10.1016/j.tecto.2011.06.010, 2012.

Corti, G., Philippon, M., Sani, F., Keir, D. and Kidane, T.: Re-orientation of the extension direction and pure extensional faulting at oblique rift margins: Comparison between the Main Ethiopian Rift and laboratory experiments, Terra Nov., 25(5), 396–404, doi:10.1111/ter.12049, 2013.

Cowie, P. A., Roberts, G. P., Bull, J. M. and Visini, F.: Relationships between fault geometry, slip rate variability and earthquake recurrence in extensional settings, Geophys. J. Int., 189(1), 143–160, doi:10.1111/j.1365-246X.2012.05378.x, 2012.

Cox, S. C., Stirling, M. W., Herman, F., Gerstenberger, M. and Ristau, J.: Potentially active faults in the rapidly eroding landscape adjacent to the Alpine Fault, central Southern Alps, New Zealand, Tectonics, 31(2), doi:10.1029/2011TC003038, 2012.

Craig, T. J., Jackson, J. A., Priestley, K. and Mckenzie, D.: Earthquake distribution patterns in Africa: Their relationship to variations in lithospheric and geological structure, and their rheological implications, Geophys. J. Int., 185(1), 403–434, doi:10.1111/j.1365-246X.2011.04950.x, 2011.

Daly, M. C., Green, P., Watts, A. B., Davies, O., Chibesakunda, F. and Walker, R.: Tectonics and Landscape of the Central African Plateau and their Implications for a Propagating Southwestern Rift in Africa, Geochemistry, Geophys. Geosystems, 21(6), doi:10.1029/2019GC008746, 2020.

Delvaux, D.: Age of Lake Malawi (Nyasa) and water level fluctuations, Mus. roy. Afrr. centr., Tervuren (Belg.), Dept. Geol. Min., Rapp. ann. 1993 1994, 108, 99–108, 1995.

Delvaux, D. and Barth, A.: African stress pattern from formal inversion of focal mechanism data, Tectonophysics, 482(1–4), 105–128, doi:10.1016/j.tecto.2009.05.009, 2010.

Delvaux, D., Mulumba, J. L., Sebagenzi, M. N. S., Bondo, S. F., Kervyn, F. and Havenith, H. B.: Seismic hazard assessment of the Kivu rift segment based on a new seismotectonic zonation model (western branch, East African Rift system), J. African Earth Sci., 134, 831–855, doi:10.1016/j.jafrearsci.2016.10.004, 2017.

Dixey, F.: The Nyasaland section of the great rift valley, Geogr. J., 68(2), 117–137, 1926.

Dixey, F.: The Nyasa-Shire Rift, Geogr. J., 91(1), 51–56, 1938.

Dulanya, Z.: A review of the geomorphotectonic evolution of the south Malawi rift, J. African Earth Sci., 129, 728–738, doi:10.1016/j.jafrearsci.2017.02.016, 2017.

DuRoss, C. B., Personius, S. F., Crone, A. J., Olig, S. S., Hylland, M. D., Lund, W. R. and Schwartz, D. P.: Fault segmentation: New concepts from the Wasatch Fault Zone, Utah, USA, J. Geophys. Res. Solid Earth, 121(2), 1131–1157, doi:10.1002/2015JB012519, 2016.

Ebinger, C.: Continental break-up: The East African perspective, Astron. Geophys., 46(2), 2.16-2.21, doi:10.1111/j.1468-4004.2005.46216.x, 2005.

Ebinger, C. J.: Tectonic development of the western branch of the East African rift system, Geol. Soc. Am. Bull., 101(7), 885–903, doi:10.1130/0016-7606(1989)101<0885:TDOTWB>2.3.CO;2, 1989.

Ebinger, C. J., Rosendahl, B. R. and Reynolds, D. J.: Tectonic model of the Malaŵi rift, Africa, Tectonophysics, 141(1–3), 215–235, doi:10.1016/0040-1951(87)90187-9, 1987.

Ebinger, C. J., Oliva, S. J., Pham, T. Q., Peterson, K., Chindandali, P., Illsley-Kemp, F., Drooff, C., Shillington, D. J., Accardo, N. J., Gallacher, R. J., Gaherty, J., Nyblade, A. A. and Mulibo, G.: Kinematics of Active Deformation in the Malawi Rift and Rungwe Volcanic Province, Africa, Geochemistry, Geophys. Geosystems, 20(8), 3928–3951, doi:10.1029/2019GC008354, 2019.

England, P. and Jackson, J.: Uncharted seismic risk, Nat. Geosci., 4(6), 348–349, doi:10.1038/ngeo1168, 2011.

Fagereng, Å.: Fault segmentation, deep rift earthquakes and crustal rheology: Insights from the 2009 Karonga sequence and seismicity in the Rukwa-Malawi rift zone, Tectonophysics, 601, 216–225, doi:10.1016/j.tecto.2013.05.012, 2013.

Field, E. H., Arrowsmith, R. J., Biasi, G. P., Bird, P., Dawson, T. E., Felzer, K. R., Jackson, D. D., Johnson, K. M., Jordan, T. H. and Madden, C.: Uniform California earthquake rupture forecast, version 3 (UCERF3)—The time-independent model, Bull. Seismol. Soc. Am., 104(3), 1122–1180, 2014.

Fritz, H., Abdelsalam, M., Ali, K. A., Bingen, B., Collins, A. S., Fowler, A. R., Ghebreab, W., Hauzenberger, C. A., Johnson, P. R., Kusky, T. M., Macey, P., Muhongo, S., Stern, R. J. and Viola, G.: Orogen styles in the East African Orogen: A review of the Neoproterozoic to Cambrian tectonic evolution, J. African Earth Sci., 86, 65–106, doi:10.1016/j.jafrearsci.2013.06.004, 2013.

Fullgraf, T., Zammit, C., Bailly, L., Terrier, M., Hyvonen, E., Backman, B., Karinen, T., Konnunaho, J., Thomas, R. and Tychsen, J.: Geological Mapping and Mineral Assessment Project (GEMMAP) of Malawi. Report Inception Phase - February 2017., 2017.

Gaherty, J. B., Zheng, W., Shillington, D. J., Pritchard, M. E., Henderson, S. T., Chindandali, P. R. N., Mdala, H., Shuler, A., Lindsey, N., Oliva, S. J., Nooner, S., Scholz, C. A., Schaff, D., Ekström, G. and Nettles, M.: Faulting processes during early-stage rifting: Seismic and geodetic analysis of the 2009-2010 Northern Malawi earthquake sequence, Geophys. J. Int., 217(3), 1767–1782, doi:10.1093/gji/ggz119, 2019.

Gawthorpe, R. L. and Leeder, M. R.: Tectono-sedimentary evolution of active extensional basins, Basin Res., 12(3–4), 195–218, doi:10.1111/j.1365-2117.2000.00121.x, 2000.

Gerstenberger, M. C., Marzocchi, W., Allen, T., Pagani, M., Adams, J., Danciu, L., Field, E. H., Fujiwara, H., Luco, N., Ma, K. F., Meletti, C. and Petersen, M. D.: Probabilistic Seismic Hazard Analysis at Regional and National Scales: State of the Art and Future Challenges, Rev. Geophys., 58(2), e2019RG000653, doi:10.1029/2019RG000653, 2020.

Goda, K., Gibson, E. D., Smith, H. R., Biggs, J. and Hodge, M.: Seismic risk assessment of urban and rural settlements around lake malawi, Front. Built Environ., 2, doi:10.3389/fbuil.2016.00030, 2016.

Goda, K., Kloukinas, P., Risi, R., Hodge, M., Kafodya, I., Ngoma, I., Biggs, J., Crewe, A., Fagereng, Å. and Macdonald, J.: Scenario-based seismic risk assessment for Malawi using improved information on earthquake sources and local building characteristics, in 16th European Conference on Earthquake Engineering, pp. 1–12., 2018.

Goitom, B., Werner, M. J., Goda, K., Kendall, J. M., Hammond, J. O. S., Ogubazghi, G., Oppenheimer, C., Helmstetter, A., Keir, D. and Illsley-Kemp, F.: Probabilistic seismic-hazard assessment for Eritrea, Bull. Seismol. Soc. Am., 107(3), 1478–1494, doi:10.1785/0120160210, 2017.

Gómez-Vasconcelos, M. G., Villamor, P., Procter, J., Palmer, A., Cronin, S., Wallace, C., Townsend, D. and Leonard, G.: Characterisation of faults as earthquake sources from geomorphic data in the Tongariro Volcanic Complex, New Zealand, New Zeal. J. Geol. Geophys., 1–12, 2018.

Gupta, H. K.: The Malawi earthquake of March 10, 1989: A report of the macroseismic survey, Tectonophysics, 209(1–4), 165–166, doi:10.1016/0040-1951(92)90018-2, 1992.

Gupta, S., Cowie, P. A., Dawers, N. H. and Underhill, J. R.: A mechanism to explain rift-basin subsidence and stratigraphic patterns through fault-array evolution, Geology, 26(7), 595–598, doi:10.1130/0091-7613(1998)026<0595:AMTERB>2.3.CO, 1998.

Habgood, F.: The geology of the country west of the Shire River between Chikwawa and Chiromo, Bull. Geol. Surv. Malawi, 14, 1963.

Habgood, F., Holt, D. N. and Walshaw, R. D.: The geology of the Thyolo Area, Bull. Geol. Surv. Malawi, 22, 1973.

Hamiel, Y., Baer, G., Kalindekafe, L., Dombola, K. and Chindandali, P.: Seismic and aseismic slip evolution and deformation associated with the 2009-2010 northern Malawi earthquake swarm, East African Rift, Geophys. J. Int., 191(3), 898–908, doi:10.1111/j.1365-246X.2012.05673.x, 2012.

Hart, E. and Bryant, W.: Fault-rupture hazard zones in California: Alquist-Priolo Earthquake Fault Zoning Act with Index to Earthquake Fault Zones Maps., 1999.

Heimpel, M. and Olson, P.: A seismodynamical model of lithosphere deformation: Development of continental and oceanic rift networks, J. Geophys. Res. Solid Earth, 101(B7), 16155–16176, doi:10.1029/96jb00168, 1996.

Hellebrekers, N., Niemeijer, A. R., Fagereng, Å., Manda, B. and Mvula, R. L. S.: Lower crustal earthquakes in the East African Rift System: Insights from frictional properties of rock samples from the Malawi rift, Tectonophysics, 767, 228167, doi:10.1016/j.tecto.2019.228167, 2019.

Hodge, M., Biggs, J., Goda, K. and Aspinall, W.: Assessing infrequent large earthquakes using geomorphology and geodesy: the Malawi Rift, Nat. Hazards, 76(3), 1781–1806, doi:10.1007/s11069-014-1572-y, 2015.

Hodge, M., Fagereng, A., Biggs, J. and Mdala, H.: Controls on Early-Rift Geometry: New Perspectives From the Bilila-Mtakataka Fault, Malawi, Geophys. Res. Lett., 45(9), 3896–3905, doi:10.1029/2018GL077343, 2018a.

Hodge, M., Fagereng and Biggs, J.: The Role of Coseismic Coulomb Stress Changes in Shaping the Hard Link Between Normal Fault Segments, J. Geophys. Res. Solid Earth, 123(1), 797–814, doi:10.1002/2017JB014927, 2018b.

Hodge, M., Biggs, J., Fagereng, A., Elliott, A., Mdala, H. and Mphepo, F.: A semi-automated algorithm to quantify scarp morphology (SPARTA): Application to normal faults in southern Malawi, Solid Earth, 10(1), 27–57, doi:10.5194/se-10-27-2019, 2019.

Hodge, M., Biggs, J., Fagereng, Mdala, H., Wedmore, L. N. J. and Williams, J. N.: Evidence From High-Resolution Topography for Multiple Earthquakes on High Slip-to-Length Fault Scarps: The Bilila-Mtakataka Fault, Malawi, Tectonics, 39(2), e2019TC005933, doi:10.1029/2019TC005933, 2020.

Iezzi, F., Roberts, G., Walker, J. F. and Papanikolaou, I.: Occurrence of partial and total coseismic ruptures of segmented normal fault systems: Insights from the Central Apennines, Italy., J. Struct. Geol., doi:10.1016/j.jsg.2019.05.003, 2019.

Ivory, S. J., Blome, M. W., King, J. W., McGlue, M. M., Cole, J. E. and Cohen, A. S.: Environmental change explains cichlid adaptive radiation at Lake Malawi over the past 1.2 million years, Proc. Natl. Acad. Sci. U. S. A., 113(42), 11895–11900, doi:10.1073/pnas.1611028113, 2016.

Jackson, J.: Living with earthquakes: Know your faults, J. Earthq. Eng., 5, 5–123, doi:10.1080/13632460109350530, 2001.

Jackson, J. and Blenkinsop, T.: The Malaŵi Earthquake of March 10, 1989: Deep faulting within the East African Rift System, Tectonics, 12(5), 1131–1139, doi:10.1029/93TC01064, 1993.

Jackson, J. and Blenkinsop, T.: The Bilila-Mtakataka fault in Malawi: an active, 100-km long, normal fault segment in thick seismogenic crust, Tectonics, 16(1), 137–150, doi:10.1029/96TC02494, 1997.

Jackson, J. A. and White, N. J.: Normal faulting in the upper continental crust: observations from regions of active extension, J. Struct. Geol., 11(1–2), 15–36, doi:10.1016/0191-8141(89)90033-3, 1989.

Jomard, H., Marc Cushing, E., Palumbo, L., Baize, S., David, C. and Chartier, T.: Transposing an active fault database into a seismic hazard fault model for nuclear facilities - Part 1: Building a database of potentially active faults (BDFA) for metropolitan France, Nat. Hazards Earth Syst. Sci., doi:10.5194/nhess-17-1573-2017, 2017.

Kagan, Y. Y., Jackson, D. D. and Geller, R. J.: Characteristic earthquake model, 1884-2011, R.I.P., Seismol. Res. Lett., 83(6), 951–953, doi:10.1785/0220120107, 2012.

King, A. W. and Dawson, A. L.: The Geology of the Mangochi-Makanjila Area, Bull. Geol. Surv. Malawi, 35, 1976.

Kloukinas, P., Novelli, V., Kafodya, I., Ngoma, I., Macdonald, J. and Goda, K.: A building classification scheme of housing stock in Malawi for earthquake risk assessment, J. Hous. Built Environ., 1–31, doi:10.1007/s10901-019-09697-5, 2019.

Kolawole, F., Atekwana, E. A., Laó-Dávila, D. A., Abdelsalam, M. G., Chindandali, P. R., Salima, J. and Kalindekafe, L.: Active Deformation of Malawi Rift's North Basin Hinge Zone Modulated by Reactivation of Preexisting Precambrian Shear Zone Fabric, Tectonics, 37(3), 683–704, doi:10.1002/2017TC004628, 2018a.

Kolawole, F., Atekwana, E. A., Laó-Dávila, D. A., Abdelsalam, M. G., Chindandali, P. R., Salima, J. and Kalindekafe, L.: High-resolution electrical resistivity and aeromagnetic imaging reveal the causative fault of the 2009 Mw 6.0 Karonga, Malawi earthquake, Geophys. J. Int., 213(2), 1412–1425, doi:10.1093/gji/ggy066, 2018b.

Langridge, R. M., Ries, W. F., Litchfield, N. J., Villamor, P., Van Dissen, R. J., Barrell, D. J. A., Rattenbury, M. S., Heron, D. W., Haubrock, S., Townsend, D. B., Lee, J. M., Berryman, K. R., Nicol, A., Cox, S. C. and Stirling, M. W.: The New Zealand Active Faults Database, New Zeal. J. Geol. Geophys., 59(1), 86–96, doi:10.1080/00288306.2015.1112818, 2016.

Laõ-Dávila, D. A., Al-Salmi, H. S., Abdelsalam, M. G. and Atekwana, E. A.: Hierarchical segmentation of the Malawi Rift: The influence of inherited lithospheric heterogeneity and kinematics in the evolution of continental rifts, Tectonics, 34(12), 2399–2417, doi:10.1002/2015TC003953, 2015.

Lavayssière, A., Drooff, C., Ebinger, C., Gallacher, R., Illsley-Kemp, F., Oliva, S. J. and Keir, D.: Depth Extent and Kinematics of Faulting in the Southern Tanganyika Rift, Africa, Tectonics, 38(0), doi:10.1029/2018TC005379, 2019.

Leonard, M.: Earthquake fault scaling: Self-consistent relating of rupture length, width, average displacement, and moment release, Bull. Seismol. Soc. Am., 100(5 A), 1971–1988, doi:10.1785/0120090189, 2010.

Litchfield, N., Van Dissen, R., Sutherland, R., Barnes, P., Cox, S., Norris, R., Beavan, R., Langridge, R., Villamor, P., Berryman, K., Stirling, M., Nicol, A., Nodder, S., Lamarche, G., Barrell, D., Pettinga, J., Little, T., Pondard, N., Mountjoy, J. and Clark, K.: A model of active faulting in New Zealand, New Zeal. J. Geol. Geophys., 57(1), 32–56, doi:10.1080/00288306.2013.854256, 2014.

Litchfield, N. J., Villamor, P., van Dissen, R. J., Nicol, A., Barnes, P. M., Barrell, D. J. A., Pettinga, J. R., Langridge, R. M., Little, T. A., Mountjoy, J. J., Ries, W. F., Rowland, J., Fenton, C., Stirling, M. W., Kearse, J., Berryman, K. R., Cochran, U. A., Clark, K. J., Hemphill-Haley, M., Khajavi, N., Jones, K. E., Archibald, G., Upton, P., Asher, C., Benson, A., Cox, S. C., Gasston, C., Hale, D., Hall, B., Hatem, A. E., Heron, D. W., Howarth, J., Kane, T. J., Lamarche, G., Lawson, S., Lukovic, B., McColl, S. T., Madugo, C., Manousakis, J., Noble, D., Pedley, K., Sauer, K., Stahl, T., Strong, D. T., Townsend, D. B., Toy, V., Williams, J., Woelz, S. and Zinke, R.: Surface rupture of multiple crustal faults in the 2016 Mw 7.8 Kaikōura, New Zealand, earthquake, Bull. Seismol. Soc. Am., 108(3B), 1496–1520, doi:10.1785/0120170300, 2018.

Lyons, R. P., Scholz, C. A., Cohen, A. S., King, J. W., Brown, E. T., Ivory, S. J., Johnson, T. C., Deino, A. L., Reinthal, P. N., McGlue, M. M. and Blome, M. W.: Continuous 1.3-million-year record of East African hydroclimate, and implications for patterns of evolution and biodiversity, Proc. Natl. Acad. Sci., 201512864, doi:10.1073/pnas.1512864112, 2015.

Macgregor, D.: History of the development of the East African Rift System: A series of interpreted maps through time, J. African Earth Sci., 101, 232–252, doi:10.1016/j.jafrearsci.2014.09.016, 2015.

Machette, M., Haller, K. and Wald, L.: Quaternary Fault and Fold Database for the nation. United States Geological Survey Fact Sheet. [online] Available from: https://pubs.usgs.gov/fs/2004/3033/FS2004-3033.pdf, 2004.

Macheyeki, A. S., Mdala, H., Chapola, L. S., Manhiça, V. J., Chisambi, J., Feitio, P., Ayele, A., Barongo, J., Ferdinand, R. W., Ogubazghi, G., Goitom, B., Hlatywayo, J. D., Kianji, G. K., Marobhe, I., Mulowezi, A., Mutamina, D., Mwano, J. M., Shumba, B. and Tumwikirize, I.: Active fault mapping in Karonga-Malawi after the December 19, 2009 Ms 6.2 seismic event, J. African Earth Sci., 102, 233–246, doi:10.1016/j.jafrearsci.2014.10.010, 2015.

Malawi, N. S. O.: 2018 Malawi Population & Housing Census Main Report, Gov. Malawi, 2018.

Manda, B. W. C., Cawood, P. A., Spencer, C. J., Prave, T., Robinson, R. and Roberts, N. M. W.: Evolution of the Mozambique Belt in Malawi constrained by granitoid U-Pb, Sm-Nd and Lu-Hf isotopic data, Gondwana Res., 68, 93–107, doi:10.1016/j.gr.2018.11.004, 2019.

McCalpin, J. P.: Paleoseismology, Academic press., 2009.

McCartney, T. and Scholz, C. A.: A 1.3 million year record of synchronous faulting in the hangingwall and border fault of a half-graben in the Malawi (Nyasa) Rift, J. Struct. Geol., 91, 114–129, doi:10.1016/j.jsg.2016.08.012, 2016.

Mesko, G.: Magmatism at the Southern End of the East African Rift System: Origin and Role During Early Stage Rifting, 2020.

Midzi, V., Hlatywayo, D. J., Chapola, L. S., Kebede, F., Atakan, K., Lombe, D. K., Turyomurugyendo, G. and Tugume, F. A.: Seismic hazard assessment in Eastern and Southern Africa, Ann. di Geofis., V42(No 6), 1067–1083, doi:10.4401/ag-3770, 1999.

Molnar, P.: Earthquake recurrence intervals and plate tectonics, Bull. Seismol. Soc. Am., 69(1), 115–133, 1979.

Morell, K. D., Styron, R., Stirling, M., Griffin, J., Archuleta, R. and Onur, T.: Seismic hazard analyses from geologic and geomorphic data: Current and future challenges, Tectonics, e2018TC005365, doi:10.1029/2018tc005365, 2020.

Morley, C. K.: Variable extension in Lake Tanganyika, Tectonics, 7(4), 785–801, doi:10.1029/TC007i004p00785, 1988.

Mortimer, E. J., Paton, D. A., Scholz, C. A., Strecker, M. R. and Blisniuk, P.: Orthogonal to oblique rifting: Effect of rift basin orientation in the evolution of the North basin, Malawi Rift, East Africa, Basin Res., 19(3), 393–407, doi:10.1111/j.1365-2117.2007.00332.x, 2007.

Mortimer, E. J., Kirstein, L. A., Stuart, F. M. and Strecker, M. R.: Spatio-temporal trends in normal-fault segmentation recorded by low-temperature thermochronology: Livingstone fault scarp, Malawi Rift, East African Rift System, Earth Planet. Sci. Lett., 455, 62–72, doi:10.1016/j.epsl.2016.08.040, 2016.

Muirhead, J. D., Kattenhorn, S. A., Lee, H., Mana, S., Turrin, B. D., Fischer, T. P., Kianji, G., Dindi, E. and Stamps, D. S.: Evolution of upper crustal faulting assisted by magmatic volatile release during early-stage continental rift development in the East African Rift, Geosphere, 12(6), 1670–1700, doi:10.1130/GES01375.1, 2016.

Muirhead, J. D., Wright, L. J. M. and Scholz, C. A.: Rift evolution in regions of low magma input in East Africa, Earth Planet. Sci. Lett., 506, 332–346, doi:10.1016/j.epsl.2018.11.004, 2019.

Ngoma, I., Kafodya, I., Kloukinas, P., Novelli, V., Macdonald, J. and Goda, K.: Building classification and seismic vulnerability of current housing construction in Malawi, Malawi J. Sci. Technol., 11(1), 57–72, 2019.

Nicol, A., Walsh, J. J., Watterson, J. and Underhill, J. R.: Displacement rates of normal faults, Nature, 390(6656), 157–159, doi:10.1038/36548, 1997.

Nicol, A., Walsh, J., Berryman, K. and Villamor, P.: Interdependence of fault displacement rates and paleoearthquakes in an active rift, Geology, 34(10), 865–868, doi:10.1130/G22335.1, 2006.

Nicol, A., Van Dissen, R. J., Stirling, M. W. and Gerstenberger, M. C.: Completeness of the Paleoseismic Active-Fault Record in New Zealand, Seismol. Res. Lett., 87(6), 1299–1310, doi:10.1785/0220160088, 2016a.

Nicol, A., Robinson, R., Van Dissen, R. J. and Harvison, A.: Variability of recurrence interval and single-event slip for surface-rupturing earthquakes in New Zealand, New Zeal. J. Geol. Geophys., 59(1), 97–116, doi:10.1080/00288306.2015.1127822, 2016b.

Njinju, E. A., Kolawole, F., Atekwana, E. A., Stamps, D. S., Atekwana, E. A., Abdelsalam, M. G. and Mickus, K. L.: Terrestrial heat flow in the Malawi Rifted Zone, East Africa: Implications for tectono-thermal inheritance in continental rift basins, J. Volcanol. Geotherm. Res., 387, doi:10.1016/j.jvolgeores.2019.07.023, 2019.

Novelli, V., Kloukinas, P., De Risi, R., Kafodya, I., Ngoma, I., Macdonald, J. and Goda, K.: Seismic Mitigation Framework for Non-engineered Masonry Buildings in Developing Countries: Application to Malawi in the East African Rift, in Resilient Structures and Infrastructure, pp. 195–223, Springer., 2019.

Nyblade, A. A. and Langston, C. A.: East African earthquakes below 20 km depth and their implications for crustal structure, Geophys. J. Int., 121(1), 49–62, doi:10.1111/j.1365-246X.1995.tb03510.x, 1995.

Olive, J. A., Behn, M. D. and Malatesta, L. C.: Modes of extensional faulting controlled by surface processes, Geophys. Res. Lett., 41(19), 6725–6733, doi:10.1002/2014GL061507, 2014.

Page, M. and Felzer, K.: Southern San Andreas fault seismicity is consistent with the Gutenberg–Richter magnitude–frequency distribution, Bull. Seismol. Soc. Am., 105(4), 2070–2080, doi:10.1785/0120140340, 2015.

De Pascale, G. P., Araya, J., Perisco, M., Sandoval, F., Sepulveda, S. and Moncada, D.: New school faults and seismic hazard, guilty (i.e. active) until proven innocent (i.e. inactive), in PATA DAYS 2017; 8th International Workshop on Paleoseismology, Active Tectonics and Archeoseismology, 13th-16th November 2017, Blenheim, New Zealand., 2017.

Pérouse, E. and Wernicke, B. P.: Spatiotemporal evolution of fault slip rates in deforming continents: The case of the Great Basin region, northern Basin and Range province, Geosphere, 13(1), 112–135, doi:10.1130/GES01295.1, 2017.

Philippon, M., Willingshofer, E., Sokoutis, D., Corti, G., Sani, F., Bonini, M. and Cloetingh, S.: Slip re-orientation in oblique rifts, Geology, 43(2), 147–150, doi:10.1130/G36208.1, 2015.

Pike, J. G.: A pre-colonial history of Malawi, Nyasal. J., 18(1), 22–54, 1965.

Poblet, J. and Lisle, R. J.: Kinematic evolution and structural styles of fold-and-thrust belts, Geol. Soc. Spec. Publ., 349, 1–24, doi:10.1144/SP349.1, 2011.

Poggi, V., Durrheim, R., Tuluka, G. M., Weatherill, G., Gee, R., Pagani, M., Nyblade, A. and Delvaux, D.: Assessing seismic hazard of the East African Rift: a pilot study from GEM and AfricaArray, Bull. Earthq. Eng., 1–31, doi:10.1007/s10518-017-0152-4, 2017.

Quigley, M., Van Dissen, R., Litchfield, N., Villamor, P., Duffy, B., Barrell, D., Furlong, K., Stahl, T., Bilderback, E. and Noble, D.: Surface rupture during the 2010 Mw 7.1 darfield(canterbury) earthquake: Implications for fault rupture dynamics and seismic-hazard analysis, Geology, 40(1), 55–58, doi:10.1130/G32528.1, 2012.

Rabinowitz, N. and Steinberg, D. M.: Seismic hazard sensitivity analysis: a multi-parameter approach, Bull. - Seismol. Soc. Am., 81(3), 796–817, 1991.

Roberts, E. M., Stevens, N. J., O'Connor, P. M., Dirks, P. H. G. M., Gottfried, M. D., Clyde, W. C., Armstrong, R. A., Kemp, A. I. S. and Hemming, S.: Initiation of the western branch of the East African Rift coeval with the eastern branch, Nat. Geosci., 5(4), 289–294, doi:10.1038/ngeo1432, 2012.

Robertson, E. A. M., Biggs, J., Cashman, K. V., Floyd, M. A. and Vye-Brown, C.: Influence of regional tectonics and pre-existing structures on the formation of elliptical calderas in the Kenyan Rift, in Geological Society Special Publication, vol. 420, pp. 43–67., 2016.

Sandwell, D., Mellors, R., Tong, X., Wei, M. and Wessel, P.: Open radar interferometry software for mapping surface Deformation, Eos, Trans. Am. Geophys. Union, doi:10.1029/2011EO280002, 2011.

Saria, E., Calais, E., Altamimi, Z., Willis, P. and Farah, H.: A new velocity field for Africa from combined GPS and DORIS space geodetic Solutions: Contribution to the definition of the African reference frame (AFREF), J. Geophys. Res. Solid Earth, 118(4), 1677–1697, doi:10.1002/jgrb.50137, 2013.

Saria, E., Calais, E., Stamps, D. S., Delvaux, D. and Hartnady, C. J. H.: Present-day kinematics of the East African Rift, J. Geophys. Res. Solid Earth, 119(4), 3584–3600, doi:10.1002/2013JB010901, 2014.

Scholz, C., Shillington, D., Wright, L., Accardo, N., Gaherty, J. and Chindandali, P.: Intrarift fault fabric, segmentation, and basin evolution of the Lake Malawi (Nyasa) Rift, East Africa, Geosphere, doi:10.1130/GES02228.1, 2020.

Scholz, C. H.: The Mechanics of Earthquakes and Faulting, 2nd ed., Cambridge University Press, Cambridge., 2002.

Scholz, C. H. and Contreras, J. C.: Mechanics of continental rift architecture, Geology, 26(11), 967–970, doi:10.1130/0091-7613(1998)026<0967:MOCRA>2.3.CO, 1998.

Scholz, C. H., Aviles, C. A. and Wesnousky, S. G.: Scaling differences between large interplate and intraplate earthquakes, Bull. Seismol. Soc. Am., 76(1), 65–70, doi:10.1144/gsjgs.141.4.0763, 1986.

Shillington, D. J., Scholz, C. A., Chindandali, P. R. N., Gaherty, J. B., Accardo, N. J., Onyango, E., Ebinger, C. J. and Nyblade, A. A.: Controls on Rift Faulting in the North Basin of the Malawi (Nyasa) Rift, East Africa, Tectonics, 39(3), e2019TC005633, doi:10.1029/2019TC005633, 2020.

Shudofsky, G. N., Cloetingh, S., Stein, S. and Wortel, R.: Unusually deep earthquakes in East Africa: Constraints on the thermo-mechanical structure of a continental rift system, Geophys. Res. Lett., 14(7), 741–744, doi:10.1029/GL014i007p00741, 1987.

Shyu, J. B. H., Chuang, Y. R., Chen, Y. L., Lee, Y. R. and Cheng, C. T.: A new on-land seismogenic structure source database from the Taiwan earthquake model (TEM) project for seismic hazard analysis of Taiwan, Terr. Atmos. Ocean. Sci., 27(3), 311–323, doi:10.3319/TAO.2015.11.27.02(TEM), 2016.

Sibson, R. H.: Earthquake faulting as a structural process, J. Struct. Geol., 11(1–2), 1–14, doi:10.1016/0191-8141(89)90032-1, 1989.

Siegburg, M., Bull, J. M., Nixon, C. W., Keir, D., Gernon, T. M., Corti, G., Abebe, B., Sanderson, D. J. and Ayele, A.: Quantitative Constraints on Faulting and Fault Slip Rates in the Northern Main Ethiopian Rift, Tectonics, 39(8), doi:10.1029/2019TC006046, 2020.

Stahl, K.: Some notes on the development of Zomba, Soc. Malawi J., 63(2), 39–55, 2010.

Stamps, D. S., Calais, E., Saria, E., Hartnady, C., Nocquet, J. M., Ebinger, C. J. and Fernandes, R. M.: A kinematic model for the East African Rift, Geophys. Res. Lett., 35(5), doi:10.1029/2007GL032781, 2008.

Stamps, D. S., Saria, E. and Kreemer, C.: A Geodetic Strain Rate Model for the East African Rift System, Sci. Rep., 8(1), doi:10.1038/s41598-017-19097-w, 2018.

Stamps, D. S., Kreemer, C., Fernandes, R., Rajaonarison, T. A. and Rambolamanana, G.: Redefining East African Rift System kinematics, Geology, doi:10.1130/g47985.1, 2020.

Stein, S., Geller, R. J. and Liu, M.: Why earthquake hazard maps often fail and what to do about it, Tectonophysics, doi:10.1016/j.tecto.2012.06.047, 2012.

Steinbruch, F.: Geology and geomorphology of the Urema Graben with emphasis on the evolution of Lake Urema, J. African Earth Sci., 58(2), 272–284, doi:10.1016/j.jafrearsci.2010.03.007, 2010.

Stirling, M. and Gerstenberger, M.: Applicability of the Gutenberg-Richter relation for major active faults in New Zealand, Bull. Seismol. Soc. Am., 108(2), 718–728, doi:10.1785/0120160257, 2018.

Stirling, M., McVerry, G., Gerstenberger, M., Litchfield, N., Van Dissen, R., Berryman, K., Barnes, P., Wallace, L., Villamor, P., Langridge, R., Lamarche, G., Nodder, S., Reyners, M., Bradley, B., Rhoades, D., Smith, W., Nicol, A., Pettinga, J., Clark, K. and Jacobs, K.: National seismic hazard model for New Zealand: 2010 update, Bull. Seismol. Soc. Am., 102(4), 1514–1542, doi:10.1785/0120110170, 2012.

Styron, R. and Pagani, M.: The GEM Global Active Faults Database, Earthq. Spectra, 1–21, doi:10.1177/8755293020944182, 2020.

Styron, R., García-Pelaez, J. and Pagani, M.: CCAF-DB: The Caribbean and Central American active fault database, Nat. Hazards Earth Syst. Sci., 20(3), 831–857, doi:10.5194/nhess-20-831-2020, 2020.

Taylor-Silva, B. I., Stirling, M. W., Litchfield, N. J., Griffin, J. D., van den Berg, E. J. and Wang, N.: Paleoseismology of the Akatore Fault, Otago, New Zealand, New Zeal. J. Geol. Geophys., 63(2), 151–167, doi:10.1080/00288306.2019.1645706, 2020.

Taylor, M. and Yin, A.: Active structures of the Himalayan-Tibetan orogen and their relationships to earthquake distribution, contemporary strain field, and Cenozoic volcanism, Geosphere, 5(3), 199–214, doi:10.1130/GES00217.1, 2009.

U.S. Department of the Interior U.S. Geological Survey: M 5.5 - 24km NE of Nsanje, Malawi [available at https://earthquake.usgs.gov/earthquakes/eventpage/us1000d1cy#executive, last accessed 26 Sept 2018], 2018.

Valentini, A., DuRoss, C. B., Field, E. H., Gold, R. D., Briggs, R. W., Visini, F. and Pace, B.: Relaxing Segmentation on the Wasatch Fault Zone: Impact on Seismic Hazard, Bull. Seismol. Soc. Am., 110(1), 83–109, doi:10.1785/0120190088, 2020.

Vallage, A. and Bollinger, L.: Testing Fault Models in Intraplate Settings: A Potential for Challenging the Seismic Hazard Assessment Inputs and Hypothesis?, Pure Appl. Geophys., 1–11, doi:10.1007/s00024-019-02129-z, 2019.

Villamor, P., Litchfield, N., Barrell, D., Van Dissen, R., Hornblow, S., Quigley, M., Levick, S., Ries, W., Duffy, B., Begg, J., Townsend, D., Stahl, T., Bilderback, E., Noble, D., Furlong, K. and Grant, H.: Map of the 2010 Greendale Fault surface rupture, Canterbury, New Zealand: Application to land use planning, New Zeal. J. Geol. Geophys., 55(3), 223–230, doi:10.1080/00288306.2012.680473, 2012.

Villamor, P., Barrell, D. J. A., Gorman, A., Davy, B., Hreinsdóttir, S., Hamling, I. J., Stirling, M. W., Cox, S. C., Litchfield, N. J., Holt, A., Todd, E., Denys, P., Pearson, C., C, S., Garcia-Mayordomo, J., Goded, T., Abbot, E., Ohneiser, C., Lepine, P. and F, C.-T.: Unknown faults under cities, Lower Hutt., 2018.

Wallace, L. M., Barnes, P., Beavan, J., Van Dissen, R., Litchfield, N., Mountjoy, J., Langridge, R., Lamarche, G. and Pondard, N.: The kinematics of a transition from subduction to strike-slip: An example from the central New Zealand plate boundary, J. Geophys. Res. Solid Earth, 117(2), doi:10.1029/2011JB008640, 2012.

Wallace, R. E.: Earthquake recurrence intervals on the San Andreas fault, Bull. Geol. Soc. Am., 81(10), 2875–2890, doi:10.1130/0016-7606(1970)81[2875:ERIOTS]2.0.CO;2, 1970.

Wallace, R. W.: Degradation of the Hebgen Lake fault scarps of 1959., Geology, 8(5), 225–229, doi:10.1130/0091-7613(1980)8<225:DOTHLF>2.0.CO;2, 1980.

Walshaw, R. D.: The Geology of the Nchue-Balaka Area, Bull. Geol. Surv. Malawi, 19, 1965.

Wedmore, L. N. J., Biggs, J., Williams, J. N., Fagereng, Dulanya, Z., Mphepo, F. and Mdala, H.: Active Fault Scarps in Southern Malawi and Their Implications for the Distribution of Strain in Incipient Continental Rifts, Tectonics, 39(3), e2019TC005834, doi:10.1029/2019TC005834, 2020a.

Wedmore, L. N. J., Williams, J. N., Biggs, J., Fagereng, Å., Mphepo, F., Dulanya, Z., Willoughby, J., Mdala, H. and Adams, B. A.: Structural inheritance and border fault reactivation during active early-stage rifting along the Thyolo fault, Malawi, J. Struct. Geol., 139, 104097, doi:10.1016/j.jsg.2020.104097, 2020b.

Wells, D. L. and Coppersmith, K. J.: New Empirical Relationships among Magnitude, Rupture Length, Rupture Width, Rupture Area, and Surface Displacement, Bull. Seismol. Soc. Am., 84(4), 974–1002, doi:<p></p>, 1994.

Wesnousky, S. G.: Displacement and geometrical characteristics of earthquake surface ruptures: Issues and implications for seismic-hazard analysis and the process of earthquake rupture, Bull. Seismol. Soc. Am., 98(4), 1609–1632, doi:10.1785/0120070111, 2008.

Wessel, B., Huber, M., Wohlfart, C., Marschalk, U., Kosmann, D. and Roth, A.: Accuracy assessment of the global TanDEM-X Digital Elevation Model with GPS data, ISPRS J. Photogramm. Remote Sens., 139, 171–182, 2018.

Wheeler, W. H. and Rosendahl, B. R.: Geometry of the Livingstone Mountains Border Fault, Nyasa (Malawi) Rift, East Africa, Tectonics, 13(2), 303–312, doi:10.1029/93TC02314, 1994.

Willemse, E. J. M.: Segmented normal faults: Correspondence between three-dimensional mechanical models and field data, J. Geophys. Res. Solid Earth, 102(B1), 675–692, 1997.

Williams, J. N., Fagereng, Å., Wedmore, L. N. J., Biggs, J., Mphepo, F., Dulanya, Z., Mdala, H. and Blenkinsop, T.: How Do Variably Striking Faults Reactivate During Rifting? Insights From Southern Malawi, Geochemistry, Geophys. Geosystems, 20(7), 3588–3607, doi:10.1029/2019GC008219, 2019.

World: Tectonic Shift : Rift 2018 - Regional Seismic Risk and Resilience Workshop (English). [online] Available from:

http://documents.worldbank.org/curated/en/325121555063464245/Tectonic-Shift-Rift-2018-Regional-Seismic-Risk-and-Resilience-Workshop, 2019.

WorldPop: www.worldpop.org - School of Geography and Environmental Science, University of Southampton; Department of Geography and Geosciences, University of Louisville; Departement de Geographie, Universite de Namur) and Center for International Earth Science Info, , doi:DOI: 10.5258/SOTON/WP00538, 2018.

Wright, L. J. M., Muirhead, J. D. and Scholz, C. A.: Spatio-temporal variations in upper crustal extension across the different basement terranes of the Lake Tanganyika Rift, East Africa, Tectonics, doi:10.1029/2019tc006019, 2020.

Yeats, R.: Active faults of the world, Cambridge University Press., 2012.

Youngs, R. R. and Coppersmith, K. J.: Implications of fault slip rates and earthquake recurrence models to probabilistic seismic hazard estimates, Bull. Seismol. Soc. Am., 75(4), 939–964, 1985.

Zeng, Y. and Shen, Z. K.: Fault network modeling of crustal deformation in California constrained using GPS and geologic observations, Tectonophysics, 612–613, 1–17, doi:10.1016/j.tecto.2013.11.030, 2014.

Zhang, P., Slemmons, D. B. and Mao, F.: Geometric pattern, rupture termination and fault segmentation of the Dixie Valley-Pleasant Valley active normal fault system, Nevada, U.S.A., J. Struct. Geol., 13(2), 165–176, doi:10.1016/0191-8141(91)90064-P, 1991.

Zielke, O. and Strecker, M. R.: Recurrence of large earthquakes in magmatic continental rifts: Insights from a paleoseismic study along the Laikipia-Marmanet fault, Subukia Valley, Kenya rift, Bull. Seismol. Soc. Am., 99(1), 61–70, doi:10.1785/0120080015, 2009.

4332

List of Figures

Figure 1

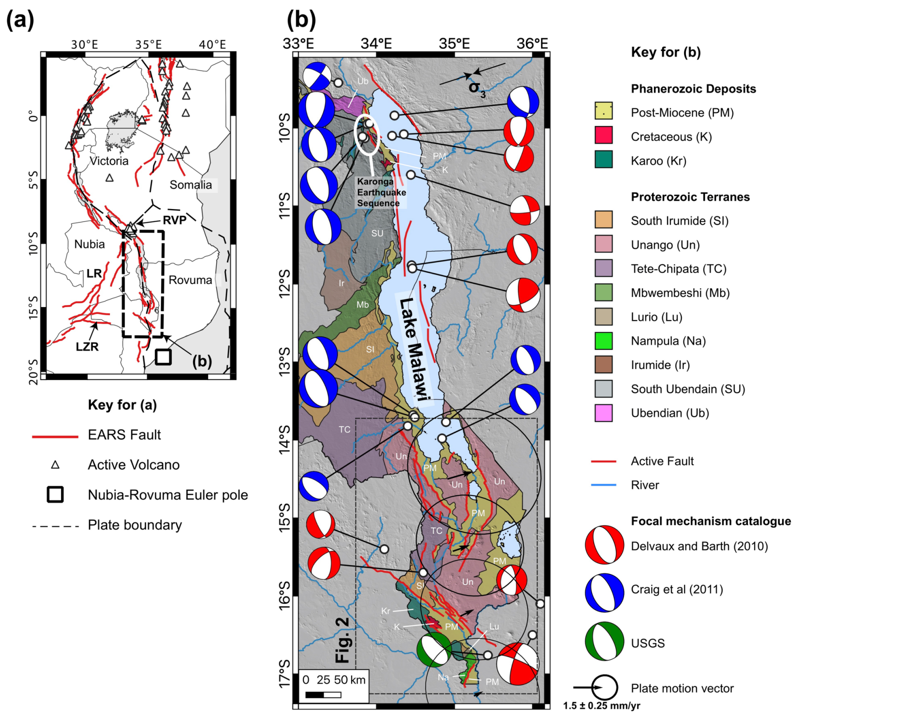

Figure 1: (a) Location of Malawi in the context of major faults in the East African Rift (Daly et al., 2020; Hodge et al., 2018a; Macgregor, 2015) and plate boundaries proposed by Saria et al., (2013). LZR; Lower Zambezi Rift, LR; Luangwa Rift; RVP; Rungwe Volcanic Province. (b) Simplified geological map of Malawi, with Proterozoic Terranes after Fullgraf et al., (2017). Map is underlain by Shuttle Radar Topography Mission (STRM) 30-m digital elevation model (DEM; Sandwell et al., 2011). Extent of Fig. 2 also shown. Active faults within this area are those included in the South Malawi Active Fault Database (SMAFD). Active faults outside this region mapped as in (a). Focal mechanisms collated from Delvaux and Barth, (2010), Craig et al., (2011), and U.S. Department of

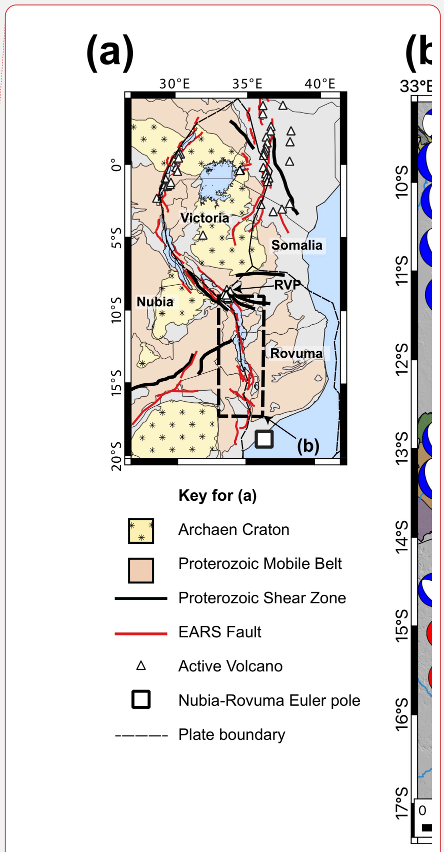

Deleted:

Deleted: the

Deleted: within East Africa

Deleted: . Distribution of Archean Cratons, Proterozoic Mobile Belts and shear zones modified after Fritz et al., (2013), …

Deleted: modified after Hodge et al., (2018). and Macgregor, (2015). P

Deleted: and the Euler pole between the Nubia and Rovuma plates after Saria et al., (2013) the Interior U.S. Geological Survey, (2018). Minimum principal compressive stress (σ_3) trend from focal mechanism stress inversion (Williams et al., 2019). Plate motion vector for central point of each basin in southern Malawi (Fig. S1) for Nubia-Rovuma Euler pole (Saria et al., 2013), modelled using methods described in Robertson et al., (2016).

Deleted: graben

Deleted: A2

Figure 2

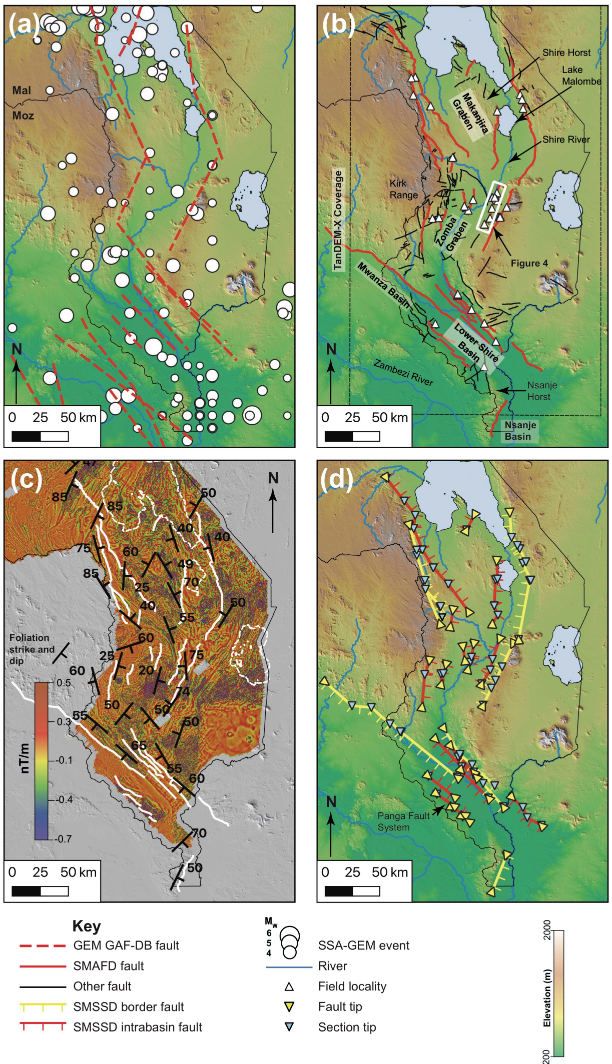

Figure 2: (a) Global Earthquake Model Global Active Fault Database map for southern Malawi and (GAF-DB; Macgregor, 2015; Styron and Pagani, 2020). Sub-Saharan African Global Earthquake Model (SSA-GEM; Poggi et al., 2017) event locations also shown. (b) Map of active fault traces

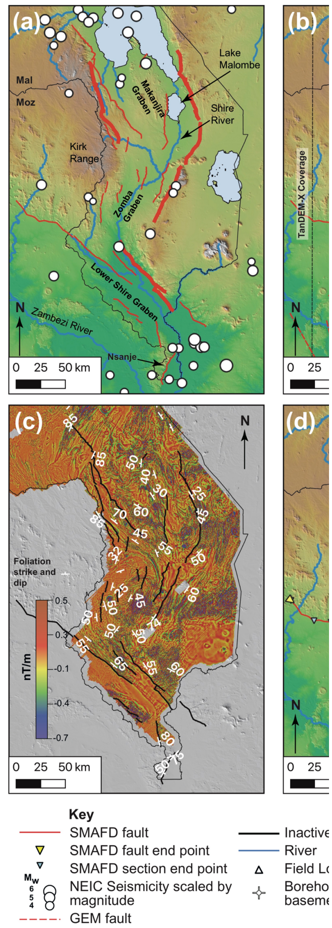

Deleted:

Deleted: Active fault map for south Malawi underlain by SRTM 30 m resolution DEM, division of its principal grabens (with border faults heavily weighted)

Deleted: (

Deleted: , and National Earthquake Information Centre (NEIC) record for events M_W>2.5 from 1900-February 2019 also shown…

compiled in the South Malawi Active Fault Database (SMAFD) with field locations and TanDEM-X coverage. Faults not interpreted to be active also shown. (c) Aeromagnetic image created from the vertical derivative, with foliation orientations digitised from geological maps (Bloomfield, 1958, 1965; Bloomfield and Garson, 1965; Habgood et al., 1973; Walshaw, 1965). SMAFD faults shown in white and outline of lakes are shown by dashed white lines. For full details of the acquisition of the aeromagnetic data, see Laõ-Dávila et al., (2015). (d) Simplified geometry of faults in the South Malawi Seismogenic Source Database (SMSSD), with faults sorted into border and intrabasin faults. Ticks indicate fault hanging-wall. Extent of all maps is equivalent and outlined in Fig. 1b. All maps underlain by SRTM 30 m Digital Elevation Model. Mal: Malawi, Moz: Mozambique.

Deleted: Information on methods used to collate

Deleted: and previous fault mapping

Deleted: . Combined

Deleted: , and underlain with the

Deleted: black

Deleted: The SMAFD faults and section geometry

Deleted: is

Deleted: GEM: Global Earthquake Model,

Figure 3

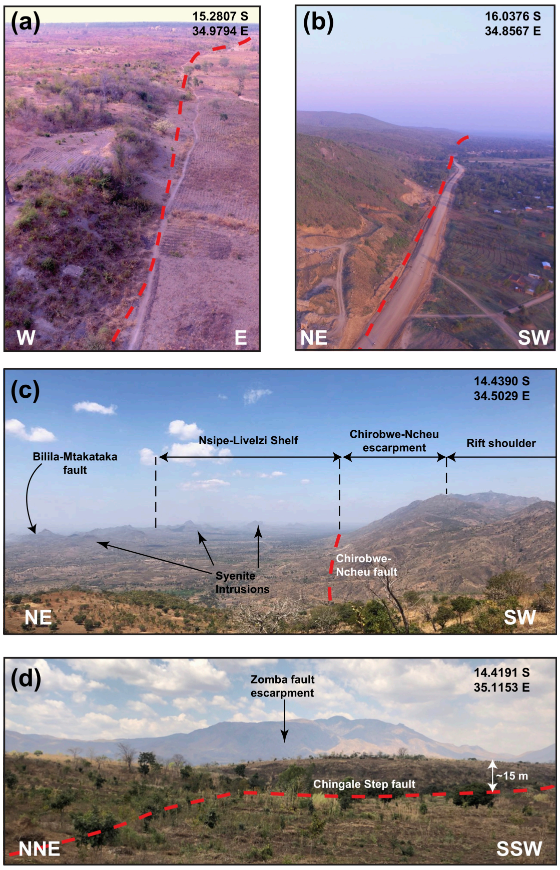

Figure 3: Field examples of border and intrabasin faults in southern Malawi. Unmanned Aerial Vehicle (UAV) images of scarps (dashed red line) along (a) intrabasin Mlungusi fault in the Zomba Graben, and (b) the Thyolo fault, the border fault for the Lower Shire Basin, (c) View across the western edge of the Makanjira Graben showing the Chirobwe Ncheu and Bilila-Mtakataka faults, and Proterozoic syenite intrusions (Walshaw, 1965). (d) Minor step in the scarp along the intrabasin Chingale Step fault, with the escarpment of the Zomba border fault behind.

Deleted: al

Deleted: al

Deleted: Graben

Deleted: al

Figure 4

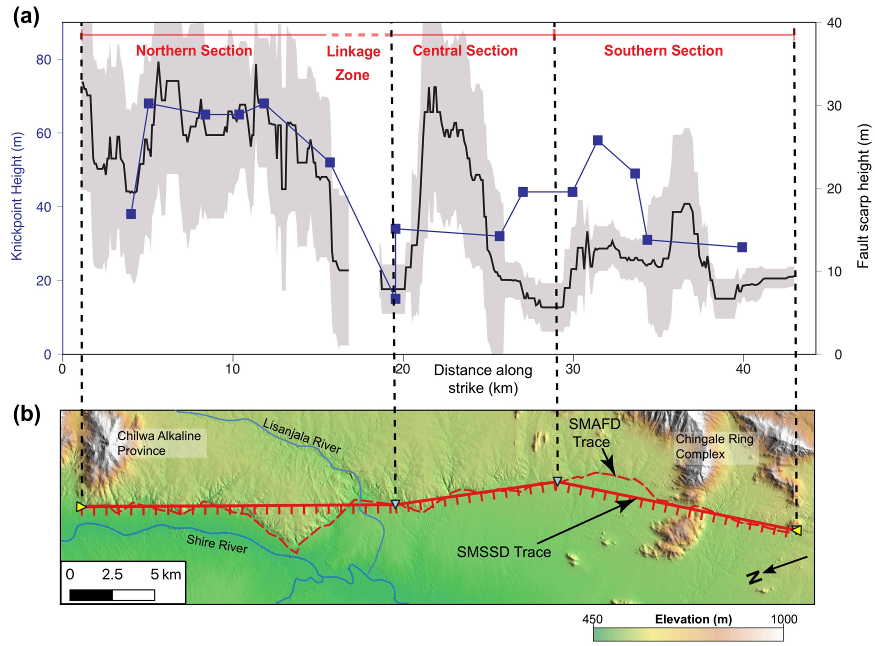

Figure 4: Fault segmentation along the Chingale Step fault, modified after Wedmore et al., (2020a). (a) Along strike variation in stream knickpoint (blue points) and fault scarp height (black line), with the gap due to erosion by the Lisanjala River. Grey shading represents one standard deviation error in scarp height measurements (Wedmore et al., 2020a). (b) Map of Chingale Step fault underlain by TanDEM-X DEM, extent of area shown in Fig. 2b. The dashed red line shows the surface trace of the fault as per the South Malawi Active Fault Database (SMAFD). The solid red line shows the simplified geometry of the fault in the South Malawi Seismogenic Source Database (SSMSD), where it is defined by straight lines between section endpoints (blue triangles). Ticks indicate fault hanging-wall. An along-strike scarp height minima at the boundary between the northern and central section occurs at a bend in the fault scarp, however, there is no obvious geometrical complexity at the along strike scarp height minima between the southern and central sections. Topography

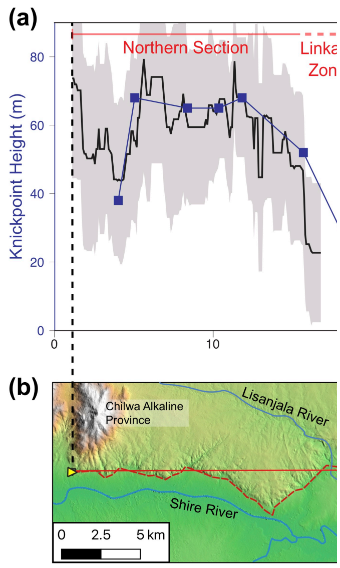

Deleted:

Deleted: used

Deleted: in earthquake source modelling, associated with the Proterozoic Chingale Ring Structure and Chilwa Alkaline Province (Bloomfield, 1965; Manda et al., 2019) is also indicated. For full details on (a) see Wedmore et al., (2020a).

Figure 5

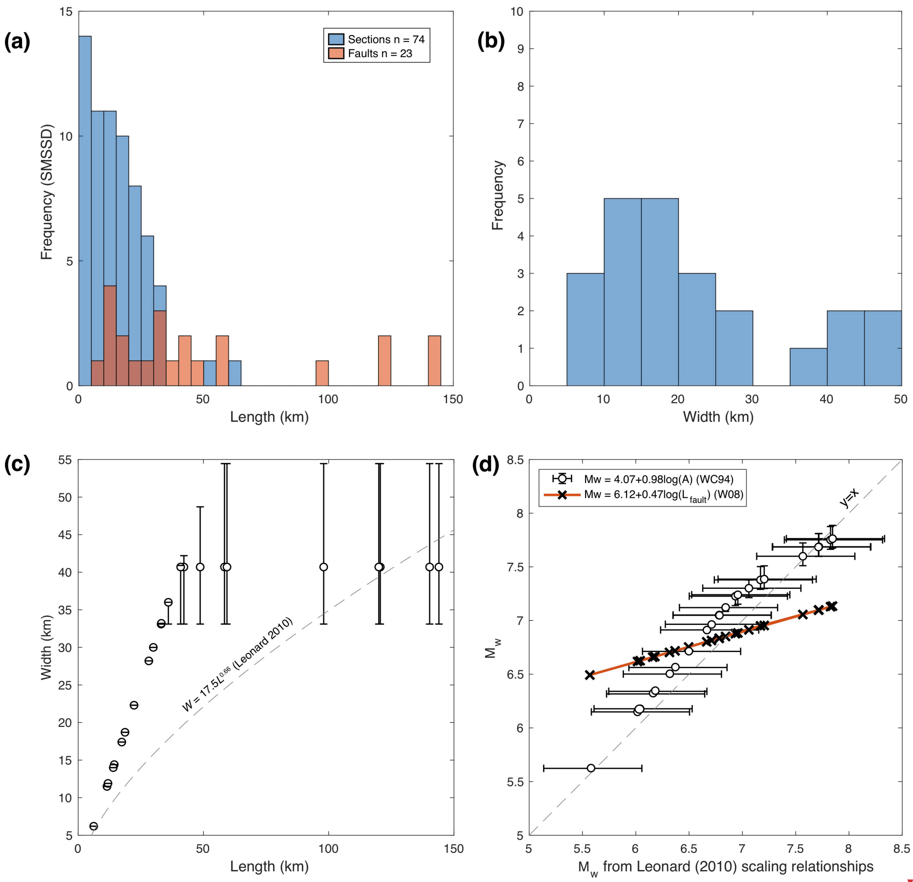

Figure 5: Assessment of fault geometry in the SMSSD, (a) Histograms showing distribution of (a) fault (L_{fault}) and section (L_{sec}) lengths in the SMSSD, (b) Histogram of fault widths in the SMSSD as derived from the Leonard, (2010) scaling relationship (Eq. (2)), and in (c) the predicted aspect ratio of faults following this relationship (dashed grey line) in comparison to an alternative method to estimate W using Eq. (1) (white circles). (d) A comparison of empirical scaling relationships used to estimate earthquake magnitudes (M_W) from fault geometry in the SMSSD. Leonard, (2010) magnitudes estimated using Eq. (4), with error bars representing range of C_1 and C_2 values derived

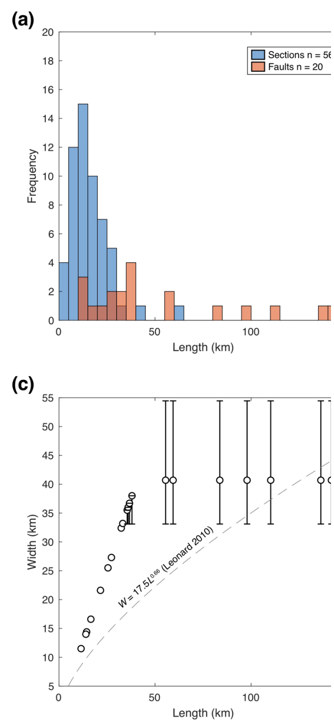

Deleted:

Deleted: AFD

Deleted: , and (b) fault widths (W)

Deleted: AF

Deleted: in comparison to normal faults in the Global Earthquake Model Global Active Fault Database (GAF-DB; Styron and Pagani, 2020). Note this comparison excludes 104 >150 km long faults in the GAF-DB

Deleted: The latter is

Deleted: s

Deleted: ed

Deleted: AF

for interplate dip-slip faults. A, fault area calculated from L_{fault} and W using Eq. (1); WC 94, Wells and Coppersmith (1994); W08, Wesnousky (2008).

Figure 6

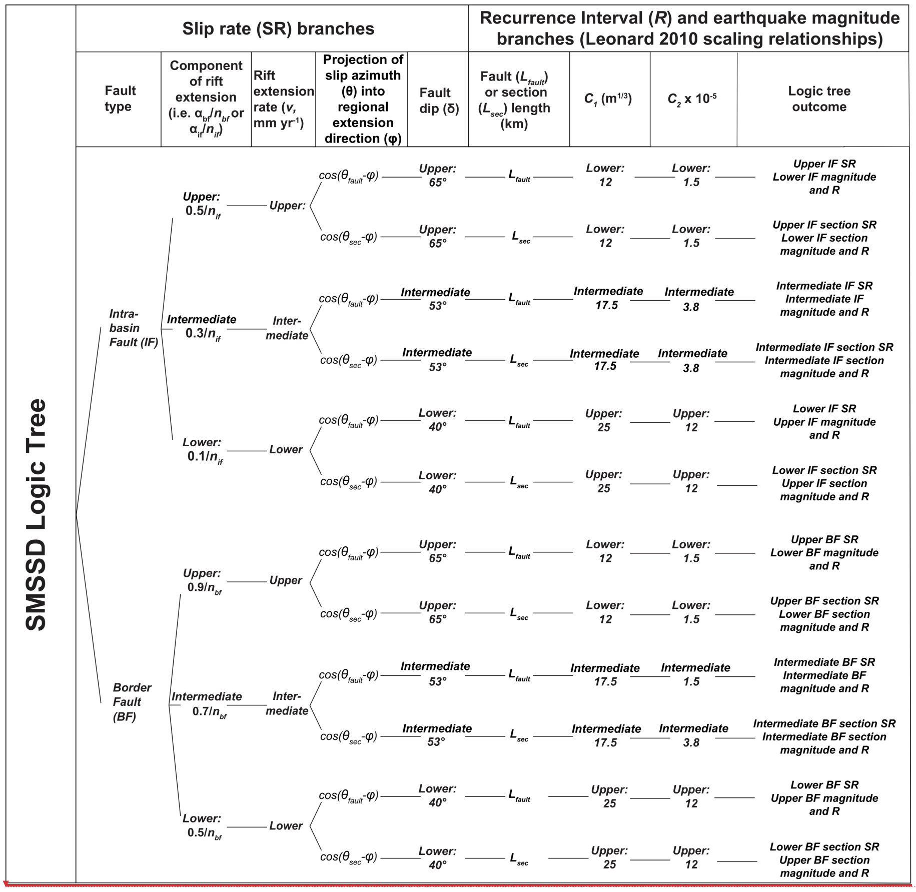

Deleted:

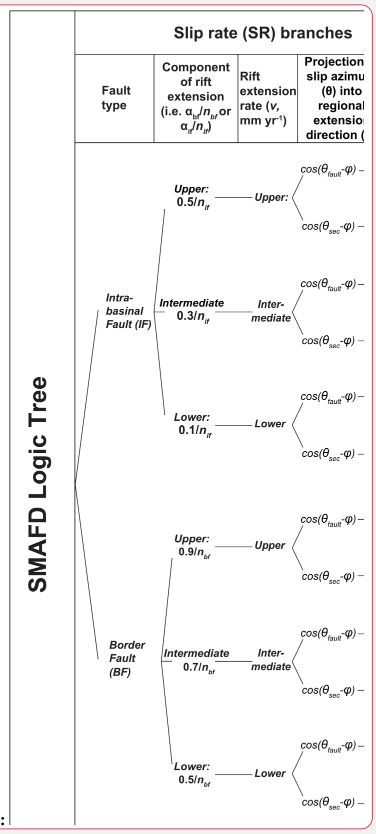

Figure 6: Logic tree for calculating lower, intermediate, and upper estimates of fault slip rates and earthquake magnitudes and recurrence intervals in the SMSSD; α_{bf} and α_{if} are the rift extension weighting assigned to border faults (BF) and intrabasin faults (IF) respectively; n_{bf} and n_{if} are the number of border or intrabasin faults in a basin, θ_{fault} and θ_{sec} are whole fault and individual section slip azimuth.

Deleted: AFD

Deleted: al

Deleted: al

Deleted: grabe

Deleted: n

Figure 7

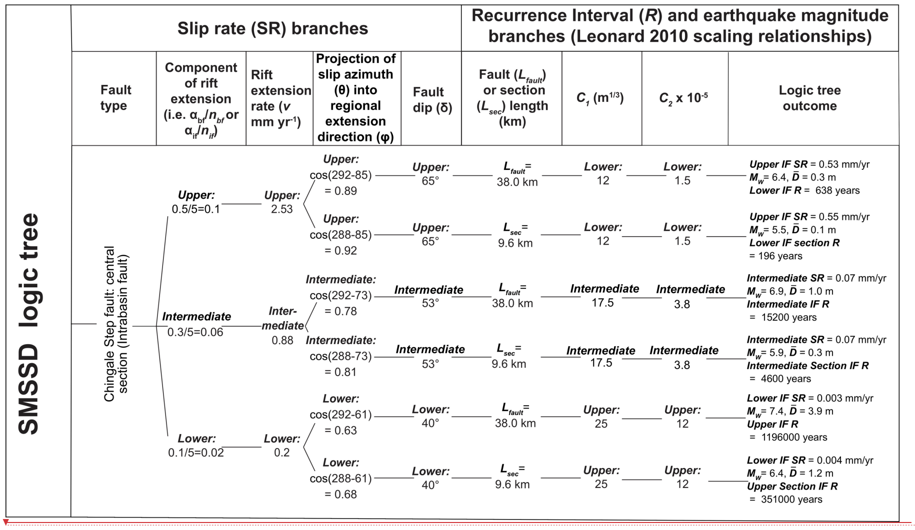

Figure 7: Example of the calculations in the SMSSD logic tree (Fig. 6), performed for the central section of the Chingale Step Fault (Fig. 4b). This is an intrabasin fault in the Zomba Graben, where the number of intrabasin faults (n_{if}) is five. A multiparameter sensitivity analysis for these calculations is documented in Appendix A.

Deleted:

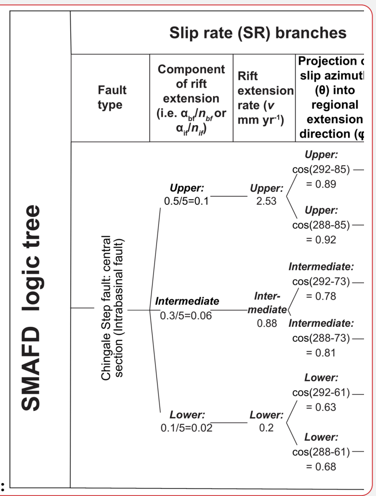

Deleted: AF

Deleted: al

Deleted: al

Deleted: B

Figure 8

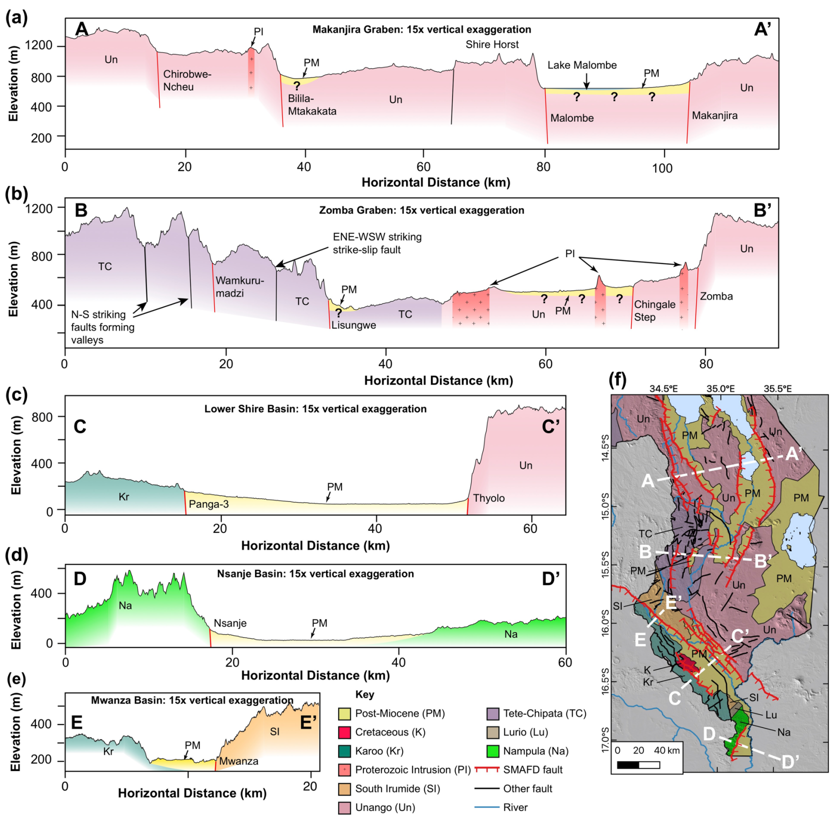

Figure 8: (a-e) Cross sections through each basin in southern Malawi. Topography from TanDEM-X 12 m Digital Elevation Model (DEM) except (d) which is from SRTM 30 m DEM. Tectonic terranes from Fullgraf et al., (2017), except for Proterozoic intrusions (Bloomfield, 1965; Walshaw, 1965). All normal faults in cross sections inferred to dip at 60°. Post-Miocene deposits in (a) and (b) shown to be 50-100 m thick, as estimated by borehole data (Fig. S1). (f) Simplified geological map for southern Malawi showing extent of cross sections. Underlain by SRTM 30 m DEM.

Formatted: Line spacing: Double

Field Code Changed

Deleted: (

Deleted:

Formatted: Font: Not Bold

Figure 9

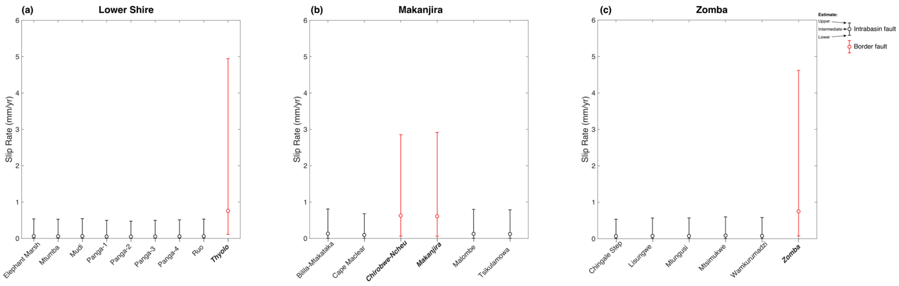

Figure 9: Fault slip rate estimates in the SMSSD, calculated following approach outlined in Fig. 6, and sorted into different basins in southern Malawi.

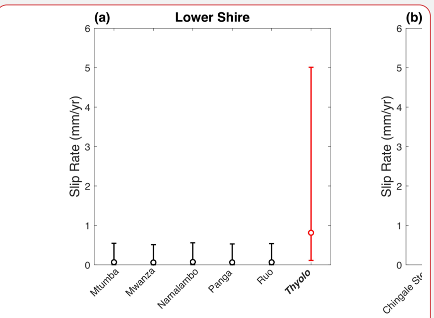

Deleted:

Deleted: 8

Deleted: AFD

Deleted: for faults in (a) Lower Shire graben, (b) Zomba graben, and (c) Makanjira graben. Middle point represents intermediate estimate with error bars representing upper and lower estimates. Faults with red data points, and names that are bold and italicised are classified as border faults in the SMAFD, the remaining faults are intrabasinal.

Figure 10

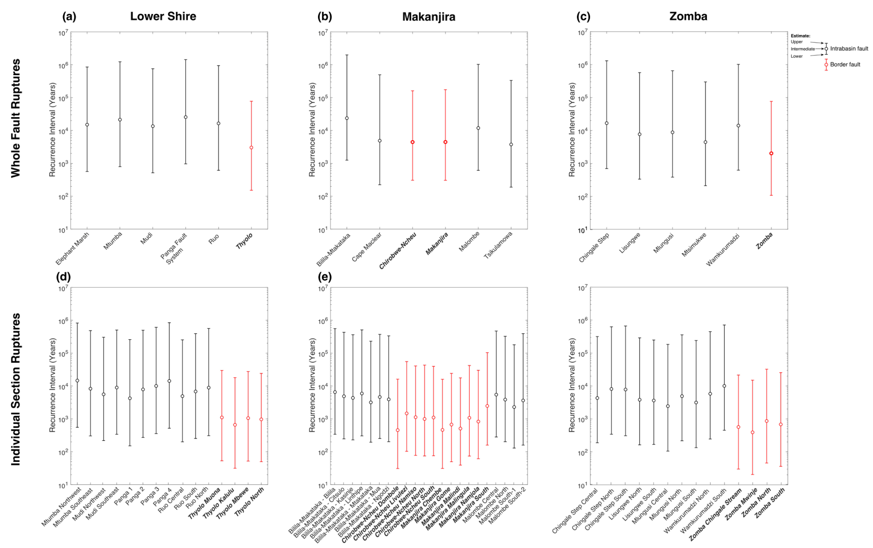

Figure 10: Recurrence interval (R) estimates in the SMSSD for (a-c) whole fault ruptures and (d-f) individual fault section ruptures. Note, R estimates for each Panga fault included in (d), whilst a multi-fault rupture is shown in (a)

Deleted: 9

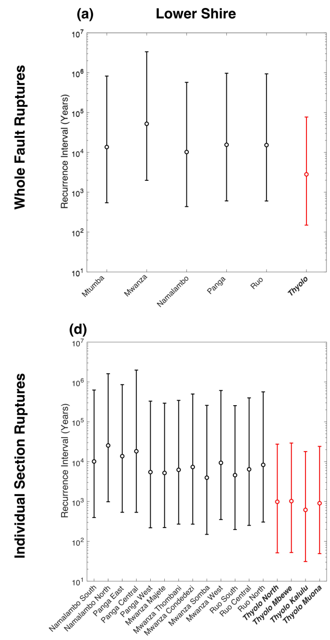

Deleted:

Deleted: 9

Deleted: AFD

Deleted: Calculated following approach outlined in Fig. 6, with middle point representing intermediate estimate, and error bars representing lower and upper estimates. Faults that are bold and italicised are classified as border faults.

Figure 11

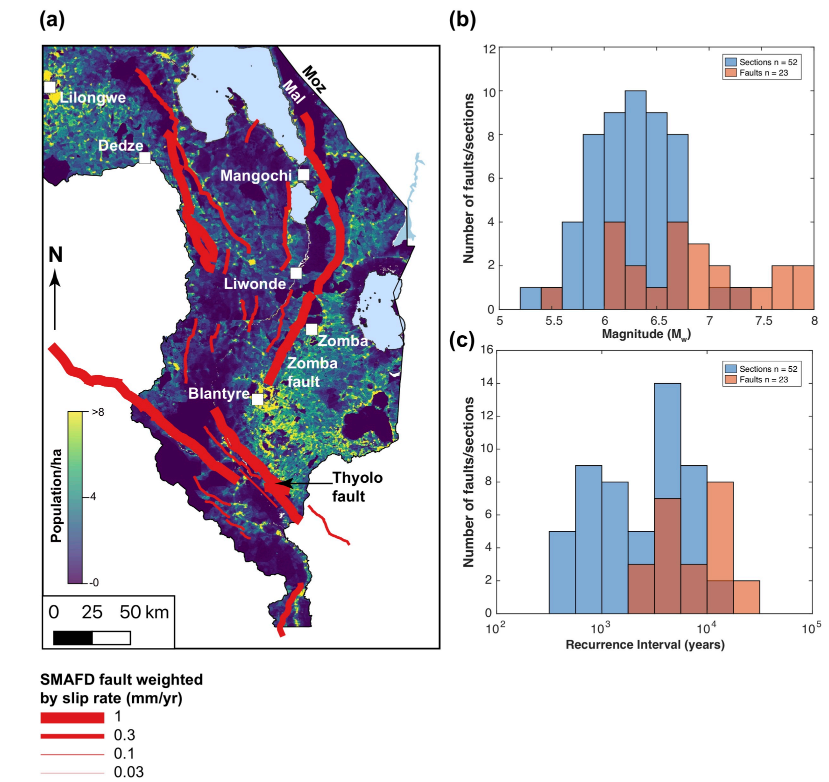

Figure 11: (a) Faults in the SMAFD with lines weighted by intermediate estimates of fault slip rate in the SMSSD. Fault map is underlain by population density where the pixel size is 3 arcseconds (approximately 1 ha) as derived from WorldPop predicted 2020 datasets for Malawi (WorldPop, 2018) with major population centres also highlighted. Note that population density in these places may exceed 100 people/ha. Area shown is same as in Fig. 2. Histograms to show range of (b) earthquake magnitudes and (c) recurrence interval estimates in the SMSSD from intermediate branches in Fig. 6.

Deleted: 0

Deleted:

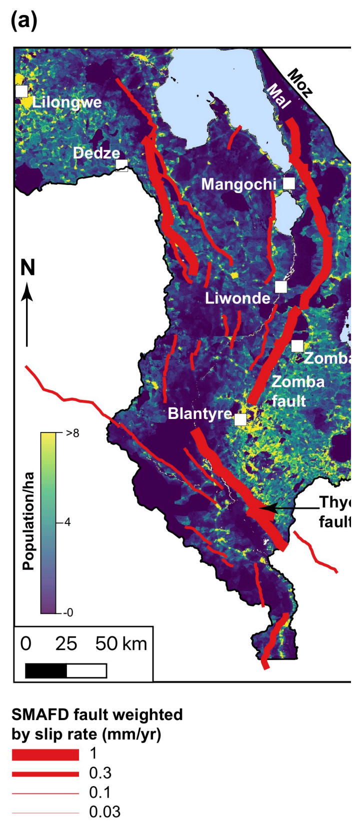

Deleted: 0

Deleted: SMAFD

Figure A1

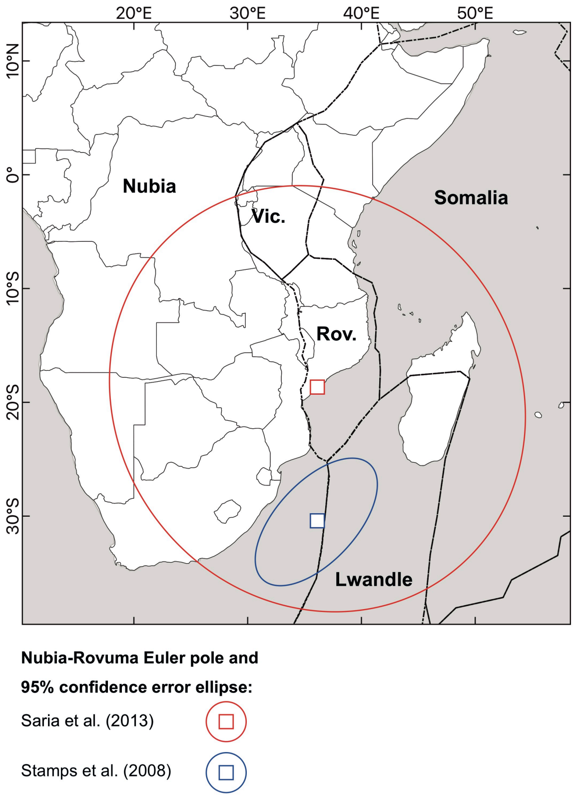

Figure A1: Plate boundaries in East Africa with location and uncertainty of the Nubia-Rovuma Euler pole derived by Saria et al. (2013) and Stamps et al. (2008). Vic., Victoria; Rov., Rovuma. Modified after Saria et al. (2013).

Deleted: Figure A1¶

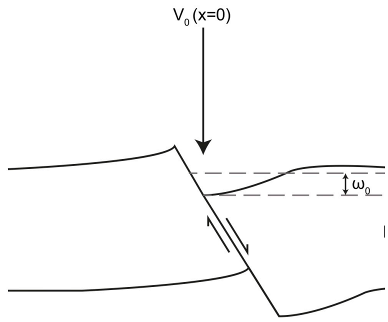

Figure A1: Set-up for hanging wall deflection equations. A vertical load (V_0) is applied to the point where the hanging-wall intersects the surface (i.e. where *x*=0) and where there is a maximum deflection (ω_0). The elastic thickness, Young's Modulus, density, and Poisson's ratio of the crust are represented by *h*, *E*, ρ_0, and *v* respectively.

Section Break (Next Page)

Figure A2¶
Figure A2¶ ... [43]

Deleted: B1

Deleted: B1

Figure A2

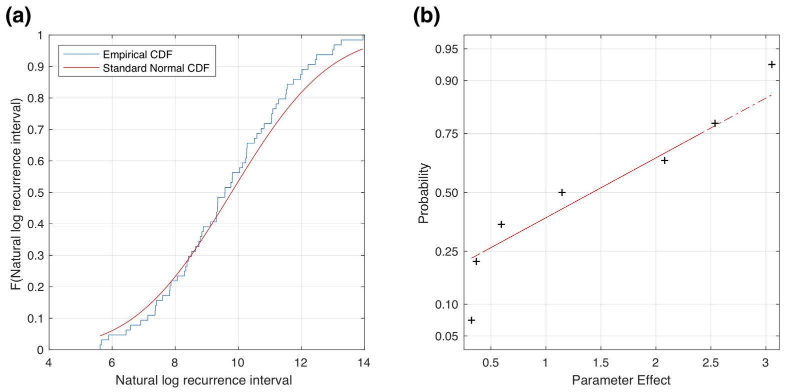

Figure A2: (a) Cumulative distribution function (CDF) of the natural log of the recurrence intervals calculated for the Chingale Step fault central section using the various parameter combinations listed in Table S1 (blue line). This CDF is compared to a standard normal CDF (red line) with the same mean value and standard deviation as the values in Table S1. (b) Normal probability plot of the parameter effects assessed in the sensitivity analysis and reported in Table 5. The most important effects are those that plot above a standard normal distribution (red line). Line is solid when within first and third quartiles of data and dashed when outside.

Deleted: B2

Deleted: B

Deleted: 1

Deleted: B1

Deleted: B1

Deleted: 4

List of Tables

Table 1

Attribute	**Type**	**Description**	**Notes**
SMAFD-ID	Numeric, assigned	Unique two-digit numerical reference ID for each trace	
name	Text		Assigned based on previous mapping or local geographic feature.
Geomorphic Expression	Text	Geomorphological feature used to identify and map fault trace.	E.g. scarp, escarpment
Location Method	Text	Dataset used to map trace.	E.g. type of digital elevation model
Accuracy	Numeric, assigned	Coarsest scale at which trace can be mapped. Expressed as denominator of map scale.	Reflects the prominence of the fault's geomorphic expression.
activity_confidence	Numeric, assigned	Certainty of neotectonic activity	1 if certain, 2 if uncertain
exposure_quality	Numeric, assigned	Fault exposure quality	1 if high, 2 if low
epistemic_quality	Numeric, assigned	Certainty that fault exists there	1 if high, 2 if low
last_movement	Text		Currently this is unknown for all faults in southern Malawi but can be updated when new information becomes available.
references	Text	Relevant geological maps/literature where fault has been previously described.	
SMSSD ID	Numeric, assigned	ID of equivalent structure in South Malawi Seismogenic Source Database	Will be multiple ID's for multi-segment faults, as these consist of multiple potential earthquake sources

Table 1: List and brief description of attributes in the SMAFD. Attributes are based on the Global Earthquake Model Global Active Faults Database (Styron and Pagani, 2020).

Deleted: Trace
Deleted: Fault N
Deleted: Fault that trace belongs to.
Deleted: Graben ... [44]
Deleted: Scale
Deleted: C
Deleted: Score between 1-4 that geomorphic feature used to map trace is an active fault.
Deleted: Trace notes
Deleted: Text
Deleted: Any remaining miscellaneous geomorphological information about fault trace.
Deleted: Author ... [45]
Deleted: 1
Deleted: Representative values for numeric attributes are reported in Table 3.

Table 2

Attribute	Type	Description	Notes
SMSSD-ID	Numeric, assigned	Unique numerical reference ID for each seismic source	
Fault Name	Text	Fault that section belongs to	Assigned based on previous mapping or local geographic feature.
Section Name	Text		Assigned based on previous mapping, local geographic feature, or location along fault.
Basin	Text	Basin that fault is located within.	Used in slip rate calculations.
Fault Type	Text	Intrabasin or border fault	
Section Length (L_{sec})	Numeric, assigned	Straight-line distance between section tips.	Measured in km. Except for linking sections, must be >5 km.
Section strike	Numeric, assigned	Measured from section tips, using bearing that is <180°.	
Fault Length (L_{fault})	Numeric, assigned	Straight-line distance between fault tips or sum of L_{sec} for segmented faults.	Measured in km
Fault strike	Numeric, assigned	Measured from fault tips using bearing <180°.	For segmented (i.e. non-planar) this is an 'averaged' value of fault geometry, which is required for slip rate estimates (Eq. (3)).
Dip (δ)	Numeric, assigned		Attribute parameterised by a set of representative values (40, 53, 65°).
Dip Direction	Text	Compass quadrant that fault dips in.	
Fault Width (W)	Numeric, calculated	Calculated from Eq. (2) from Leonard, (2010) scaling relationship using L_{fault}.	Not equivalent to rupture width for individual section earthquakes.
Slip Type	Text	Fault kinematics	All faults in the SMSSD assumed to be normal
Section net slip rate	Numeric, calculated	Calculated from Eq. (3).	In mm/yr. All faults in the SMSSD assumed to be normal, so is equivalent to dip-slip rate.

Fault net slip rate	Numeric, calculated	Calculated from Eq. (3).	In mm/yr. All faults in the SMSSD assumed to be normal, so is equivalent to dip-slip rate. Different from section net slip rate where fault strike ≠ section strike.
Section earthquake magnitude	Numeric, calculated	Calculated from Leonard, (2010) scaling relationship using Eq. (4) and L_{sec}.	Lower, intermediate, and upper values calculated.
Fault earthquake magnitude	Numeric, calculated	Calculated from Leonard, (2010) scaling relationship using Eq. (4) and L_{fault}.	Lower, intermediate, and upper values calculated.
Section earthquake recurrence interval (*R*)	Numeric, calculated	Calculated from Eq. (6) and using L_{sec} to calculate average single event displacement in Eq. (5).	Lower, intermediate, and upper values calculated.
Fault earthquake recurrence interval (*R*)	Numeric, calculated	Calculated from Eq. (6) and using L_{fault} to calculate average single event displacement in Eq. (5).	Lower, intermediate, and upper values calculated.
Fault notes	Text	Remaining miscellaneous information about fault.	
References	Text	Relevant geological maps/literature where fault has been previously described.	
SMAFD-ID	Numeric, assigned	ID of equivalent structure in South Malawi Active Fault Database	

Table 2: List and brief description of fault geometry, slip rate estimates, and earthquake source attributes in the SMSSD.

Formatted: Line spacing: single

Deleted: Graben ... [46]

Table 3

Basin	Centre of basin longitude (E)	Centre of basin latitude (S)	Geodetic Model	Velocity and velocity uncertainty of plate motion (mm/yr)	Azimuth, and azimuthal uncertainty of plate motion
Makanjira	34.88	14.51	S13	1.08 ± 1.66	075° ± 089°
			S08	3.01 ± 0.28	085° ± 002°
Zomba	34.93	15.42	S13	0.88 ± 1.65	072° ± 110°
			S08	2.84 ± 0.28	085° ± 002°
Lower Shire	35.08	16.26	S13	0.69 ± 1.65	069° ± 141°
			S08	2.69 ± 0.28	086° ± 002°
Nsanje	35.23	17.28	S13	0.46 ± 1.63	063° ± 212°
			S08	2.49 ± 0.27	086° ± 002°
Mwanza	NA	NA	N/A	0.6 ± 0.4	N/A

Table 3: Coordinates from which the Nubia-Rovuma plate motion vector for different basins in southern Malawi was derived (Fig. 1b). The velocity, azimuth, and uncertainties of each vector is also reported given the Nubia-Rovuma Euler poles reported in Saria et al. (2013) (S13), or in Stamps et al., (2008) (S08; Fig. A1), and where the uncertainties associated with the Euler pole are derived from the methods presented in Robertson et al. (2016). For justification of basin centre locations, see Fig. S1.

Formatted: Normal
Formatted: Font: Bold
Deleted: Graben
Deleted: graben
Deleted: graben
Deleted: 9
Deleted: 2
Deleted: 74
Deleted: 3
Deleted: 63
Deleted: 31
Deleted: 34.66
Deleted: 16.16
Deleted: 71
Deleted: 4
Deleted: ¶
Deleted: 2
Deleted: each
Deleted: graben
Deleted: B
Deleted: graben
Deleted: A2

Table 4

Attribute	Minimum	Median	Maximum
Section Length (L_{sec}, km)	0.7	13.4	62.4
Fault Length (L_{fault}, km)	6.2	33.2	144.0
Fault Width (W, km)	5.9	18.1	48.0
Section net slip rate (mm/yr)	0.05	0.13	0.90
Fault net slip rate (mm/yr)	0.05	0.08	0.81
Section earthquake magnitude (M_W)	5.4	6.3	7.2
Fault earthquake magnitude (M_W)	5.6	6.8	7.8
Section earthquake recurrence interval (R, years)	380	2814	14600
Fault earthquake recurrence interval (R, years)	2020	7870	23690

To demonstrate how calculated attributes vary across different faults in the SMSSD, as opposed to variation from the set of parameters used to calculate them, the values shown are for the intermediate branches in the SMSSD logic tree (Fig. 6).

Deleted: 3
Deleted: 3
Deleted: 0
Deleted: 3
Deleted: 9
Deleted: 11
Deleted: 5
Deleted: 5
Deleted: 7
Deleted: 1
Deleted: 8
Deleted: 8
Deleted: 19
Deleted: 0
Deleted: 7
Deleted: 6
Deleted: 3
Deleted: 0
Deleted: 84
Deleted: 06
Deleted: 13
Deleted: 2
Deleted: 6
Deleted: 0
Deleted: 8
Deleted: 390
Deleted: 4580
Deleted: 25
Deleted: 5
Deleted: Fault earthquake recurrence interval (R, years) ... [47]
Deleted: AF
Deleted: AF

Table 5

Parameter	**Lower Level**	**Upper Level**	**S08 Parameter Main Effect (*A*)**	**S13 Parameter Main Effect (*A*)**
Component of regional extensional strain (α_{if}/n_{if})	0.1	0.02	1.88	3.05
Rift extension rate (*v*, mm/yr)	2.56 (S08) 0.2 (S13)	3.12 (S08) 2.53 (S13)	0.20	2.54
Rift extension azimuth (ϕ)	085°	061°	0.32	0.32
Fault dip (δ)	65°	40°	0.59	0.59
Leonard, (2010) empirically derived scaling parameter C_1 ($m^{1/3}$)	12	25	0.37	0.37
Leonard, (2010) empirically derived scaling parameter C_2	1.5	12	2.08	2.08
Rupture length (*L*, km)	9.6 (individual section, L_{sec})	38.0 (whole fault, L_{fault})	1.15	1.15

Deleted: 4

Deleted: Parameter ... [48]

Table 4: Parameters and their associated upper and lower levels used in the sensitivity analysis for recurrence interval (*R*) calculations for the Chingale Step fault central section using the Stamps et al. (2008) (S08) and Saria et al. (2013) (S13) Nubia-Rovuma Euler poles (Fig. A1). The main effect of each parameter (*A*) for each geodetic model is then also reported. See Appendix A for full details of this analysis.

Deleted: 4

Deleted: B

Deleted: B

Deleted: ¶

Deleted: Page Break

Page 30: [1] Deleted	Jack Williams	12/10/2020 20:10:00

Page 30: [2] Deleted	Jack Williams	15/10/2020 13:50:00

Page 30: [3] Deleted	Jack Williams	09/10/2020 08:32:00

Page 30: [4] Deleted	Jack Williams	19/10/2020 10:47:00

Page 34: [5] Deleted	Jack Williams	15/10/2020 14:14:00

Page 34: [6] Deleted	Jack Williams	15/10/2020 14:36:00

Page 34: [7] Deleted	Jack Williams	12/10/2020 13:44:00

Page 34: [8] Deleted	Jack Williams	25/09/2020 09:12:00

Page 38: [9] Deleted	Jack Williams	13/09/2020 08:50:00

Page 44: [10] Deleted	Jack Williams	09/10/2020 10:08:00

Page 44: [11] Deleted	Jack Williams	13/09/2020 10:31:00

Page 44: [12] Deleted	Jack Williams	19/10/2020 11:41:00

Page 44: [13] Deleted	Jack Williams	15/10/2020 19:32:00

Page 44: [14] Deleted	Jack Williams	12/10/2020 14:32:00

Page 49: [15] Deleted	Jack Williams	09/10/2020 19:13:00

Page 49: [16] Deleted	Jack Williams	14/09/2020 08:45:00

Page 49: [17] Deleted	Jack Williams	12/10/2020 17:57:00

Page 49: [18] Deleted	Jack Williams	14/09/2020 08:51:00

Page 49: [19] Deleted	Jack Williams	13/10/2020 08:29:00

Page 51: [20] Deleted	Jack Williams	14/09/2020 08:56:00

Page 53: [21] Deleted	Jack Williams	15/10/2020 19:42:00

Page 53: [21] Deleted	Jack Williams	15/10/2020 19:42:00

Page 53: [21] Deleted	Jack Williams	15/10/2020 19:42:00

Page 53: [21] Deleted	Jack Williams	15/10/2020 19:42:00

Page 53: [22] Deleted	Jack Williams	14/09/2020 14:16:00

Page 53: [22] Deleted	Jack Williams	14/09/2020 14:16:00

Page 53: [23] Deleted	Jack Williams	15/10/2020 19:42:00

Page 53: [23] Deleted	Jack Williams	15/10/2020 19:42:00
Page 53: [23] Deleted	Jack Williams	15/10/2020 19:42:00
Page 53: [24] Deleted	Jack Williams	14/09/2020 14:19:00
Page 53: [24] Deleted	Jack Williams	14/09/2020 14:19:00
Page 53: [25] Deleted	Jack Williams	25/09/2020 10:31:00
Page 53: [25] Deleted	Jack Williams	25/09/2020 10:31:00
Page 53: [26] Deleted	Jack Williams	19/10/2020 09:02:00
Page 53: [26] Deleted	Jack Williams	19/10/2020 09:02:00
Page 53: [26] Deleted	Jack Williams	19/10/2020 09:02:00
Page 53: [26] Deleted	Jack Williams	19/10/2020 09:02:00
Page 53: [27] Deleted	Jack Williams	13/10/2020 21:09:00
Page 53: [27] Deleted	Jack Williams	13/10/2020 21:09:00
Page 53: [28] Deleted	Jack Williams	09/10/2020 20:15:00
Page 53: [28] Deleted	Jack Williams	09/10/2020 20:15:00

Page 53: [29] Deleted	Jack Williams	15/10/2020 19:43:00

Page 53: [29] Deleted	Jack Williams	15/10/2020 19:43:00

Page 53: [29] Deleted	Jack Williams	15/10/2020 19:43:00

Page 53: [29] Deleted	Jack Williams	15/10/2020 19:43:00

Page 53: [29] Deleted	Jack Williams	15/10/2020 19:43:00

Page 53: [29] Deleted	Jack Williams	15/10/2020 19:43:00

Page 53: [30] Deleted	Jack Williams	26/09/2020 11:21:00

Page 53: [30] Deleted	Jack Williams	26/09/2020 11:21:00

Page 53: [30] Deleted	Jack Williams	26/09/2020 11:21:00

Page 53: [30] Deleted	Jack Williams	26/09/2020 11:21:00

Page 53: [31] Moved to page 53 (Move #3)	Jack Williams	14/09/2020 14:11:00

Page 53: [31] Moved to page 53 (Move #3)	Jack Williams	14/09/2020 14:11:00

Page 53: [32] Deleted	Jack Williams	14/09/2020 18:59:00
Page 55: [33] Deleted	Jack Williams	14/09/2020 15:47:00
Page 55: [34] Deleted	Jack Williams	12/10/2020 20:00:00
Page 55: [35] Deleted	Jack Williams	09/10/2020 20:22:00
Page 55: [36] Deleted	Jack Williams	13/10/2020 08:38:00
Page 55: [37] Deleted	Jack Williams	14/09/2020 19:00:00
Page 55: [38] Deleted	Jack Williams	09/10/2020 10:42:00
Page 55: [39] Deleted	Jack Williams	15/10/2020 19:47:00
Page 55: [40] Deleted	Jack Williams	25/09/2020 10:48:00
Page 55: [41] Deleted	Jack Williams	25/09/2020 10:54:00
Page 56: [42] Deleted	Jack Williams	15/10/2020 15:12:00
Page 100: [43] Deleted	Jack Williams	15/10/2020 15:25:00
Page 102: [44] Deleted	Jack Williams	14/09/2020 19:16:00
Page 102: [45] Deleted	Jack Williams	14/09/2020 19:27:00
Page 104: [46] Deleted	Jack Williams	14/09/2020 19:45:00
Page 106: [47] Deleted	Jack Williams	19/10/2020 08:37:00
Page 107: [48] Deleted	Jack Williams	13/10/2020 09:13:00